

Chapter II.13

Radiation safety

Xavier Queralt

UKRI-STFC-ISIS Neutron and Muon Source, Didcot, United Kingdom

The purpose of this lecture is to provide insight into the importance of managing ionising radiation hazard. Unfortunately, this hazard cannot be removed when operating with accelerators, and the level of the risk depends on the type and usage of the accelerators. Understanding why radiation safety is needed and the lessons learned from serious accidents involving the ionising radiation hazard is essential. Also, the role of international organisations providing an external and rigorous approach to handling this hazard is covered, as well as the main principles of radiation safety, in particular, the term ALARA. A brief definition of the most relevant magnitudes and the meaning of the limit values are essential to understand how to interpret the official dosimetry data. A very simple and general approach to how the main particles interact with the matter is given through some characteristic examples. As a very summarised guidance, it explains how to proceed with a radiation shielding analysis and also the objective of the interlock systems. Finally, a recommendation on what type of radiation detector to use depending on the radiation environment is given in a very broad outline. Most of the examples provided come from electron and proton synchrotron accelerators due to the experience and background of the author.

II.13.1 Introduction

II.13.1.1 Scope

This “radiation safety” lecture provides a general overview of ionising radiation hazard in the accelerator technology environment. Almost all accelerators can produce ionising radiation, regardless of their accelerated particles or energy. The benefits of using ionising radiation cover a huge range of applications in very different fields of our lives, such as in medicine (radiodiagnosis and radiotherapy), products sterilisation, security access control, industrial radiography, communication broadcasting and fundamental research (high energy colliders) or applied research (synchrotron light sources) among others.

However, the risk that ionising radiation can produce any damage to somebody working with or close to the accelerators, or their environment, could be relevant. In order to minimise the ionising radiation risk, it is essential to understand the hazard and how to implement the control measures that will allow reducing the risk to levels comparable to the natural ionising radiation background.

The structure of this lecture is presented in seven parts, starting with the radiation safety background explaining some historical accidents and how the non governmental bodies propose practical guidance on how to control the ionising radiation risk. After that, the dose magnitudes are used to describe and quantify the hazard level.

This chapter should be cited as: Radiation safety, X. Queralt, DOI: [10.23730/CYRSP-2024-003.1653](https://doi.org/10.23730/CYRSP-2024-003.1653), in: Proceedings of the Joint Universities Accelerator School (JUAS): Courses and exercises, E. Métral (ed.), CERN Yellow Reports: School Proceedings, CERN-2024-003, DOI: [10.23730/CYRSP-2024-003](https://doi.org/10.23730/CYRSP-2024-003), p. 1653.
© CERN, 2024. Published by CERN under the [Creative Commons Attribution 4.0 license](https://creativecommons.org/licenses/by/4.0/).

Three sections cover how radiation is produced in high-energy electron and proton accelerators, specific situations when the beam is on and off, how to shield the accelerators depending on the radiation fields, and the engineering systems in place to ensure better control of the ionising radiation risk, such as radiation shielding and interlock systems.

Finally, a descriptive and basic explanation of the most used radiation monitors in high-energy accelerators is presented.

Although it is a qualitative description of radiation safety, some quantitative examples and exercises will be given to understand better how to approach this kind of risk.

II.13.1.2 Examples of facilities based on high-energy accelerator

II.13.1.2.1 ALBA synchrotron light source

ALBA is a 3rd generation synchrotron light facility located in Cerdanyola del Vallès [1], (Barcelona-Spain), in operation since 2012 (see Fig. II.13.1). ALBA's users are split in 65% from Spanish institutions and 35% from other countries. CELLS consortium is funded by Spanish and Catalanian governments, 50% each.



Fig. II.13.1: ALBA synchrotron light source is in the south of Europe (bottom left) and an aerial photo of the ALBA site (top right) [2]. The blue dots represent the location of synchrotron light sources as of 2005.

ALBA source is produced by a 3 GeV electron beam energy by means of a sequence arrangement of a LINear ACcelerator (LINAC) and a low-emittance, full-energy BOOSTER placed in the same tunnel

as the STORAGE RING (SR), see Fig. II.13.2. The nominal (designed) beam current is 400 mA, and nowadays is running above 255 mA in top-up mode, and the beam emittance is 4.3 nm-rad. ALBA's 270-metre perimeter has 17 straight sections, all of which are available for the installation of magnetic structures called insertion devices.

ALBA currently has ten operational state-of-the-art beamlines, comprising soft and hard X-rays, which are devoted mainly to biosciences, condensed matter (magnetic and electronic properties, nanoscience) and materials science. Additionally, four beamlines are in construction (low-energy ultra-high-resolution angular photoemission for complex materials, microfocus for macromolecular crystallography, absorption and diffraction and fast X-ray tomography & radioscopy).

The magnetic design of the ALBA SR is based on a modified Chasman-Green (Double Bend) lattice. The basic unit cell (repetitive structure) is an arrangement of two bending magnets accompanied by quadrupoles that produce non-zero dispersion in the straight lines between cells. Despite the fact that dispersion contributes to the radiation apparent beam size, the ALBA lattice design minimizes it while maximizing the available space in the straight sections.

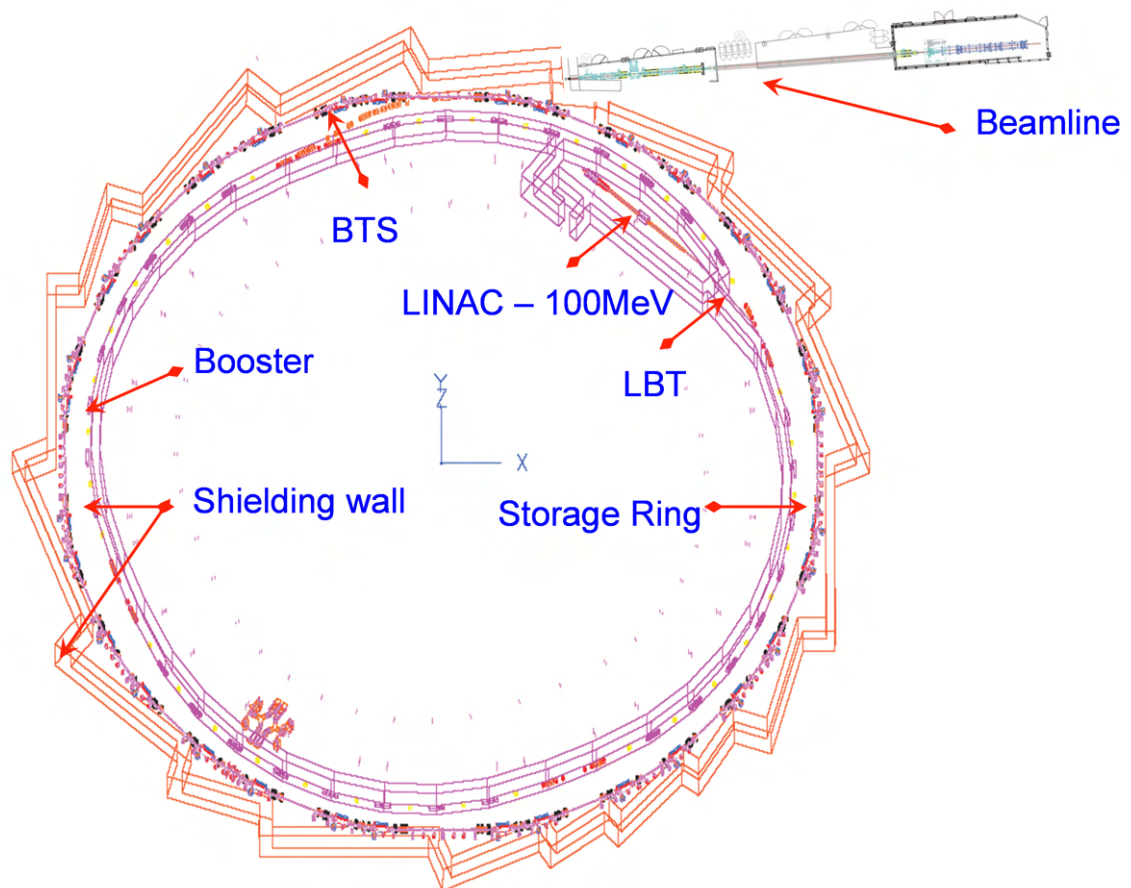


Fig. II.13.2: Top view of the ALBA LINAC-Booster-Storage Ring accelerators and the shielding structure, where the LBT (LINAC to Booster) and BTS (Booster to Storage Ring) transfer lines are indicated. On the top of the figure, the experimental beamline and its shielding structure are shown.

The straight sections at ALBA are called LSS (long), MSS (medium) and SSS (short). There are

3 LLS, 9 MSS and 5 SSS. The unit cell has MSS with small beta values which has very good properties to allow the installation of insertion devices, however they are not long enough to accommodate the injection straight. Therefore, modified cells, called matching cells, are used to accommodate LSS. The maximum number of direct beamlines is 33.

II.13.1.2.2 *ISIS neutron and muon spallation source*

ISIS Neutron and Muon [3] Source is based at Rutherford Appleton Laboratory (RAL) in Oxfordshire (see Fig. II.13.3 and Fig. II.13.4) and is a world-leading centre for research in the physical and life sciences. It is owned and operated by the Science and Technology Facilities Council (STFC), one of the councils that forms UK Research and Innovation (UKRI).



Fig. II.13.3: UKRI-STFC site in Great Britain, ISIS is at Rutherford Appleton Laboratory, which is part of the Harwell Science and Innovation Campus (Didcot, Oxfordshire) [4].

ISIS neutron and muon source produces beams of neutrons and muons that allow scientists to study materials at the atomic level using a suite of instruments, often described as “super-microscopes”, each of which is individually optimised for the study of different types of matter. Neutron and muon experiments are non-destructive and provide results that cannot be achieved by other techniques. ISIS supports a national and international community of more than 2,000 scientists who use neutrons and muons for research in physics, chemistry, materials science, geology, engineering, and biology.

In a typical year at ISIS, 1,200 experiments are carried out by 3,000 users from 30 countries generating 600 publications.

The first neutron beam was produced back in December 1984, and routine operations began in



Fig. II.13.4: Aerial view of the Rutherford Appleton Laboratory (RAL) showing the two research facilities based on high energy accelerators. DIAMOND (on the top) is a 3rd generation synchrotron light source and ISIS at the bottom showing the two buildings where the neutron and muon targets are installed [4].

June 1985, and in October 1985 at its official inauguration the neutron source was named ISIS by the then Prime Minister Margaret Thatcher.

ISIS is a high-intensity pulsed source of neutrons and muons, whereby neutron energies can be defined using time-of-flight techniques. The production of the 800 MeV proton beam is achieved in essentially four stages: ion source, radiofrequency quadrupole (RFQ), LINAC, and synchrotron as shown schematically in Fig. II.13.5. The RFQ, LINAC and synchrotron are all accelerators using radiofrequency (RF) power. All RF-based accelerators produce bunched beams in which the bunch structures reflect the RF frequencies.

Throughout the entire H^- and proton acceleration process (since 2017 the foil to remove the electrons in each H^- atom is carbon, not alumina), the beam must be kept under good vacuum. Accordingly, many tens of vacuum pumps are used, and vacuum is maintained typically between 10^{-8} and 10^{-9} of atmospheric pressure.

At ISIS protons from the synchrotron are guided by the electromagnet structures, which form the Extracted Proton Beam (EPB, see point 5 in Fig. II.13.5) and delivered to the neutron-producing targets in the two target stations as beams of 800 MeV protons. Target Station 1 (TS-1, see point 6 in Fig. II.13.5) and Target Station 2 (TS-2, see point 7 in Fig. II.13.5) run at pulse repetition rates of 40 and 10 pulses per

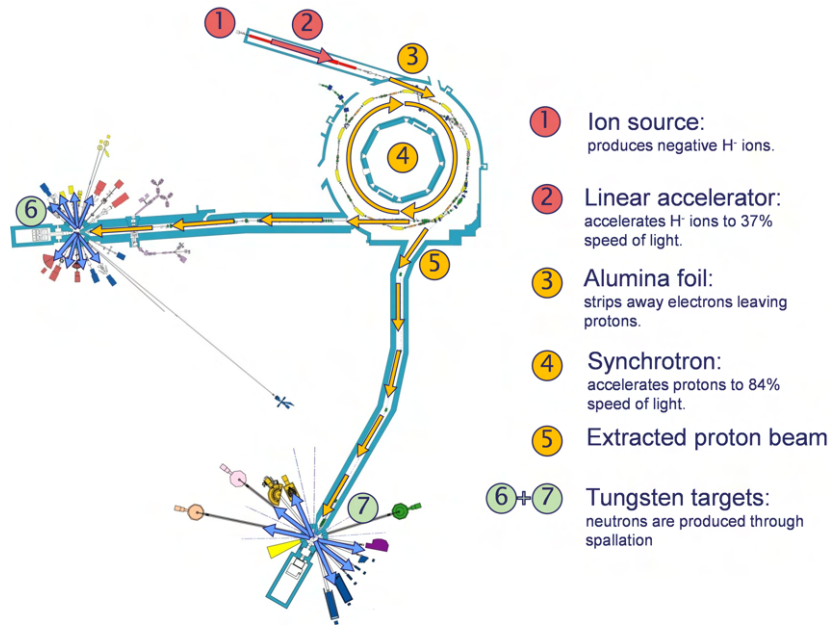


Fig. II.13.5: Diagram showing how ISIS works from the H^- ion source to the instruments which use the neutron and muons beam produced in the targets.

second (pps) respectively, and the mean proton currents delivered to the targets are $180 \mu A$ and $45 \mu A$ respectively. TS-1 therefore runs at a quarter of the repetition rate of TS-2, but for both targets cases the charge in each pulse of protons is $4.5 \mu C$ or $\sim 2.8 \times 10^{13}$ protons.

A high-energy proton hitting a heavy-metal nucleus can knock a few particles or clusters of particles out of the nucleus and can also split the rest of the nucleus into two excited fragments which de-excite by emitting neutrons with energies of the order of 1 MeV, and the knocked-out particles can go on to induce further spallation reactions (see Fig. II.13.6). The overall result, at ISIS, is some 10–15 neutrons produced per incident proton.

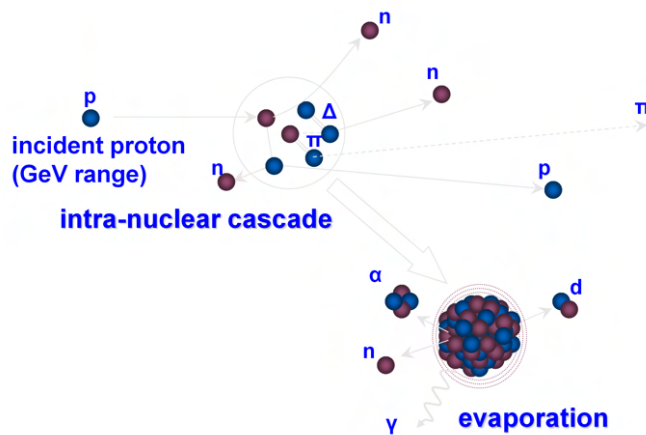


Fig. II.13.6: A schematic representation of the spallation process, where a high-energy proton beam hits a high-Z nucleus and produces more than ten neutrons per incident proton.

The neutrons emitted from spallation targets have energies of the order of ~ 100 MeV, whereas the neutron beam-line instruments for looking at the structure of materials require neutrons with energies in the eV range or even in the meV region. To achieve such reductions in energy, i.e. to moderate the neutrons, the primary-neutron-producing target is surrounded by moderator(s) made from low-atomic-number material in which neutron absorption is small. The primary neutrons then lose energy rapidly by scattering repeatedly off the light (low-Z) nuclei.

II.13.2 Radiation safety background

II.13.2.1 Definition of hazard and risk

High-energy particle accelerators are designed in such a way that all the charged particles accelerated by RF fields describe an ideal-theoretical orbit guided by magnetic and electric fields. In a first approach, it is assumed that there is no interaction between the accelerated particles with the residual gas (vacuum pressures are not zero) or with the vacuum vessel walls. However, in real cases, this interaction between the beam current and its surroundings will produce high-energy radiation that can be hazardous for the environment of the accelerator in general and for the people.

When this radiation carries enough energy to liberate electrons from atoms or molecules, thereby ionising them, it is called Ionising Radiation (IR). It consists of energetic subatomic particles (alpha, beta and neutron), ions or atoms moving at relativistic speeds, and electromagnetic waves on the high-energy end of the electromagnetic spectrum (X-ray or gamma ray).

The exposure to IR produces biological damage to human cells, and IR is considered as a hazard in the working environment. If there is a possibility that the damage caused by IR will produce misfortune or loss to any individual, then we are referring to IR risk.

All the control measures put in place to minimise this risk is the subject of the radiation safety. According to International Atomic Energy Agency-IAEA [5], the aim of radiation safety is the protection of people and the environment against radiation risks, and the safety of facilities and activities that give rise to radiation risks. It covers the radiation risks under normal circumstances and radiation risks as a consequence of incidents, as well as with other possible direct consequences of a loss of control over a nuclear reactor core, nuclear chain reaction, radioactive source or any other source of radiation. Safety measures include actions to prevent incidents and arrangements put in place to mitigate their consequences if they were to occur. As part of the radiation safety is the Radiation Protection (RP), which compresses all the measures oriented to the protection of people from harmful effects of exposure to ionising radiation.

II.13.2.1.1 Hierarchy principle

The control measure towards the risk reduction entails reducing the likelihood of the hazard occurrence or the severity of the incident where the IR is present. It is achieved only if it is possible to eliminate the hazard.

Hazard elimination is the top priority to reduce (in this case to zero) the risk. However, this is not always achievable, and therefore the next step is to replace or substitute the material, the process, or the machinery to minimise the risk. For instance, if we must use neutron beam, using accelerators

reduces the risk from using nuclear reactors. The next step towards the risk reduction is to implement engineering controls that ensure that regardless of the knowledge or experience of the operators, the risk is under control. In the case of IR, it is done using shielding and interlocks systems.

For those activities where it is not feasible or possible to implement any engineering control measures, administrative controls must be in place, such as operating procedures, training, signage, and informative material to ensure that anybody exposed to the risk is well informed and trained.

Finally, if there is still any risk that could affect an individual, we must put in place personal protection equipment (PPE), such as shoe covers, overalls, air hoods to avoid breathing contaminated radioactive material or leaded aprons to reduce the IR exposure.

In summary, the measures to follow are elimination, substitution, engineering controls, administrative controls, and personal protection clothes and equipment.

II.13.2.1.2 The Swiss cheese model

The “Swiss cheese model” is an image which explains how to reduce the likelihood of system failures in the presence of a hazard. In this model, each cheese slice represents a barrier put in place to minimise the probability that the hazard will produce harm or losses (risk reduction). The hole position in each slice is uncontrolled, in such a way that when by chance all holes are aligned, the hazard can cause harm and losses (see Fig. II.13.7).

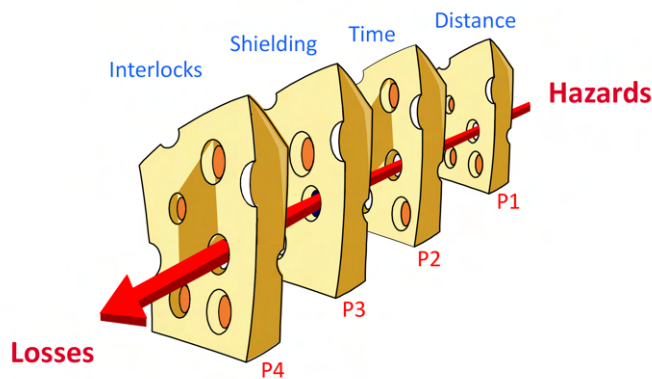


Fig. II.13.7: Graphical image of the “Swiss cheese model”, which explains how the presence of a hazardous situation ends in a loss. In this case, each cheese slice represents one control measure or barrier put in place to reduce the likelihood of the risk in the case of the IR hazard: distance, time, shielding and interlocks system.

This model draws attention to the nature of the control measures (engineering or administrative) that contain a probability of failure (P_i), and the total probability is (if all the control measures are independent) equal to $P = \prod_i P_i$.

The losses could be personal injuries, time, reputation, or equipment damage among others.

II.13.2.1.3 *Radiation safety risk assessment*

Before any work activity starts, a suitable and sufficient radiation safety risk assessment must be in place. Its content will depend on the different kinds of IR risks involved. Depending on the accelerator energy, IR can be only external radiation produced when the accelerator is on or off, or it can include any possible radionuclide intakes coming from activated particles in air, liquids or solids.

In any case, a proper assessment of the IR hazard, considering the different modes of operation, is needed to ensure that even the most unlikely situation is considered.

Although in this lecture we are focussing on the IR safety risk assessment only, it is very important to bear in mind to put in place a general Health & Safety risk assessment, where all the hazards involved in the work activity are taken into consideration.

Once it has been justified that it is not possible to avoid or replace the radiation source, the aim of the radiation safety risk assessment is to put in place all the risk control measures, both engineering and administrative controls, to reduce As Low As Reasonably Achievable (ALARA) the dose received by each individual that could be exposed to the radiation produced by the source (directly or indirectly).

The characteristics of the source (the accelerated particle, the current and the irradiation time) as well as the location, the category and number of individuals that might be exposed, will guide to decide the engineering control measures (in general the shielding characteristics and the interlock systems) and the administrative procedures.

The characteristics of the shielding material will depend on a lot of constraints such as the space available, the personal access, the penetrations for the accelerator supplies and the annual accepted dose outside the shielded area. In a first approach, the shielding is given by the material type, its density (ρ) and thickness (e), see Fig. II.13.8.

The interlock system¹ provides engineer control to ensure nobody is left inside the accelerator area when it is ready to be in operation, and if anyone opens any access door, the accelerator turns off immediately (in a fraction of a second). It is very convenient to include in the interlock system, a radiation monitor that trips the accelerator if a given dose rate or accumulated dose is achieved.

Another two parameters that must be taken into account in the radiation safety risk assessment are the distance from the source to the people exposed (D) to the radiation and the exposition time (t).

Figure II.13.8 shows, in a schematic way, the main aspects that must be taken into account for the radiation safety risk assessment.

II.13.2.2 **Historical examples**

From the early stages of the discovery of natural radioactivity and the invention of the first X-ray apparatus, there was a lot of interest in using them in different ways for human interest, from medical to military applications and commercial business. At that time, the knowledge of the damage on the human body of these kinds of radiation was not at the same level as the social and economic benefits, and the lack of proper control measures led to serious illnesses, and in some cases, deaths. In the following paragraphs, the most representative historical cases are described, but unfortunately the list is so long that it is out of

¹It is commonly called as Personnel Protection System-PPS or Personnel Safety System-PSS.

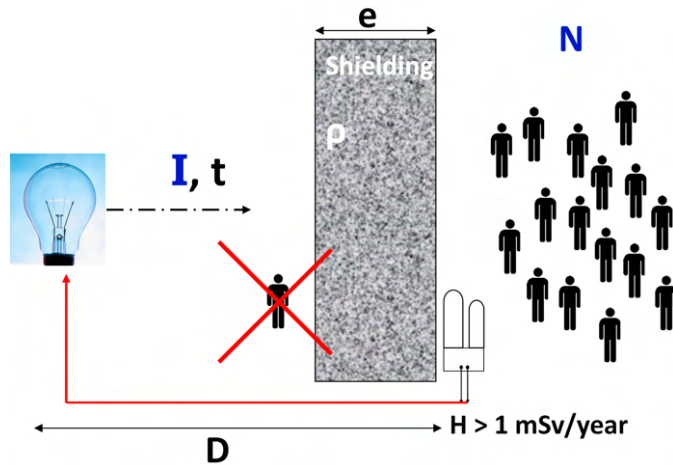


Fig. II.13.8: The purpose of the radiation safety risk assessment (for irradiation cases).

the scope of this course.

II.13.2.2.1 Radium dial paint

In December 1898 Marie and Pierre Curie demonstrated strong grounds for having come upon an additional very active substance that behaved chemically almost like pure barium. They suggested the name of radium for the new element [6]. After thousands of crystallizations, Marie finally isolated one decigram of almost pure radium chloride from several tons of the original material, and had determined radium's atomic weight as 225.

Natural radium (which is mostly Ra-226) emits mostly alpha particles, but other steps in its decay chain (the uranium or radium series) emit alpha or beta particles, and almost all particle emissions are accompanied by gamma rays. The beta particles in the presence of zinc sulphide (a phosphor) emits visible intense green light.

One of the applications of this natural green light emission was used to make the numbers on clocks and watches easier to see. In the 1920s there was a famous industrial case, known as “The Radium Girls” [7].

The sparkling, glowing, and beautiful, radium was also, according to the companies that employed these young women, completely harmless. The workers needed to coat the dials with radium paint, and the best and most efficient workers were women and girls, some as young as 14 or 15 years old (see Fig. II.13.9).

Radium's luminosity was part of its appeal. These young women were under the impression that radium was perfectly safe for them to be handling in this way.

In order to obtain the fine lines which the work required, a girl would place the bristles in her mouth, and by the action of her tongue and lips bring the bristles to a fine point.

Sadly, some of the women started having strange pains in their mouths and bones. Their teeth would loosen and fall out and their jaws, legs, and ankles would develop permanent aches or even crum-

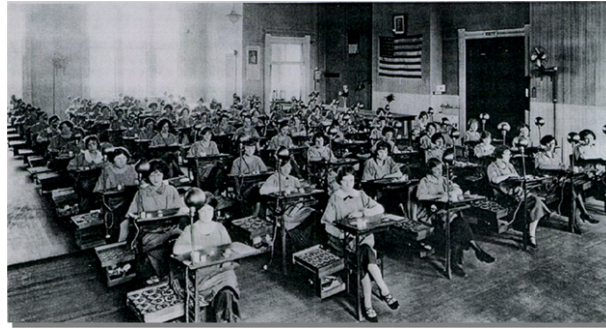


Fig. II.13.9: An image of watch painting process in an American factory in the 1920s [8].

ble. In September of 1922 the first dial painter died, and between 1922 and 1933 twenty-two dial painters are known to have died from radiation poisoning. Many of the women later began to develop anaemia, bone fractures, and necrosis of the jaw, a condition now known as radium jaw. The women also experienced suppression of menstruation, and sterility.

The inventor of radium dial paint, Dr. Sabin Arnold von Sochocky, died in November 1928, becoming the 16th known victim of poisoning by radium dial paint. He became ill from radium in his hands, not the jaw, but the circumstances of his death helped the Radium Girls in court.

II.13.2.2.2 Early X-ray radiographers

W.C. Röntgen discovered [9] X-rays in December 1895 after seven weeks of work during which he had studied the properties of this new type of radiation able to go through screens of notable thickness and densities. He named them X-rays to underline the fact that their nature was unknown. Physicians and physicists began as early as January 1896 to use X-rays on patients to investigate the skeleton and subsequently the lung and other organs. This was the birth of radiology. In June 1896 the first patient was treated by radiotherapy.

Although X-rays had already been utilized in several battlefield theatres prior to World War I (WWI) [10], during this war X-ray saw widespread development and applications (see Fig. II.13.10). The use was further precipitated by the 1913 development at the Research Laboratory of the General Electric Company of the hot-cathode X ray tube allowing for stable and reproducible operation and production of large amounts of radiation compared with the earlier gas X-ray tubes. Significant use of radiography in hospitals and on the WWI battlefields with several types of vehicles, dynamos, film processing, and X-ray equipment was quickly created out of urgent need.

Following significant exposures of X-ray operators and radiologists during WWI, acute injuries (skin and eyes) as well as cases of leukaemia and aplastic anaemia were reported. As of 1913, users understood that standardization in measurement was ultimately necessary and critical.

In 1915, the British Röntgen Society, recognizing the plight of the radiologists who operated often primitive unshielded equipment, passed a resolution which stated “that the safety of operators should be secured by universal adoption of strict rules, and that the Society should take steps to ensure this.” Later that year, the Society produced recommendations for the protection of X-ray operators, a code



Fig. II.13.10: In the first stages of using X-ray apparatus for medical applications, the patient, the doctor, and the operator were exposed to unnecessary, unjustified and unshielded dose [11].

of practice that noted the harmful effects produced by X-rays (cumulative and latent), importance of qualified medical practitioners, shielding and collimation, avoidance of operator exposures (protected spaces), not holding anything in the beam, shielded X-ray tubes, and tests of available shielding. Such guidance signified an active organizational interest in X-ray protection.

II.13.2.2.3 First nuclear bombs (1945)

Two atomic bombs made by the allied powers (USA and UK) from uranium-235 and plutonium-239 were dropped on Hiroshima and Nagasaki in early August 1945, 6th and 9th respectively. These brought the long World War II to a sudden end. The immense and previously unimaginable power of the atom had been demonstrated. In the following years several governments joined the arms race, while internationally, efforts were focused on constraining the threat of nuclear weapons proliferation.

The Hiroshima bomb was made from highly-enriched uranium-235. This was prepared by diffusion enrichment techniques using the very small differences in mass of the two main isotopes: U-235 (originally 0.7% in the uranium) and U-238, the majority. As UF₆, there is about a one percent difference in mass between the molecules, and this enables concentration of the less common isotope. About 64 kilograms of highly-enriched uranium was used in the bomb which had a 16 kiloton yield (i.e. it was equivalent to 16,000 tonnes of TNT). It was released over Hiroshima, Japan's seventh largest city, and 90% of the city was destroyed (see Fig. II.13.11).

The devastating effects of both kinds of bombs depended essentially upon the energy released at the moment of the explosion, causing immediate fires, destructive blast pressures, and extreme local radiation exposures.

By the end of 1945, 140,000 deaths in Hiroshima and 74,000 deaths in Nagasaki were attributed to the impacts of the atomic bombings.

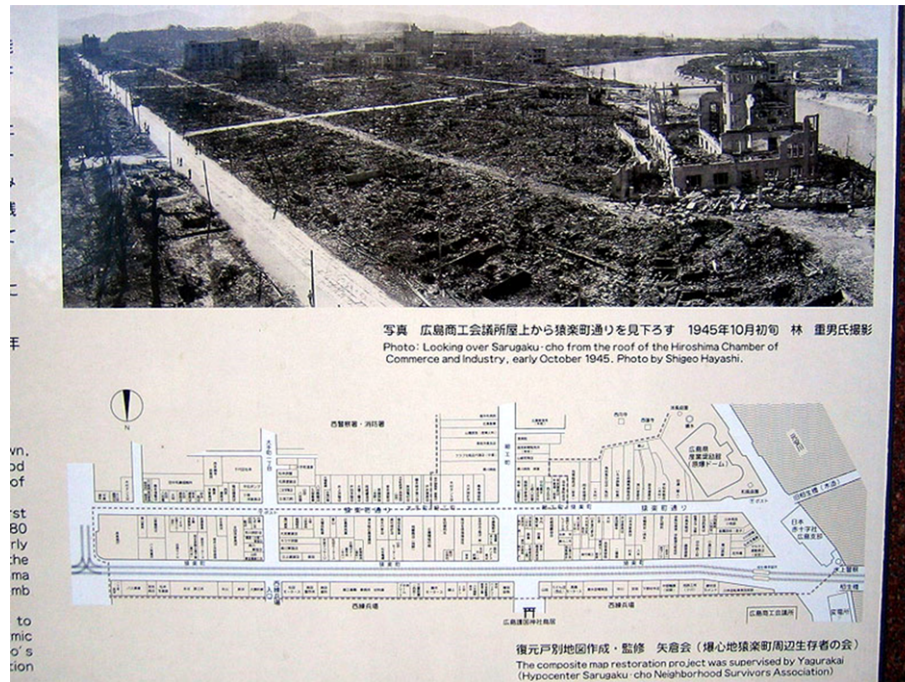


Fig. II.13.11: A photo from October 1945 showing the devastating effect of the Hiroshima atomic bomb on 6th August 1945.

II.13.2.2.4 Chernobyl accident (1986)

On 26th April 1986, in number four reactor at Chernobyl (in the former Soviet Union) there was an explosion and fire that demolished the reactor building and released large amounts of radioactive material into the atmosphere due to improper testing at low-power, which resulted in loss of control. As safety measures were ignored, the uranium fuel in the reactor overheated and melted through the protective barriers.

As a result of this explosion, a lethal dose of radiation about 5 Gy (Joules/kilogram) was released over 5 hours and as a result, unprotected workers received fatal doses in less than a minute. According to the official figures, only ten individuals were highly exposed.

Soon after the accident, the IAEA [12] provided immediate support to the Soviet Union in the area of environmental remediation, decommissioning and management of radioactive waste, to strengthen the safety levels at the plant. The IAEA worked closely with other United Nations organizations under the “International Chernobyl Project”, which provided an assessment of the radiological consequences of the accident and evaluated protective measures (see Fig. II.13.12).

Shortly after the Chernobyl accident, the IAEA drafted two conventions that were ratified by Member States—the Convention on Early Notification of a Nuclear Accident and the Convention on Assistance in the Case of a Nuclear Accident or Radiological Emergency, which establish the international framework for emergency notification, information exchange and the provision of international assistance on request. The Conventions mandate the IAEA to act as the international hub coordinating these activities.

The findings of the 1996 and 2005 conferences were considered by The United Nations Scientific

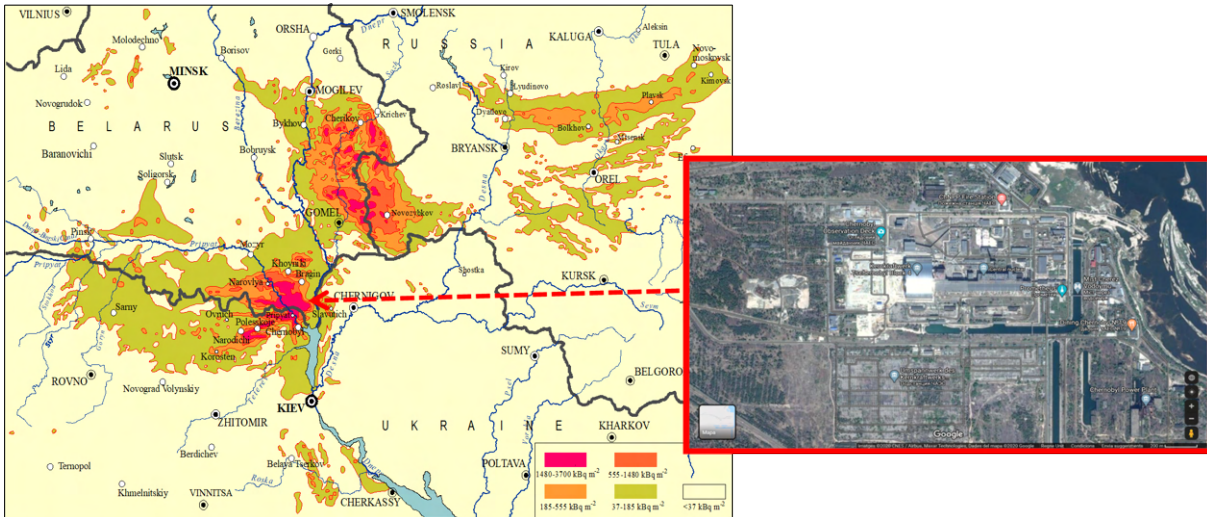


Fig. II.13.12: Surface ground contamination map (in kBq/m²) of Cs-137 released on the area close to Chernobyl reactor (left) [13], and a top view image of the power plant with the coffin covering the affected reactor (right).

Committee on the Effects of Atomic Radiation—UNSCEAR—as part of its mandate to assess and report levels and effects of ionising radiation. UNSCEAR findings are fully reflected in the IAEA standards, which are regularly reviewed and updated.

II.13.2.2.5 Fukushima accident (2011)

On March 11th 2011 Japan suffered a 9.0 magnitude earthquake and a subsequent tsunami that affected the Japanese Northeast coast. It was caused by a sudden release of energy at the interface where the Pacific tectonic plate forces its way under the North American tectonic plate. A section of the Earth’s crust, estimated to be about 500 km in length and 200 km wide, was ruptured, causing a massive earthquake and a tsunami which struck a wide area of coastal Japan, including the north-eastern coast, where several waves reached heights of more than ten metres. The earthquake and tsunami caused great loss of life and widespread devastation in Japan. More than 15,000 people were killed, over 6,000 were injured. Considerable damage was caused to buildings and infrastructure, particularly along Japan’s north-eastern coast.

At the Fukushima Daiichi nuclear power plant (see Fig. II.13.13), the earthquake caused damage to the electric power supply lines to the site, and the tsunami caused substantial destruction of the operational and safety infrastructure on the site. The combined effect led to the loss of off-site and on-site electrical power. This resulted in the loss of the cooling function at the three operating reactor units as well as at the spent fuel pools. The four other nuclear power plants along the coast were also affected to different degrees by the earthquake and tsunami.

Four reactors were written off due to damage in the accident and high radioactive material was released over days 4 to 6, reaching a total of some 940 PBq.

Despite the efforts of the operators at the Fukushima Daiichi nuclear power plant to maintain control, the reactor cores in Units 1–3 overheated, the nuclear fuel melted and the three containment

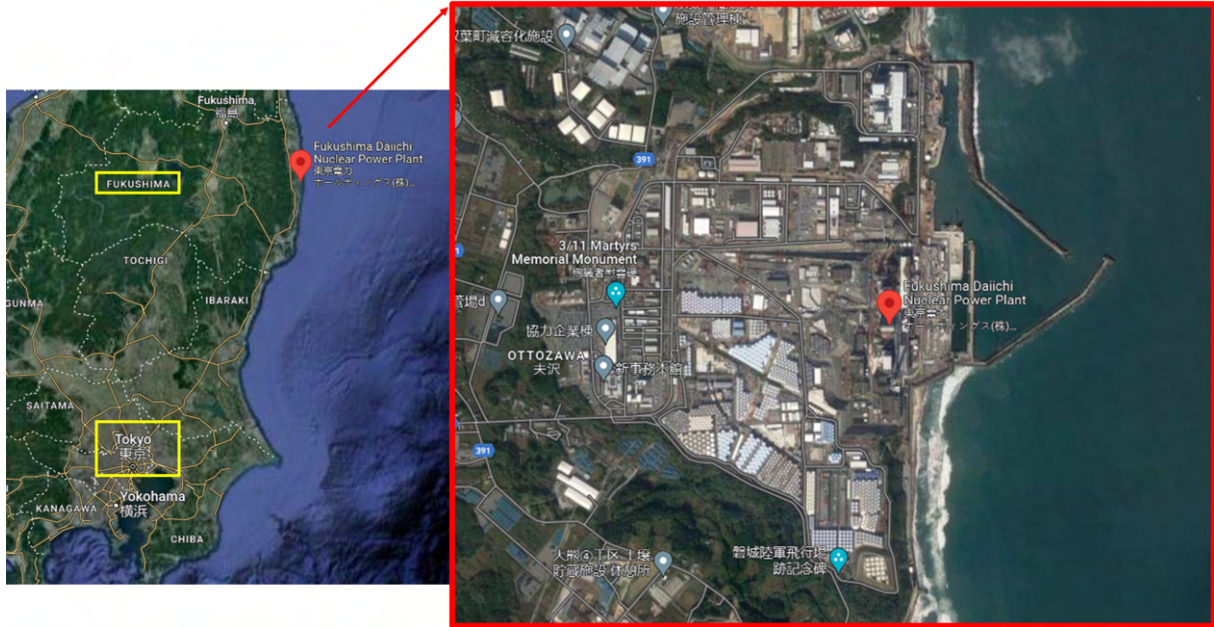


Fig. II.13.13: Google map view of Fukushima Daiichi nuclear power plant.

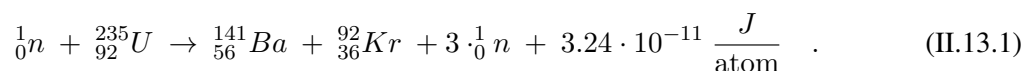
vessels were breached. Hydrogen was released from the reactor pressure vessels, leading to explosions inside the reactor buildings in Units 1, 3 and 4 that damaged structures and equipment and injured personnel.

Radionuclides were released from the plant to the atmosphere and were deposited on land and on the ocean. There were also direct releases into the sea. People within a radius of 20 km of the site and in other designated areas were evacuated, and those within a radius of 20–30 km were instructed to shelter before later being advised to voluntarily evacuate. Restrictions were placed on the distribution and consumption of food and the consumption of drinking water.

As a graphical summary, Fig. II.13.14 shows the number of overexposed accidents and overexposed people affected by these accidents, extracted from Ref. [14]. The relevant number of accidents and people involved in accidents related to medical interventions (“radiation therapy” and “Fluoroscopy”) is remarkable.

II.13.2.3 Nuclear reaction

From time to time the ionising radiation hazard in a particle accelerator environment is compared and weighted with the one in a nuclear reactor. It is out of the scope of this chapter to cover the nuclear reactor principles and technology. However, it is essential to highlight two main aspects that differentiate the same hazard in the two environments: the energy involved and the operational aspects. For the first one, the radiation effects in a nuclear reactor are based on a self-maintained nuclear reaction where very heavy atoms are involved. In the case of the U-235 reactors, the self-maintained reaction is given by Eq. (II.13.1)



II.13.2. Radiation safety background

Industrial Radiation therapy Fluoroscopy Orphan source Military Other & unknown

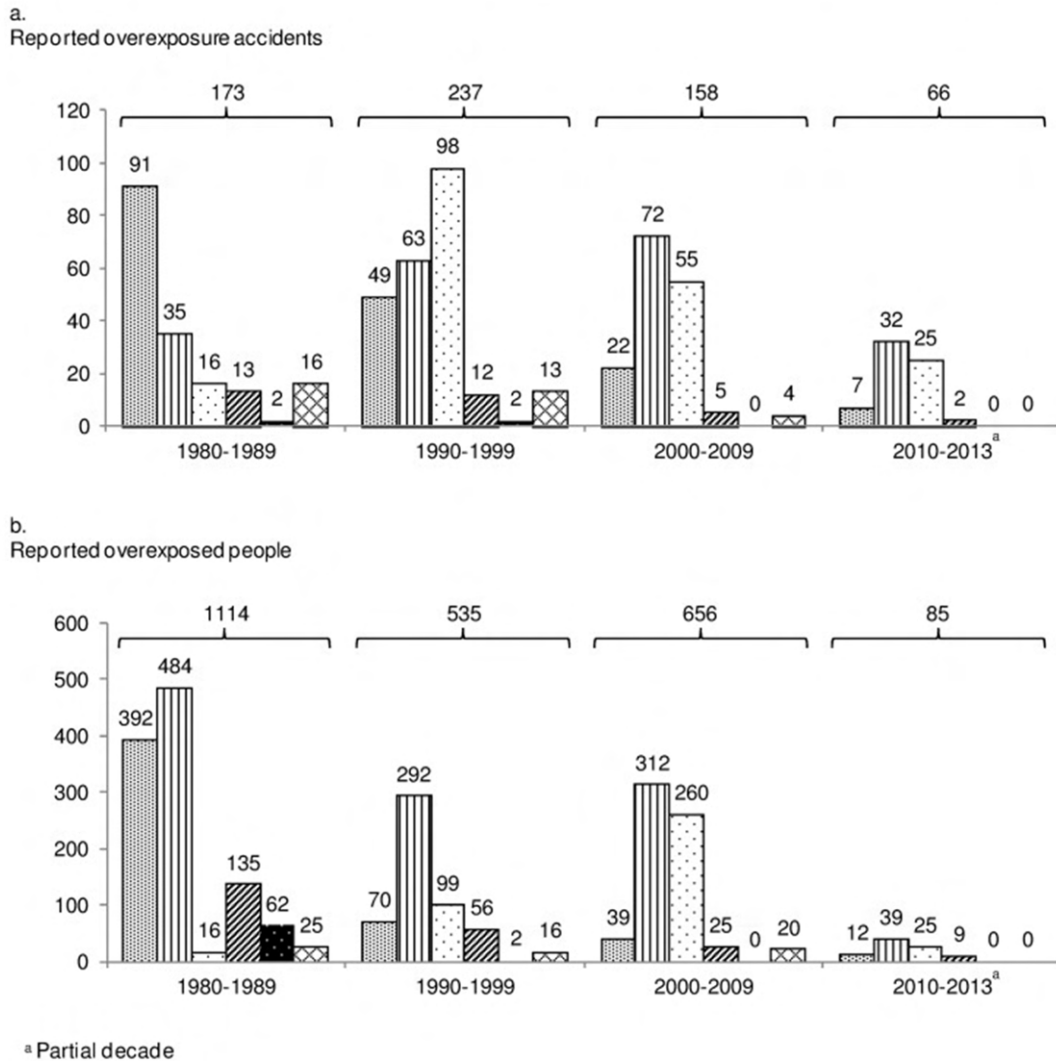


Fig. II.13.14: Number of reported accidents and overexposed people in the period 1980-2013, where the Chernobyl and Fukushima accidents occurred.

If we consider one mol of ${}_{92}^{235}\text{U}$

$$6.023 \cdot 10^{23} \frac{\text{atom}}{\text{mol}} \times 3.24 \cdot 10^{-11} \frac{\text{J}}{\text{atom}} = 19.5 \frac{\text{TJ}}{\text{mol}} ,$$

with 1 mol of ${}_{92}^{235}\text{U}$ is ~ 235 g of ${}_{92}^{235}\text{U}$.

Critical mass is defined as the smallest amount of the fissile material needed for a sustained nuclear chain reaction, and in the case of ${}_{92}^{235}\text{U}$ it is 52 kg.

Secondly, from the operational point of view and compared with a particle accelerator, a nuclear reactor is not easy to switch off because of the self-sustained chain reaction, where 1 neutron is needed for a reaction to occur, but 3 new neutrons are generated every time. Also, a large mass of highly activated material inside the reactor vessel produces high radioactive contamination (as solid, liquid and gas).

II.13.2.4 International organizations

Since the spread and wide use of radiation equipment and radioactive sources, it was clear the necessity of creating international organizations to support, monitor and control the practices where the ionising hazards were involved.

The uncontrolled and overwhelming destruction power of the two nuclear bombs, the unprecedented consequences of this new technology applied as a war weapon, and the high risk of being used again over any largely populated area showed that an international agreement had to be reached to limit its production.

Currently, there are a lot of international organisations that can be classified depending on the involvement of their respective governments. This document focuses on non-government organisations where professional-scientific recommendations are their primary objective.

II.13.2.4.1 Governmental bodies

There are two main government-related organisations: the United Nations Scientific Committee on the Effects of Atomic Radiation—UNSCEAR [15] and the International Atomic Energy Agency-IAEA [16].

The UNSCEAR was established in 1955 by the General Assembly of the United Nations—UN in response to widespread concerns about the effects of radiation on human health and the environment.

Following its mandate given by the General Assembly, UNSCEAR undertakes scientific evaluations of sources of ionising radiation and of the associated exposures, effects and risks to human health and the environment and provides an independent, objective and up-to-date scientific basis for radiation safety. Currently (2023), 193 nations adhere to the UN. There are two essential documents produced by UNSCEAR, “Sources, effects and risks of ionising radiation” (2017) [17] and “Hereditary effects of radiation” (2001) [18].

The IAEA was created two years later, in 1957, in response to the deep fears and expectations generated by the discoveries and diverse uses of nuclear technology. The Agency’s genesis was U.S. President Eisenhower’s “Atoms for Peace” address to the United Nations General Assembly on 8 December 1953. It was set up as the world’s “Atoms for Peace” organization within the United Nations family. From the beginning, it was mandated to work with its Member States and multiple partners worldwide to promote safe, secure and peaceful nuclear technologies. The IAEA’s dual mission is to encourage and control the atomic energy to peace.

II.13.2.4.2 Non-government related organisations

The leading non-government-related organisations are the International Commission on Radiological Protection-ICRP [19], the International Commission on Radiation Units and Measurements-ICRU [20], and the International Radiation Protection Association-IRPA [21].

ICRP was established in 1928 at the second International Congress of Radiology to respond to growing concerns about the effects of ionising radiation being observed in the medical community. At the time it was called the International X-ray and Radium Protection Committee (IXRPC). Subsequently, it was restructured to take better account of the uses of radiation outside the medical area and given its present name in 1950. It is an independent, international organisation that advances for the public benefit

the science of radiological protection, in particular by providing recommendations and guidance on all aspects of protection against ionising radiation.

It was established as a charity (not-for-profit organisation) registered with the Charity Commission of England and Wales. It is formed by a community of more than 250 globally recognised experts in radiological protection science, policy, and practice from more than 30 countries. Originally, ICRP published its recommendations and advice as papers in various scientific journals in medicine and physics. Since 1959, ICRP has had its own series of publications, from 1977 in the shape of a scientific journal, “Annals of the ICRP”. One of its latest documents is “The 2007 Recommendations of the International Commission on Radiological Protection” [22] (see next Section II.13.2.4.3).

The ICRU (originally known as the International X-Ray Unit Committee and later as the International Committee for Radiological Units) was conceived at the First International Congress of Radiology (ICR) in London in 1925 and officially came into being at ICR-2 in Stockholm in 1928. The primary objective was to propose a unit for measurement of radiation as applied in medicine. From 1950 the ICRU expanded its role significantly to embrace a wider field. Its mission statement is to develop and promulgate internationally accepted recommendations on radiation related quantities and units, terminology, measurement procedures, and reference data for the safe and efficient application of ionising radiation to medical diagnosis and therapy, radiation science and technology, and radiation protection of individuals and populations.

The IRPA is an independent non-profit association of national and regional radiation protection societies, and its mission is to advance radiation protection worldwide. It is the international professional association for radiation protection. IRPA is an observer on the IAEA Radiation Safety Standards Committee-RASSC [23]. It was formed in 1965 at a meeting in Los Angeles, stimulated by the desire of radiation protection professionals to have a worldwide body. Membership includes 50 Associate Societies covering 65 countries.

II.13.2.4.3 ICRP recommendations

The ICRP is an advisory body that offers its recommendations to regulatory and advisory agencies, mainly by providing guidance on the fundamental principles on which appropriate radiological protection can be based.

Since 1928, ICRP has regularly issued recommendations regarding protection against the hazards of ionising radiation.

The first report in the current series, Publication 1 [24], contained the recommendations adopted in 1958. The more recent recommendations have appeared as Publication 26 [25], and Publication 60 [26], and contain the recommendations adopted in 1977 and 1990, respectively. The latest recommendations are included in “The 2007 Recommendations of the International Commission on Radiological Protection” [22].

In this paragraph two main concepts are collected from its 2007 recommendations: the types of exposure situations and the principles of radiological protection.

According to ICRP there are **3 types of exposure situations** which are intended to cover the entire range of exposure situations: planned exposure situations, which are situations involving the planned

introduction and operation of sources, it includes situations that were previously categorised as practices; emergency exposure situations, which are unexpected situations such as those that may occur during the operation of a planned situation or from a malicious act, requiring urgent attention; existing exposure situations, which are exposure situations that already exist when a decision on control has to be taken, such as those caused by natural background radiation.

Also, ICRP continues to distinguish amongst three categories of exposure (depending on the person affected): occupational exposures, public exposures, and medical exposures of patients (and comforters, carers, and volunteers in research).

If a female worker has declared that she is pregnant, additional controls have to be considered in order to attain a level of protection for the embryo/fetus broadly similar to that provided for members of the public.

From the ICRP point of view there are **three key principles of radiological protection**: the principle of justification, any decision that alters the radiation exposure situation should do more good than harm; the principle of optimisation of protection, the likelihood of incurring exposure, the number of people exposed, and the magnitude of their individual doses should all be kept as low as reasonably achievable (ALARA), taking into account economic and societal factors; and the principle of application of dose limits, the total dose to any individual from regulated sources in planned exposure situations other than medical exposure of patients should not exceed the appropriate limits specified by ICRP.

The principles of justification and optimisation apply in all three exposure situations whereas the principle of application of dose limits applies only for doses expected to be incurred with certainty as a result of planned exposure situations.

II.13.3 Dose magnitudes

II.13.3.1 Definitions

II.13.3.1.1 Ionising radiation

Ionising radiation is the transported energy (as a particle or wave) capable of removing an electron from an atom (or molecule). The ionised atom is directly ionised if charged particles, such as electrons and protons, are involved in this process. However, if the particle is not charged, like neutrons and photons, the ionised atom is ionised indirectly.

The most common ionising radiation particles are such as alpha particles (He nuclei, formed by 2 protons plus 2 neutrons), electrons (also called beta particles if they are produced in the nuclei), neutrons and photons (either “X” or “ γ ” rays).

The energy needed to remove an electron from an atom is of the order of 10 eV, if it is given in SI units $1.6022 \cdot 10^{-18}$ J ($1 \text{ eV} = 1.6022 \cdot 10^{-19}$ J).

II.13.3.1.2 Ionisation potential

The ionisation potential, also called ionisation energy, is the amount of energy required to remove an electron from an isolated atom or molecule. Its value depends on the atom itself and the position of the electron inside the atom. Table II.13.1 shows the ionising potentials for the most external electron for

five typical atoms.

Table II.13.1: List of lowest ionisation potentials (in eV) for some relevant atoms.

Element	Ionisation potential (eV)
Carbon - C	11.260
Oxygen - O	13.618
Potassium - K	4.341
Iron - Fe	7.870
Lead - Pb	7.416

II.13.3.1.3 Energy, frequency, and wavelength relationship

In case of ionisation radiation from electromagnetic spectrum nature (photons), the ionisation potential can be expressed as the energy, frequency or wavelength of the radiation and is given by Eq. (II.13.2)

$$E = h \cdot \nu = h \cdot \frac{c}{\lambda} \quad , \quad (\text{II.13.2})$$

where $h = 6.626 \cdot 10^{-34}$ J·s is Planck's constant, and $c = 2.998 \cdot 10^8$ m·s⁻¹ is the speed of light in vacuum. In the case of the hard ultraviolet radiation,

$$E = 12.4 \text{ eV} \leftrightarrow \nu = 2.998 \cdot 10^{15} \text{ Hz} \leftrightarrow \lambda = 100 \text{ nm} .$$

II.13.3.1.4 Material activity (A), radionuclide decay law and units

Material activity (A) is the expected value of the number of nuclear transformations occurring in a given quantity of material per unit time. The SI unit of activity is per second (s⁻¹) and its special name is becquerel (Bq). Because the Bq is a tiny unit, sometimes the non-SI unit curie (Ci) is used

$$1 \text{ Ci} = 3.7 \cdot 10^{10} \text{ Bq} .$$

The number of radionuclides decay as a function of time ($N(t)$) follows Eq. (II.13.3)

$$\frac{dN(t)}{dt} = -\lambda \cdot N(t) \quad , \quad (\text{II.13.3})$$

where λ is the decay constant or decay rate (s⁻¹). The solution is given by Eq. (II.13.4)

$$N(t) = N(0) \cdot e^{-\lambda \cdot t} \quad , \quad (\text{II.13.4})$$

where $N(0)$ is the initial number of radionuclides, $N(t)$ is the number of radionuclides at time t , $\tau \equiv 1/\lambda$ is the radionuclide mean lifetime (it is the time needed to reduce the initial value $N(0)$ a factor- e ($\frac{N(0)}{e}$)), and $t_{1/2} = \frac{\ln(2)}{\lambda} = \tau \cdot \ln(2)$ is the radionuclide half-life, it is the time needed to reduce the initial value $N(0)$ by a factor of 2 ($\frac{N(0)}{2}$).

II.13.3.1.5 Fluence— Φ

The **fluence** is the quotient of the number of particles that cross an area “ a ” by the value of the area “ a ”, in a differential way (in SI, [particles/m²]). It is expressed by Eq. (II.13.5)

$$\Phi = \frac{dN}{da} \quad . \quad (\text{II.13.5})$$

A graphical representation is shown in Fig. II.13.15.

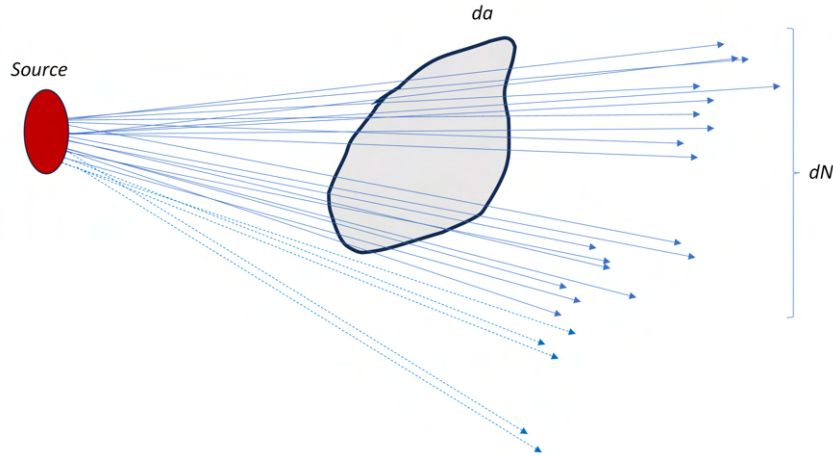


Fig. II.13.15: Schematic fluence representation.

The fluence follows the scaling of $1/r^2$, where “ r ” is the distance to the source. Fluence is one quantity that defines the radiation source, and it is one of the radiometric quantities.

II.13.3.1.6 Exposure

The **exposure** is the action where a body experiences a fluence of particles after a given period.

II.13.3.1.7 Absorbed dose- D

The **absorbed dose- D** is the fundamental dose quantity given by Eq. (II.13.6)

$$D = \frac{d\bar{\epsilon}}{dm} \quad , \quad (\text{II.13.6})$$

where $d\bar{\epsilon}$ is the mean energy imparted to matter of mass dm by a given ionising radiation. The SI unit for absorbed dose is joule per kilogram (J kg⁻¹) and its special name is Gray (Gy). Also another common unit is “rad”, where 1 rad = 0.01 Gy.

The absorbed dose rate \dot{D} is given by Eq. (II.13.7)

$$\dot{D} = \frac{dD}{dt} = \frac{d^2\bar{\epsilon}}{dt dm} \quad . \quad (\text{II.13.7})$$

The absorbed dose is one of the quantities that provide a measure of the absorbed dose by a body, and it is one of the dosimetric quantities.

II.13.3.1.8 Absorbed organ dose— D_T

If the mass- m_T refers to an organ from a human body, the absorbed organ dose is calculated as follows

$$D_T = \frac{1}{m_T} \cdot \int_{m_T} D \cdot dm \quad . \quad (\text{II.13.8})$$

II.13.3.1.9 Dose equivalent- H

The **dose equivalent- H** is the product of D and Q at a point for a given tissue- T (if it refers to an organ it is called tissue or **organ equivalent dose**), where D is the absorbed dose by the tissue- T and Q (or w_R) is the radiation weighting factors for a given radiation- R at this point (see Table II.13.2 for values), thus follows Eq. (II.13.9)

$$H_{T,R} = D_T \cdot Q = D_{T,R} \cdot w_R \quad , \quad (\text{II.13.9})$$

where

$$w_R = \begin{cases} 2.5 + 18.2 \cdot e^{-[\ln(E_n)]^2/6} & \text{for } E_n < 1 \text{ MeV} \\ 5.0 + 17.0 \cdot e^{-[\ln(2 \cdot E_n)]^2/6} & \text{for } 1 \text{ MeV} \leq E_n \leq 50 \text{ MeV} . \\ 2.5 + 3.25 \cdot e^{-[\ln(0.04 \cdot E_n)]^2/6} & \text{for } E_n > 50 \text{ MeV} \end{cases} \quad (\text{II.13.10})$$

The unit of dose equivalent is Joule per kilogram (J kg^{-1}), and its special name is **sievert (Sv)**. Also another common unit is “rem”, where $1 \text{ rem} = 0.01 \text{ Sv}$. The dose equivalent is one of the protection quantities.

Table II.13.2: Radiation weighting factors values (w_R) given by ICRP [22].

Radiation type	Radiation weighting factor, w_R
Photons (all energies)	1
Electrons and muons	1
Protons and charged pions	2
Alpha particles, fission fragments, heavy ions	20
Neutrons	Depending on the neutron energy E_n , see Eq. (II.13.10)

If an organ (T) is irradiated with more than one type of radiation, Eq. (II.13.9) is written as follows

$$H_T = \sum_{R_i} D_{T,R_i} \cdot w_{R_i} \quad . \quad (\text{II.13.11})$$

This quantity is used as a dose limit for workers (operational quantity).

II.13.3.1.10 Effective dose- E

The **effective dose- E** is the calculated dose from the tissue-weighted sum of the equivalent doses in all specified tissues (T_i) and organs of the body and for all the radiation considered (R_i), given by

$$E = \sum_{T_i} w_{T_i} \cdot \left(\sum_{R_i} D_{T,R_i} \cdot w_{R_i} \right) = \sum_{T_i} w_{T_i} \cdot H_{T_i} \quad , \quad (\text{II.13.12})$$

where

$$H_{T_i} = \sum_{R_i} D_{T,R_i} \cdot w_{R_i}$$

is the equivalent dose in a tissue or organ T_i , and w_{T_i} is the tissue weighting factor (see Table II.13.3 for values). The unit for the effective dose is the same as for absorbed dose, $\text{J} \cdot \text{kg}^{-1}$, and its special name is **sievert (Sv)**. D_{T_i,R_i} is the absorbed dose of a radiation R_i in the tissue T_i .

The Sievert is the dose unit for the equivalent and the effective dose. Effective dose is one of the protection quantities used to control the exposure to the workers.

Table II.13.3: Tissue weighting factor given by ICRP [22].

Tissue	w_T	$\sum w_T$
Bone-marrow (red), Colon, Lung, Stomach, Breast, Remainder Tissues ¹	0.12	0.72
Gonads	0.08	0.08
Bladder, Oesophagus, Liver, Thyroid	0.04	0.16
Bone surface, Brain, Salivary glands, Skin	0.01	0.04
Total		1.00

¹ *Remainder Tissues (14 in total): Adrenals, Extrathoracic (ET) region, Gall bladder, Heart, Kidneys, Lymphatic nodes, Muscle, Oral mucosa, Pancreas, Prostate, Small intestine, Spleen, Thymus, Uterus/cervix.*

The tissue weighting factors w_{T_i} proposed in Table II.13.3 have changed depending on the radiation detriment studies since 1977. In Table II.13.4 the values proposed by ICRP in 1977 and 1991 are given, showing in some cases the big difference across the years.

II.13.3.1.11 Ambient dose equivalent— $H^*(10)$

The **ambient dose equivalent**—($H^*(10)$) is the dose equivalent at a point in a radiation field that would be produced by the corresponding expanded and aligned field in the ICRU sphere ² at a depth of 10 mm on the radius vector opposing the direction of the aligned field. The unit of ambient dose equivalent is joule per kilogram ($\text{J} \cdot \text{kg}^{-1}$) and its special name is **sievert (Sv)**. It is one of the operational quantities (they are used in practical applications for monitoring and investigating situations involving external exposure, and they are defined for measurements and assessment of doses in the body).

II.13.3.1.12 Human phantoms

The **human phantoms** are the reference values for the size and composition of the organs provided by ICRP which helps with the evaluation of the transport of ionising radiation within the body and its energy

²The ICRU sphere is a sphere of tissue-equivalent material (30 cm in diameter, ICRU (soft) tissue with density of $1 \text{ g} \cdot \text{cm}^{-3}$, and mass composition: 76.2% oxygen, 11.1% carbon, 10.1% hydrogen, and 2.6% nitrogen). For radiation monitoring, in most cases it adequately approximates the human body as regards the scattering and attenuation of the radiation fields under consideration.

Table II.13.4: Tissue weighting factor given by ICRP in Pub. 26 (1977) [25] and Pub. 60 (1991) [26].

Tissue	Tissue weighting factor (w_T)	
	1977	1991
	<i>Publication 26</i>	<i>Publication 60</i>
Bone surfaces	0.03	0.01
Bladder		0.05
Breast	0.15	0.05
Colon		0.12
Gonads	0.25	0.20
Liver		0.05
Lungs	0.12	0.12
Oesophagus		0.05
Red bone marrow	0.12	0.12
Skin		0.01
Stomach		0.12
Thyroid (each)	0.03	0.05
Remainder	0.30	0.05
Total	1.0	1.0

deposition in organs and tissues.

II.13.3.2 Effects of the ionisation radiation

II.13.3.2.1 DNA modification

The deoxyribonucleic acid, shortly DNA, is a polymer (formed by hydrogen-H, oxygen-O, nitrogen-N, carbon-C and phosphorus-P) composed of two polynucleotide chains that coil around each other to form a double helix. The polymer carries genetic instructions for developing, functioning, growing and reproducing all known organisms and many viruses.

Ionising radiation can damage the DNA (known as mutagen). This type of radiation can produce physical or chemical changes in the DNA, producing cell death (early or deterministic effect) or cell transformation (stochastic effect). The type of DNA damage produced depends on the type of mutagen. Because of inherent limits in the DNA repair mechanisms, if humans lived long enough, they would all eventually develop cancer. In particular, the ionising radiation effects on DNA, such as the induction of complex forms of DNA double-strand breaks, and the problems experienced by cells in correctly repairing these complex forms of DNA damage, and the consequent appearance of gene/chromosomal mutations, can lead to cancer on the exposed person or develop hereditary effect.

II.13.3.2.2 Relationship between effective dose and health detriment probability

The health detriment of ionising radiation depends on the dose received and the exposure time. In cases where a very high (lethal) dose of 5 Gy is received in a very short time (one minute), the consequences are fatal, and survival is improbable, as was experienced by the Chernobyl workers involved at the very beginning of the accident.

The probability of developing cancer or hereditary effects is proportional to the dose received and the exposure time. An extremely low dose (20 mSv) received in a year will have a minimal effect on an exposed person so other mutagens will have a more critical impact on the health detriment.

Table II.13.5 presents the influence of the dose received on the probability of an impact on the health detriment effect.

Table II.13.5: A list of the probability per Sv received in the health effect.

Effect	Population	Exposure	Probability/Sv	20 mSv Case
Hereditary effects	Whole population	Lifetime	1.0%	0.02%
Fatal cancer	Whole population	Lifetime	5.0%	0.10%
	Working population	Age 18-65	4.0%	0.08%
Health detriment	Whole population	Lifetime	7.3%	0.15%
	Working population	Age 18-65	5.6%	0.11%

ICRP [22] recommends that members of the public, for radiological protection purposes, be subject to the public dose limit of (effective dose) 1 mSv/year. This is a tiny amount of absorbed energy because it is 1,000 times smaller than 0.25 calories/kg (1 Sv = 1 J/kg).

Regarding effective dose rate, assuming a worker is exposed to 1 mSv in a year (2,000 hours/year), it is 0.5 μ Sv/h, which means 4 μ Sv in a working day.

To get a reference of how large 1 mSv/year is, let's take the case of a smoker; the tobacco plant contains Po210, an alpha emitter. The dose absorbed per cigarette (intake dose) is \sim 1.2 μ Sv/cigarette, and if a cigarette lasts 5 minutes, the dose rate is \sim 14.4 μ Sv/h (almost 30 times higher than a public dose rate). Assuming that this smoker takes 20 cigarettes/day, after a year, the smoker will smoke 7,300 cigarettes, and his lungs will receive a yearly dose of 8.8 mSv, and after 10 years, about 90 mSv. According to the values given in Table II.13.5, this activity will increase the probability of getting fatal cancer by 0.7%, not considering the effects of nicotine as a mutagen.

II.13.3.3 Classified workers and designated zones

II.13.3.3.1 Dose limits principle

To minimise as low as reasonably achievable (ALARA) the detrimental effect of the ionising radiation, ICRP [22] recommends that the appropriate limits of the total dose should not exceed any individual planned exposure situations from regulated sources other than medical exposure of patients. Regulatory dose limits are determined by the regulatory authority, taking account of international recommendations, and apply to workers and to members of the public in planned exposure situations.

II.13.3.3.2 Classified workers

The ICRP [22] recommends using the effective dose for assessing exposure and controlling stochastic effects for regulatory purposes. It can be used to demonstrate compliance with dose limits and for dose records.

Effective dose provides a convenient quantity for the assessment of overall radiation exposure,

taking account of all exposure pathways, internal and external, for dose record keeping and regulatory purposes. Dose limits apply only in planned exposure situations but not to medical exposures of patients.

Within a category of exposure, occupational or public, dose limits apply to the sum of exposures from sources related to practices that are already justified. For occupational exposure in planned exposure situations, the limit should be expressed as an effective dose of 20 mSv per year, averaged over defined 5 year periods (100 mSv in 5 years), with the further provision that the effective dose should not exceed 50 mSv in any single year.

For public exposure in planned exposure situations, the recommendation is expressed as an effective dose of 1 mSv in a year. However, in special circumstances a higher value of effective dose could be allowed in a single year, provided that the average over defined 5-year periods does not exceed 1 mSv per year (see Table II.13.6).

Table II.13.6: Occupational dose limits for exposed workers recommended by ICRP [22].

Type of limit	Occupational	Public
Effective dose	20 mSv per year (averaged over defined periods of 5 years)	1 mSv in a year
Annual equivalent dose in:		
Lens of the eye	150 mSv	15 mSv
Skin	500 mSv	50 mSv
Hands and feet	500 mSv	—

Under the public category, ICRP [22] pays special attention to pregnant women, particularly the embryo/fetus case, with a limit of 1 mSv in total (radiation and intakes).

All the countries have adopted all these dose limit recommendations in their regulations. However, it is a common practice for all the regulators to split the two exposed categories, occupational and public, in five. This practical approach allows better monitoring and control for all the exposed workers and the general public.

The five categories of total body (radiation and intake) effective doses are as follows: exposed workers (Category A), their maximum dose of 50 mSv per official year (100 mSv for five years, 20 mSv average per year); exposed workers (Category B), their maximum dose of 6 mSv per official year; non-exposed workers, their maximum dose is 1 mSv per official year; women during pregnancy (fetus limit) their maximum dose is 1 mSv; and general public, their maximum dose is 1 mSv per official year.

All the values above are taken with the natural background subtracted in an official calendar year (from 1st January to 31st December).

II.13.3.3.3 Designated areas

One way of controlling the total dose received by any worker from regulated sources in planned exposure situations is to divide the working areas depending on the level and the type of risk. ICRP [22] defines the affected areas as follows:

- Controlled area: a defined area in which specific protection measures and safety provisions are, or could be, required for controlling normal exposures or preventing the spread of contamination

during normal working conditions and preventing or limiting the extent of potential exposures. A controlled area is often within a supervised area, but need not be. Workers in “controlled areas” of workplaces should be well informed and specially trained and form a readily identifiable group. Such workers are most often monitored for radiation exposures incurred in the workplace and occasionally may receive special medical surveillance;

- Supervised area: it is a defined area not designated as a controlled area but for which occupational exposure conditions are kept under review, even though no specific protection measures or safety provisions are usually needed.

From the regulatory point of view, the area designation follows the ICRP [22] recommendations, being more specific on the total (radiation and intake) annual dose that a worker might receive:

- Controlled area: a worker could receive more than 6 mSv per official calendar year. This area is divided into:
 - Limit access area: a worker could receive up to 100 mSv (in 5 official calendar years or 50 mSv in a single year),
 - Ruled access area: a worker could be exposed to a high dose rate in a very short time (with 100 mSv limit in 5 official calendar years or 50 mSv in a single year),
 - Prohibited access area: a worker could be exposed to a very high dose in a single exposition (with 100 mSv limit in 5 official calendar years or 50 mSv in a single year).
- Supervised area: a worker could receive less than 6 mSv per official calendar year.

All the above values are with the natural background subtracted.

If we assume that the worker is exposed 2 000 hours per year, the corresponding dose rates in each designated area are:

- Controlled area: a worker could receive more than 6 mSv per official calendar year. This area is divided into:
 - Limit access area: a worker is exposed to dose rates between 25 μ Sv/h to 100 μ Sv/h,
 - Ruled access area: a worker is exposed to dose rates between 100 μ Sv/h to 25 mSv/h,
 - Prohibited access area: a worker is exposed to dose rates higher than 25 mSv/h,
- Supervised area: a worker is exposed to dose rates between 0.5 μ Sv/h to 3.0 μ Sv/h.

Table II.13.7 presents some indicative values of the effective dose. On average, the values are far below the dose limits recommended by ICRP [22].

II.13.3.4 Background radiation

Generally speaking, background radiation refers to any external radiation to the system under study. It can be related to any part of the electromagnetic spectrum (from the radio to the gamma radiation) or any atomic or subatomic particle.

Table II.13.7: Average effective doses to workers depending on the industrial activity.

Radiation source	Number of workers	Average dose (mSv per year)
Enhanced natural sources		
Mining (excluding coal)	760,000	2.7
Coal mining	3,900,000	0.7
Air travel (crew)	250,000	3
Mineral processing	300,000	1.0
Above ground workplaces (radon)	1,250,000	4.8
Total	6,500,000	1.7

According to ICRP [22], background radiation is the existing exposure situation, and a decision on control has to be taken. The IAEA [5] refers to background radiation as “the dose or dose rate (or an observed measure related to the dose or dose rate) attributable to all sources other than the one(s) specified. Strictly speaking, this applies to measurements of dose rate or count rate from a sample, where the background dose rate or count rate must be subtracted from all measurements. However, background is used more generally, in any situation in which a particular source (or group of sources) is under consideration, to refer to the effects of other sources. It is also applied to quantities other than doses or dose rates, such as activity concentrations in environmental media”.

In this chapter, background radiation refers to the ionising radiation in the volume of the space where we will put our system to be studied. It can be expressed as the radiation dose (or dose rate) in the volume of the space considered from natural and artificial (man-made) backgrounds.

II.13.3.4.1 Natural background

The natural background source related to a person under consideration can be external or internal (see typical values per person in Table II.13.8).

Table II.13.8: Typical dose values from natural background sources.

Source	Effective dose (mSv average per year)	Typical range (mSv per year)
External exposure		
Cosmic rays	0.4	0.3–1.0
Terrestrial gamma rays	0.5	0.3–0.6
Internal exposure		
Inhalation	1.2	0.2–10
Ingestion	0.3	0.2–0.8
Total	2.4	1–10

The external radiation contribution is coming from:

- Cosmic radiation,
- Radiation from the soil: natural radioactive material in rocks and soil,
- Radiation from building materials: is mainly from radon (Rn-222) gas.

The internal radiation comes from:

- The food and drinks: K-40 and C-14,
- The gases in the air: mainly from radon (Rn-222) gas and Po-210 (smokers).

The external background radiation received per person depends strongly on where the person lives. Geographically, in Western Europe, there are regions where the annual dose can be higher than 10 mSv, and others where it can be lower than 1.3 mSv (see Fig. II.13.16).

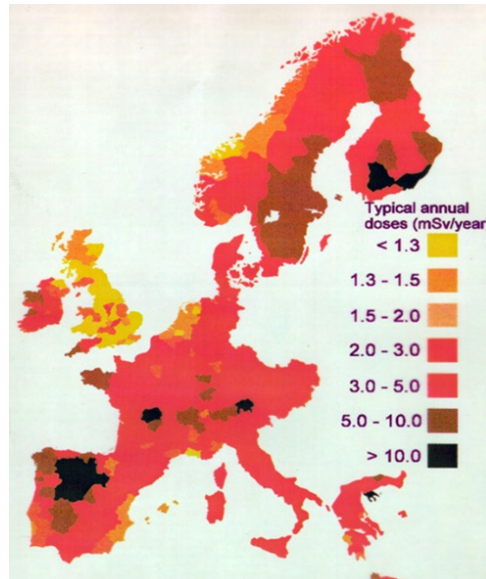


Fig. II.13.16: Typical annual doses from natural background radiation exposure in Western Europe.

II.13.3.4.2 Artificial background

The artificial background radiation caused by the human activity comes from three main sources:

- Nuclear reactor accidents: special impact caused by Chernobyl in 1986 and Fukushima 2011 (in a range of 10 to 50 mSv over 20 years),
- Nuclear weapon tests: the fallout typically contains hundreds of different radionuclides which last for more than 30 years (Am-241, Cs-137, I-131 and Sr-90),
- Medical practice: for radiodiagnosis (X-ray images) or radiotherapy treatments (external or internal).

Figure II.13.17 compares the natural and artificial background radiation from different human activities, showing the relative impact of the medical intervention growth, the nuclear weapon tests after WWII and the nuclear reactor accidents.

II.13.4 Radiation sources

The most critical aspect of radiation safety is the radiation source (i.e. ionising radiation) definition and how this source affects an individual, a group of people and the environment. ICRP [22] gives a very broad definition of radiation source as “any physical entity or procedure that results in a potentially

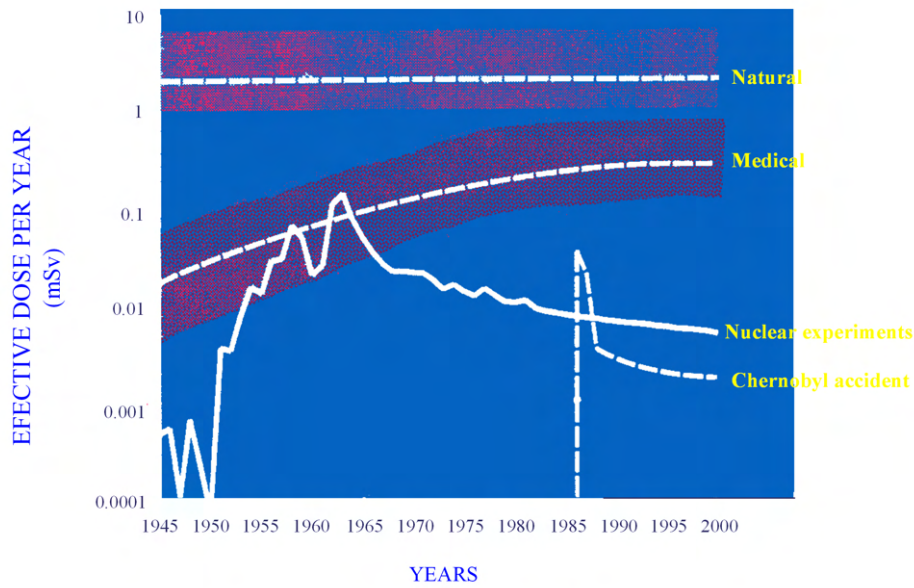


Fig. II.13.17: Comparison of the natural vs artificial background radiation from the different human interventions.

quantifiable radiation dose to a person or group of persons”. However, IAEA [5] is more specific in its definition, mainly because it emphasizes radiation sources as material or substance in a way that it is “anything that may cause radiation exposure—such as by emitting ionising radiation or by releasing radioactive substances or radioactive material—and can be treated as a single entity for purposes of protection and safety”. And IAEA is even more restricted when it defines the (radiation) source term, as “the amount and isotopic composition of radioactive material released (or postulated to be released) from a facility”, considering only the radioactive material case.

In the case of the accelerator technology, we must use the broader definition of the radiation source and source term provided by ICRP because releasing radioactive material is not always the main contribution to the radiation source; more often, the contrary.

There are a lot of parameters that define the radiation source term in each accelerator, and they can be categorised in three aspects [27]- [30]:

- The accelerator geometry: Linear or circular based,
- The accelerated particle (or particles),
- Its purpose: irradiator, collider, injector/booster/storage beam, transfer beam, neutron spallation, etc.

In an ideal world, theoretically, the radiation source term from any accelerator would be very small or residual. In this case, the ideal beam will follow the theoretical orbit and its interaction (collision) with its environment would be almost impossible. However, the losses of the accelerated particles are, in general, higher than expected and in consequence, the radiation source term is not a trivial quantity to calculate or estimate.

In particular, in the case of synchrotron light source and neutron spallation source accelerators, the radiation source term does not come only from the synchrotron radiation in the beamlines or the neutrons produced by spallation reactions in the target and guided to the beamlines. In both scenarios, the radiation source term is a complex and extended source where the production of radioactivated material plays a significant contribution.

To understand the radiation source term in any accelerator, it is necessary to understand how the main particles involved interact with the accelerator components, producing secondary radiations or creating unstable nuclei (activation process).

II.13.4.1 Particles: basic properties

Electrons, positrons, protons, and neutrons are the most relevant particles for radiation safety in accelerators (see Table II.13.9). There are other particles, such as alpha (He nuclei, $2p^+ + 2n$), beta- β (e^-), and muons- μ (μ^+ , μ^-), that also contribute to the total dose, but they are not going to be treated in this chapter.

Table II.13.9: Main physical characteristics of the main particles in radiation safety accelerators field.

Particle	Symbol	Charge [C]	Rest Mass	
			[kg]	[MeV]
Electron	e^-	$-1.602 \cdot 10^{-19}$	$9.11 \cdot 10^{-31}$	0.511
Positron	e^+	$+1.602 \cdot 10^{-19}$	$9.11 \cdot 10^{-31}$	0.511
Proton	p^+	$+1.602 \cdot 10^{-19}$	$1.67 \cdot 10^{-27}$	938.27
Photon	γ	0	0	0
Neutron	n	0	$1.68 \cdot 10^{-27}$	939.57

All the atoms are characterized by their atomic numbers, which are as follows:

- Mass number – A (or nucleons number): it is given by the number of protons and neutrons (called nucleons) in the atom,
- Atomic number – Z (or charge number): it is given by the number of proton and electrons (in a neutral atom),
- Neutron number – N : it is given by the number of neutrons.

They follow the relationship given by Eq. (II.13.13)

$$A = Z + N \quad . \quad \text{(II.13.13)}$$

Depending on these numbers, the atoms are classified as:

- Isotopes: if they have the same atomic number (Z), such as He-3 and He-4.
- Isobars: if they have the same mass number (A), such as S-40, Cl-40, Ar-40, K-40, and Ca-40.
- Isotones: if they have the same number of neutrons (N), such as B-12, C-13, N-14, and O-15.
- Isodiaphers: if the difference between proton and neutrons is the same ($N-Z$), such as C-13, N-15, and O-17.

- Isomers: if they have all the above numbers the same (Z , A , N & $(N-Z)$). The isomer decays to lower excited states or to the ground state, with the emission of gamma-ray photons. If the lifetime of a particular excited state is unusually long it is said to be isomeric, such as Tc99 and Tc99m.

II.13.4.2 Nature of radiation sources

Ionising radiation is produced in any particle accelerator when the energy of the accelerated particle is above a certain keV value. The characteristic of the radiation, intensity, energy, spatial distribution and the type of the particle depends on:

- The beam energy and intensity,
- The beam losses and their location,
- How the beam loss particle is stopped.

The accelerated particles considered in this chapter are electrons and protons, with energies in the range of tenth of keV to some GeV. The type of the particles produced are as follows:

- Photon,
- Neutron,
- e^-/e^+ ,
- Proton,
- Muon,
- Alpha,
- Ions.

The mechanism of radiation production depends on the beam particle characteristics and whether the accelerator is powered on or off. The primary mechanism of radiation production is as follows:

- Synchrotron radiation is the electromagnetic radiation (from the infrared to X-ray energies) emitted when the trajectory of the relativistic electrons (positrons) is bent.
- Solid bremsstrahlung is the electromagnetic radiation produced when the charged particles are decelerated by the collision with the atoms in solids (generally, metal components of the accelerator).
- Gas bremsstrahlung: the electromagnetic radiation produced when the charged particles are decelerated by colliding with the residual gas atoms in the vacuum chambers. This type of radiation is relevant in storage ring accelerators because the beam is kept in a closed orbit for long periods.
- Rutherford/Compton/Rayleigh photon scattering: elastic (Rutherford-Coulomb force and Rayleigh-small particles), inelastic (Compton).
- e^-/e^+ creation and annihilation process: producing two 0.511 MeV photons.
- Gamma-nuclei interaction: it produces neutrons and unstable nuclei.
- Neutron-nuclei interaction: it produces neutrons and unstable nuclei.
- Dark current & electric field structure: depending on the electromagnetic field and the material involved, it can produce X-rays and gamma rays.

- Induced activity: depending on the unstable nuclei produced, it emits any possible particle (photon, neutron, e^-/e^+ , proton, pions-muon, alpha or ions).

Table II.13.10 shows the different types of mechanisms and the accelerator component affected depending on the beam particle and if the accelerator is powered on or off.

Table II.13.10: Summary of the different types of radiation sources produced in a particle accelerator, depending on whether the accelerator is ON/OFF and the accelerated particle.

Accelerator Mode	Accelerated Particle	Particle Produced	Mechanism	At component
ON	Electron	Photon	Synchrotron radiation	Bending magnet Insertion devices
ON	Electron	Photon Neutron e^-/e^+	Solid bremsstrahlung Gas bremsstrahlung Rutherford/Compton/Rayleigh scattering e^-/e^+ Gamma-nuclei	Any component Beam dump
ON	Proton	Photon Neutron e^-/e^+ Proton Muon Alpha Ion	Solid bremsstrahlung Neutron-nuclei (and the above ones from “electrons”)	Any component Beam dump
ON	None	photon Neutron e^-/e^+	Dark current and electric field structure	RF cavity
OFF	None	Photon Neutron Electron (β) Alpha	Induced activity	Any component Beam dump Cooling circuit Airborne

II.13.4.3 Interaction of particles with the matter

To understand how ionising radiation is produced in any accelerator and how the energy is transported and reaches the human body, it is compulsory to analyse how electrons, photons, neutrons and protons interact with matter from an atomic point of view. Electrons and protons are the main particles used as primary beams, and photons and neutrons are the most important secondary particles (not charged) produced in the interactions with matter. From their interaction with matter, it is possible to know the energy deposited on it and the outcome of other particles. This interaction’s critical aspect is understanding the collision of these four particles (electrons, photons, neutrons and protons) with the atoms, the orbital electrons and the nuclei contained in the matter. To simplify the analysis, one particle from the accelerated beam and one atom (or subatomic particle) from the matter are considered in each collision.

In general, the number of collisions of the particle beam until it is incorporated in the matter is very high ($> 10^6$), as the number of particles involved in the collisions ($> 10^{23}$).

II.13.4.3.1 Electrons

When an incidental electron with energy above 1 keV interacts with matter, there are three main physical processes that might occur:

- i. Ionisation losses: inelastic collisions with orbital electrons, as a result of the interaction the incident electron loses energy,
- ii. Bremsstrahlung losses: inelastic collisions with atomic nucleus, the incident electron is losing energy by radiation (emitting photons),
- iii. Rutherford scattering: elastic collisions with atomic nucleus, the electron is deflected and keeps the initial energy.

If the incident electron interacts with a positron, it might be annihilated, emitting two 511 keV photons in opposite directions to conserve the linear momentum of the collision. On the other way around, photons with energy higher than 1.2 MeV can create pairs e^-/e^+ .

II.13.4.3.1.1 Stopping power

The stopping power of a charged particle is the quantity used to describe how relevant is the interaction of the charged particle with the material. It is characteristic of the charged particle (in this case electrons) and the material considered, and it depends on the energy of the charged particle [31].

The differential stopping power (see Eq. II.13.14) is defined as variation of the energy of the charged particle as a function of the distance of the particle in the material

$$S = \frac{dE}{dl} \quad . \quad \text{(II.13.14)}$$

It is a measure of how, as a function of the distance covered in the material, the energy of the charged particle is transferred to the exposed matter. A high value of linear-energy transfer indicates that energy is deposited within a small distance, the common unit used is $\text{MeV} \cdot \text{cm}^{-1}$.

To compare the stopping power for different material irradiated by the same charged particle beam, the stopping power is normalised by the material density ρ (see Eq. II.13.15), common unit used is $\text{MeV} \cdot \text{cm}^2 \cdot \text{g}^{-1}$

$$\frac{S}{\rho} = \frac{1}{\rho} \cdot \frac{dE}{dl} \quad . \quad \text{(II.13.15)}$$

The loss of energy of the electrons has two contributions, one is related to the energy losses from inelastic collisions, and the second one is to the energy losses from bremsstrahlung radiation, as given in Eq. (II.13.16)

$$\frac{S}{\rho} = \frac{1}{\rho} \cdot \left(\frac{dE}{dl} \right)_{\text{collision}} + \frac{1}{\rho} \cdot \left(\frac{dE}{dl} \right)_{\text{radiation}} \quad . \quad \text{(II.13.16)}$$

Figures II.13.18, II.13.19 and II.13.20 show the normalised stopping power for electron depending on the electron energy for three different materials, with low, medium and high Z numbers, carbon, copper and lead respectively.

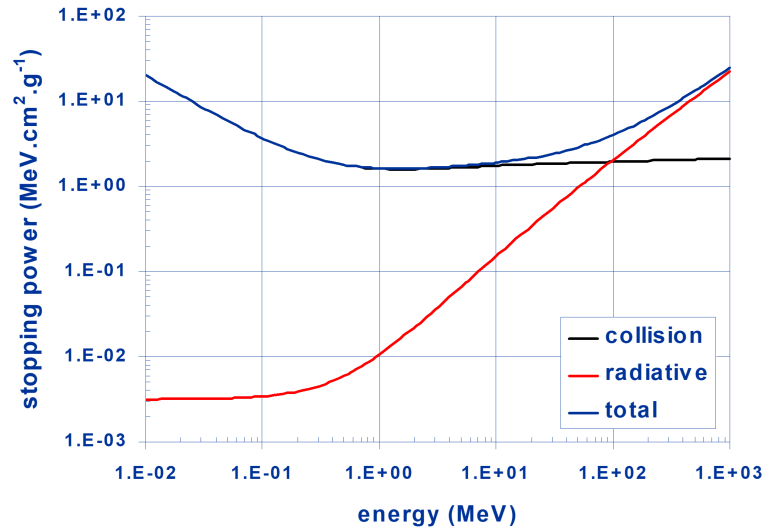


Fig. II.13.18: Graphite stopping power as a function of the electron energy (Carbon-C, $Z=6$).

Irrespective of the Z value, for low-energy electrons (below 10 MeV) the collision component of the stopping power is higher than the radiation one.

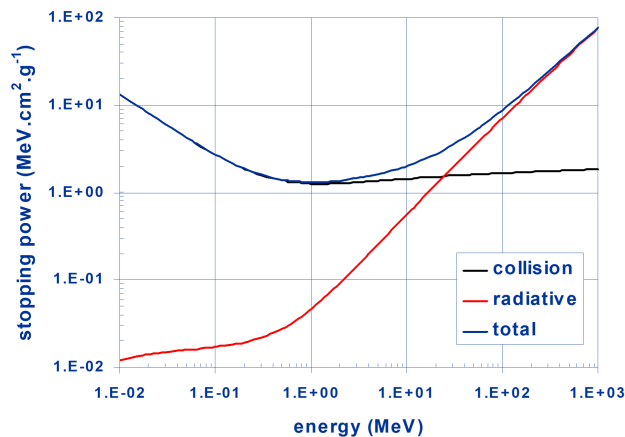


Fig. II.13.19: Copper stopping power as a function of the electron energy (Cu, $Z = 29$).

There is an electron energy value, where the radiation stopping power is linear with the energy. Also, for all of them there is an electron energy value above it, where the radiation stopping power is higher than the collision one.

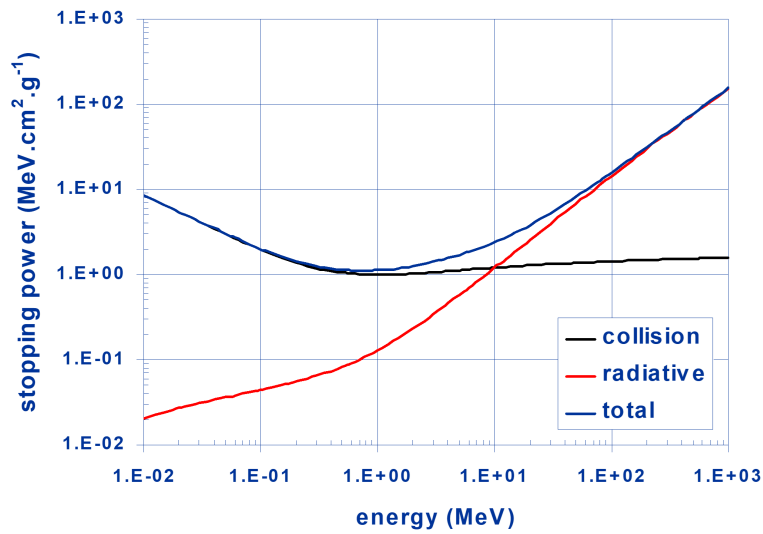


Fig. II.13.20: Lead stopping power as a function of the electron energy (Pb, $Z = 82$).

II.13.4.3.1.2 Electromagnetic cascade

In the case of high-energy electrons, where the energy radiation loss is much higher than the one from collisions, the mean length (in cm) into the material at which the energy of an electron is reduced by the factor $1/e$ is called radiation length (X_0).

The high-energy (above 100 MeV) incident electrons (incident beam particles or primary particles), produce a cascade of photons (γ), electrons (e^-), positrons (e^+) and neutrons (n), see Fig. II.13.21, which are propagated in the material until all the particles are absorbed by the material.

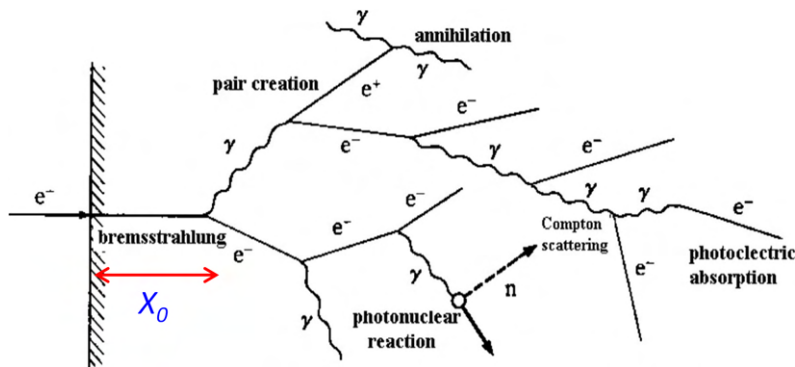


Fig. II.13.21: Schematic representation of the electromagnetic cascade for high-energy electrons.

The electromagnetic cascade produced by high-energy electrons in a material, can be calculated (“simulated”) using Montecarlo methods. Figures II.13.22 and II.13.23 show a comparison for two energetic electron beams (0.5 GeV and 6.0 GeV) in Pb. The radiation length and the number of particles created depend on the beam energy. Also the penetration length in the material and the transversal propagation are shown.

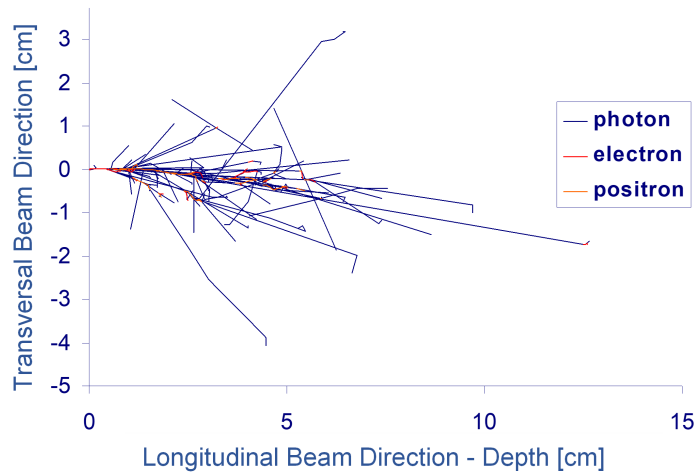


Fig. II.13.22: Montecarlo simulation of an electron beam of 500 MeV in lead.

These simulations indicate that to almost stop the incident beam lead blocks of 5 cm and 10 cm are enough for a 0.5 GeV and 6.0 GeV electron beams, respectively.

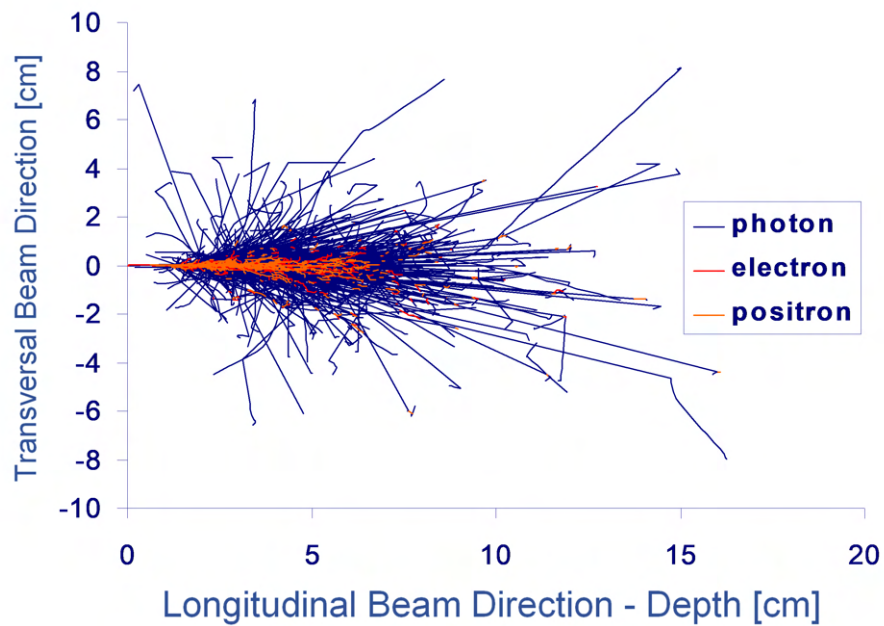


Fig. II.13.23: Montecarlo simulation of an electron beam of 6 GeV in lead.

II.13.4.3.2 Photons

Photons are massless and chargeless electromagnetic particles, in the range of X-rays to γ -rays within the electromagnetic spectrum, from 1 keV to above 1 GeV.

The physical processes when a photon (with energy above few eV) interacts with matter are as follows:

- i. Photo-electric effect,
- ii. Compton scattering,
- iii. Rayleigh (coherent) scattering: it is a photon elastic scattering with the atom, and because there is no photon energy loss it is not relevant for radiation physics,
- iv. Pair production,
- v. Photon-nuclear reaction.

II.13.4.3.2.1 Total photon cross-section

The cross-section measures the probability that a specific physical process will occur when an energetic photon (above 1 keV) intersects with an atom (with the orbital electrons or the nucleus). The cross-section is typically denoted σ and expressed in barns (in SI, area magnitude). It can be thought of as the size of the atom as a target (circular target) that produces a change (energy, direction, or consequences on subatomic particles). It is a microscopic parameter that reflects the nature of the physical process (stochastic).

The total photon cross-section is calculated from the expression below

$$\sigma_{\text{total}} = \sigma_{\text{coherent}} + \sigma_{\text{Compton}} + \sigma_{\text{photoelectric}} + \sigma_{\text{pair-production}} \quad \text{(II.13.17)}$$

Figure II.13.24 shows the total photon cross-section (normalised to the material density, $\text{cm}^2 \cdot \text{g}^{-1}$) for Pb, and the different components of the cross-section depending on the photon energy (in MeV).

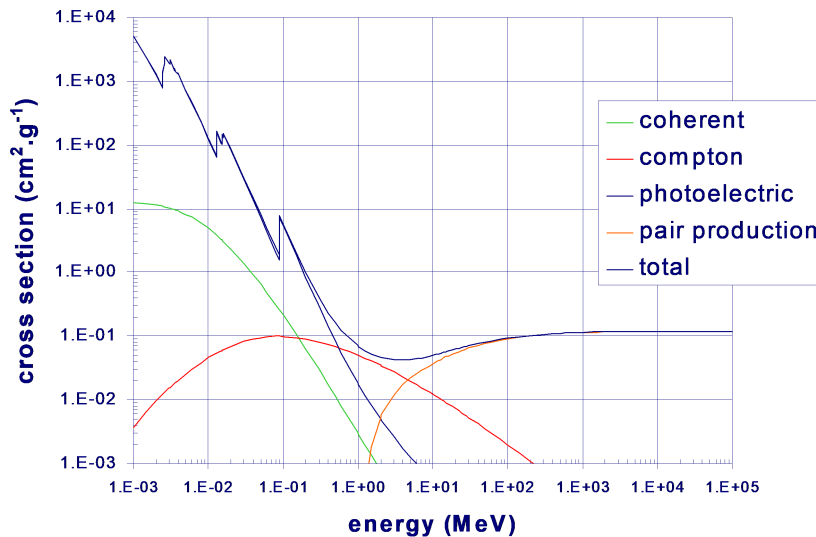


Fig. II.13.24: Total lead (Pb, $Z = 82$) cross-section and its components as a function of the photon energy.

II.13.4.3.2.2 Photon attenuation factor

The photon linear attenuation coefficient (μ) describes, in a macroscopic way for a given material and thickness (see Fig. II.13.25), the beam intensity that emerges from the material when it is irradiated by a monoenergetic photons beam. It is defined by Eq. (II.13.18) and it is commonly expressed in $\text{cm}^2 \cdot \text{g}^{-1}$

$$\mu = \frac{1}{N} \cdot \frac{dN}{dl} \quad . \quad (\text{II.13.18})$$

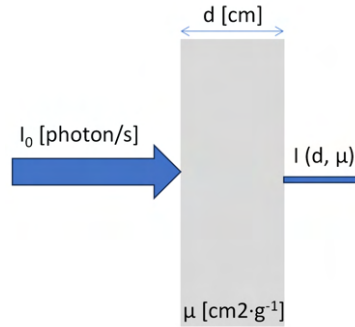


Fig. II.13.25: Schematic representation of the linear attenuation coefficient.

Therefore, solving the differential equation, the number of photons that emerge is given by Eq. (II.13.19)

$$N(d, \mu) = N_0 \cdot e^{-\mu \cdot d[\text{cm}]} \quad . \quad (\text{II.13.19})$$

If it refers to the number of photons per second (intensity), then Eq. (II.13.19) is replaced by

$$I(d, \mu) = I_0 \cdot e^{-\mu \cdot d[\text{cm}]} \quad .$$

If the mass attenuation coefficient is normalised to the material density (ρ), Eq. (II.13.18) is expressed as Eq. (II.13.20), and normally is given in cm^{-1}

$$\frac{\mu}{\rho} = \frac{1}{\rho N} \cdot \frac{dN}{dl} \quad . \quad (\text{II.13.20})$$

Then Eq. (II.13.19) is modified by Eq. (II.13.21) as follows

$$N(d) = N_0 \cdot e^{-\frac{\mu}{\rho} \cdot d[\text{g} \cdot \text{cm}^{-2}]} \quad . \quad (\text{II.13.21})$$

and graphically is given by Fig. II.13.26:

The conversion factor between the total photon cross-section (σ , in barns $\cdot \text{atom}^{-1}$; 1 barn = 10^{-28} m^2) and the normalised photon linear attenuation coefficient (μ/ρ , in $\text{cm}^2 \cdot \text{g}^{-1}$) is given by Eq. (II.13.22)

$$\frac{\mu}{\rho} = 10^{-24} \cdot \frac{N_A}{A} \cdot \sigma = n_A \cdot \sigma \quad , \quad (\text{II.13.22})$$

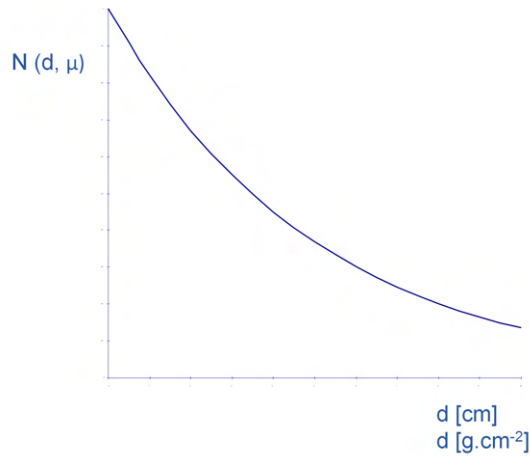


Fig. II.13.26: Graphical representation of Eq. (II.13.21).

where N_A is the Avogadro number, A is the material molar mass (g), and n_A is the material density in atoms \cdot g $^{-1}$.

II.13.4.3.2.3 Photo-electric effect

The photo-electric effect is the physical process where a photon (with an energy in the X-ray range) interacts with the orbital electrons of the inner atom shells (K,L,M), see Fig. II.13.27 (K electron involved).

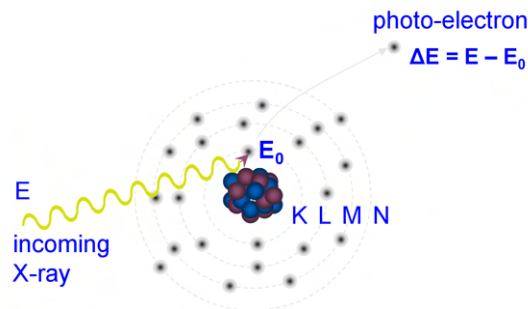


Fig. II.13.27: A photoelectron might be produced after the photon atom interaction.

As a result of this removed electron (Fig. II.13.27), two physical processes can occur:

- The vacancy created by the K-electron might be occupied by an L-electron or M-electron, producing a characteristic X-photon (called line L or M for the given material), see Fig. II.13.28, and Fig. II.13.29 if the electron removed is from line L,
- The emitted photon is absorbed by the same atom (self-absorption) and an electron called “Auger electron” is emitted (see Fig. II.13.30).

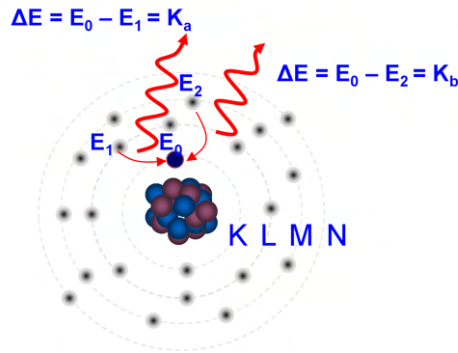


Fig. II.13.28: Emission of photons by the decay of electrons in level L or M that occupies the K-level.

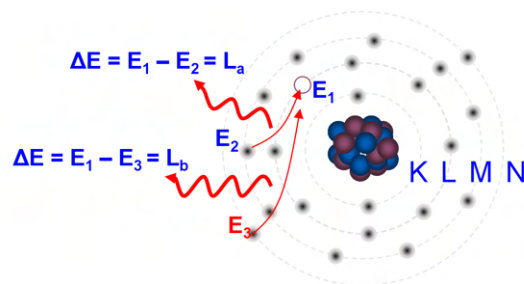


Fig. II.13.29: Emission of photons by the decay of electrons in level M or N that occupies the L-level.

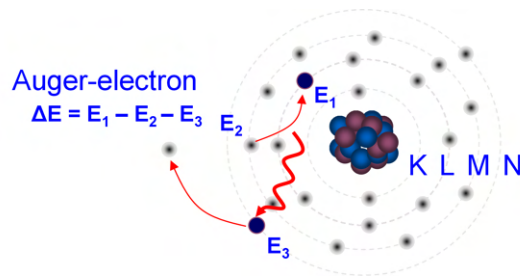


Fig. II.13.30: An Auger electron is emitted by the self-absorption of an electron in level N.

II.13.4.3.2.4 Compton scattering

The Compton scattering process is the inelastic scattering interaction between an energetic photon and an external electron in an atom (loosely bound electrons). As a result of this interaction, the incident photon is deflected with less energy and the atomic electron (Compton electron, see Fig. II.13.31) is emitted. It is a very relevant process for radiation safety because the incident photon loses energy, and the atom is ionised.

The energy of the scattered photon is given by Eq. (II.13.23), which is a function of the energy of the incident photon (E_0) and the scattered angle (θ),

$$E_C = \frac{E_0}{1 + \frac{E_0}{m_e \cdot c^2} \cdot (1 - \cos \theta)} \quad (\text{II.13.23})$$

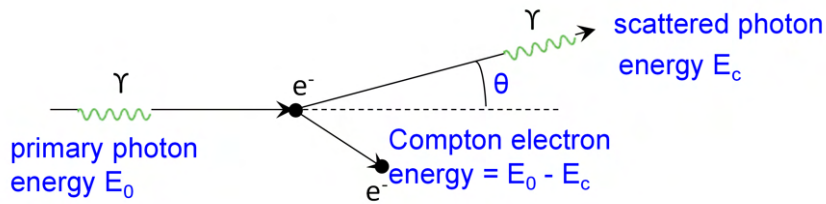


Fig. II.13.31: Schematic of the Compton scattering process.

Figure II.13.32 shows the dependence of the Compton photon energy as a function of the scattered angle for different incident photon energies for lead.

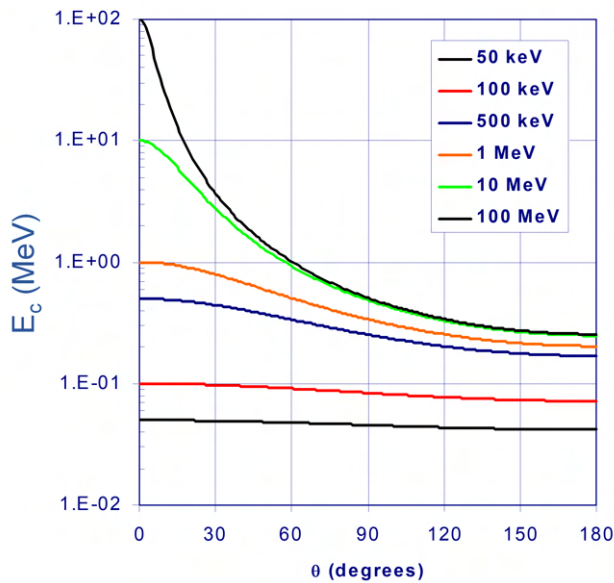


Fig. II.13.32: Angular dependence of the Compton photon scattered by lead atoms for different photon incident energies.

Figure II.13.33 shows the dependence of the variation of the Compton photon cross-section in relation to the considered solid angle (Ω) as a function of the scattered angle for different incident photon energies for lead.

II.13.4.3.2.5 Pair (e^-/e^+) production

The pair (e^-/e^+) production process happens only for gamma rays of high energy. In the pair production process, an incident gamma-ray of sufficiently high energy is annihilated in the Coulomb field of a nearby charged particle, creating an e^-/e^+ pair. As with the photoelectric effect described previously, the conservation of momentum requires the presence of a third body, which takes up the balance of the momentum in the form of a recoil. For a recoil nucleus of mass much greater than the mass of the electron, the threshold energy for pair production is simply

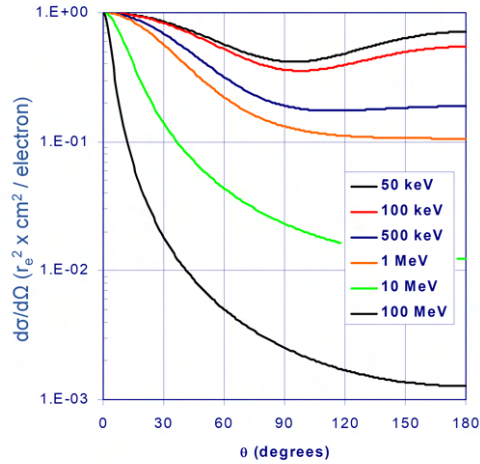


Fig. II.13.33: Angular dependence of the variation of the Compton photon cross-section with the solid angle (Ω) for different photon incident energies.

$$E_{th} \approx 2m_e \cdot c^2 = 1.022 \text{ MeV} .$$

The total cross-section for pair production rises rapidly above the threshold (see Fig. II.13.24) and quickly approaches kinetic energies for the pair e^-/e^+ in the relativistic range. The value of the cross-section reaches an asymptotic limit almost independent of the energy of the photon that creates the pair.

Any excess energy of the pair creation, produced by gamma-rays, is given to the e^-/e^+ pair as kinetic energy. Most probably, the positron will undergo annihilation by interacting with an electron and creating two gamma photons of 0.511 MeV.

The pair (e^-/e^+) production cross-section depends on the atomic charge and if the photon is in the presence of the electric field created by the nucleus (see Eq. II.13.24), or by the electrons (see Eq. II.13.25)

$$\sigma_{\text{nucleus}} \propto Z^2 \quad (\text{II.13.24})$$

with a photon energy threshold of 1.022 MeV,

$$\sigma_{\text{electron}} \propto Z \quad (\text{II.13.25})$$

with a photon energy threshold of 2.044 MeV.

As shown in Fig. II.13.24, the pair production cross-section threshold energy is 1.022 MeV, and for photon energies higher than 200 MeV, it is the only contribution to the total photon cross-section.

II.13.4.3.2.6 Photonuclear reactions

High-energy photons (above 10 MeV, see Fig. II.13.34) can interact with the nucleus being absorbed as a result of this interaction a neutron is generated. As a function of the photon energy, there are three

possible mechanisms:

- Photonuclear reactions (see Fig. II.13.35),
- Giant resonance mechanism (see Fig. II.13.35),
- Photon-pion reaction (quasi deuteron approximation model, see Fig. II.13.36).

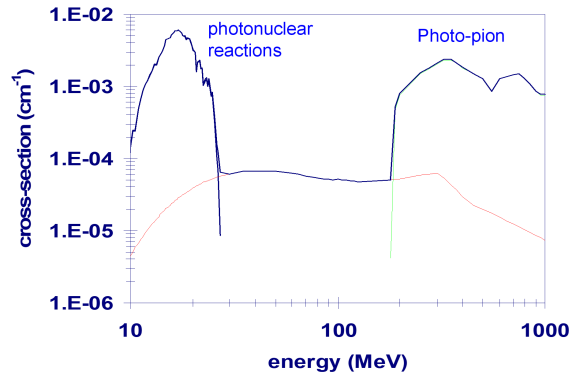


Fig. II.13.34: Photonuclear cross-section as a function of the photon energy for lead.

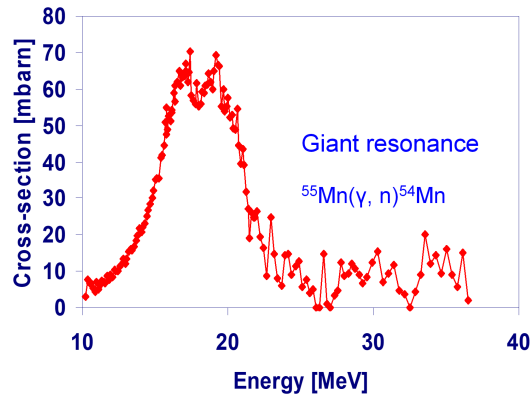


Fig. II.13.35: An example of the photonuclear reaction and the giant resonance cross-section (for lead) as a function of the photon energy.

In the quasi-deuteron approximation, the macroscopic cross-section is given by Eq. (II.13.26)

$$\Sigma_{QD} = \frac{(A - Z) \cdot Z}{A} \cdot \frac{N_A}{A} \cdot \rho \cdot \sigma_d \quad , \quad (II.13.26)$$

where N_A is the Avogadro number, A , Z are the mass and atomic numbers, ρ is the material density, and σ_d is deuteron (microscopic) cross-section for photons.

II.13.4.3.3 Neutrons

Since the neutron is electrically neutral, it interacts only weakly with matter into which it can penetrate deeply. Contrary to X-rays, which interact dominantly with the electron shell of the atom, the neutron

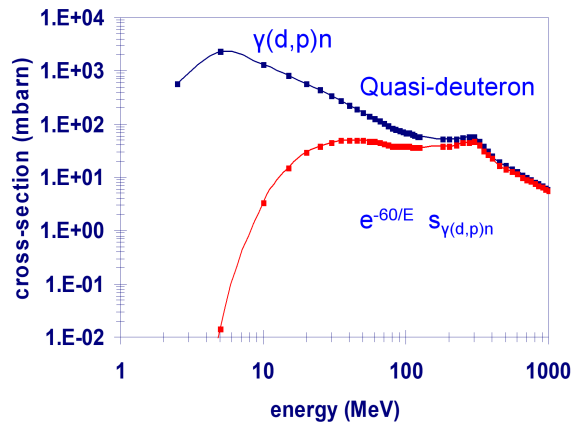


Fig. II.13.36: Photonuclear cross-section (for lead) in the quasi-deuteron approximation as a function of the photon energy.

interacts with the nucleus (see Fig. II.13.37). The interaction of a neutron with the nucleus follows one

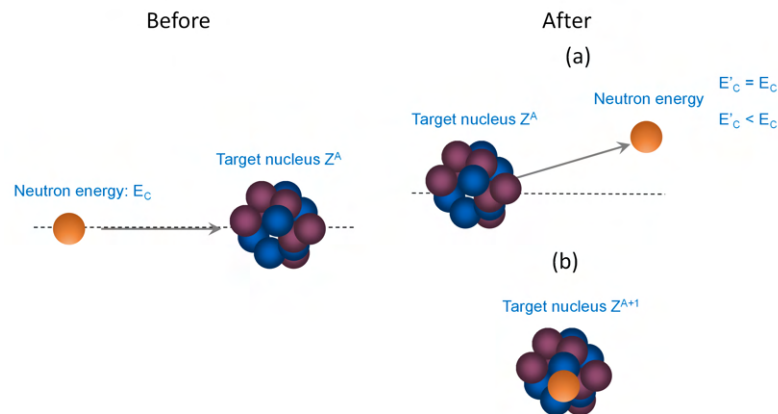


Fig. II.13.37: Schematic diagram of the interaction of a neutron with a nucleus, showing the (a) scattering result or (b) the neutron absorption.

of the following physical processes:

i. Scattering:

- Elastic scattering (n,n): the energy of the incident neutron is conserved,
- Inelastic scattering (n,n'): the energy of the incident neutron is not conserved.

ii. Absorption: where the nucleus will have some recoil velocity and it may be left in an excited state that will lead to the eventual release of radiation. Depending on the incident neutron energy and nuclei atomic mass number (see Fig. II.13.38), the emitted particle can be

- Electromagnetic: emitting a photon,
- Charged: emitting a charged particle, such as proton, alpha, deuterium, etc,

- Neutral: emitting 2, 3, 4 or more neutrons,
- Fission: emitting fission fragments.

Neutron-nucleus interaction involves the interaction with more particles compared with the interaction of photons with the atomic electronic shell. The number of nucleons in a nucleus varies from 1 (H) to almost 300 (see Fig. II.13.38) for the case of the oganesson Og-294.

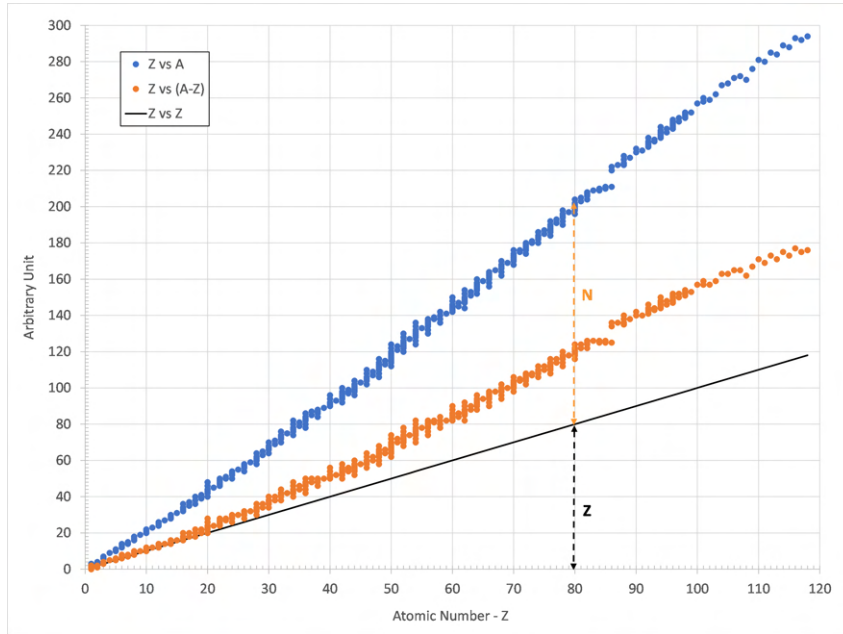


Fig. II.13.38: Mass number (A) and neutron number ($N = A - Z$) as a function of the atomic number (Z) for the stable nuclei.

Once the neutron is absorbed by the nucleus, the decay process of the excited nucleus depends on the incident neutron energy and the nucleus mass number (A). Figure II.13.39 shows different ways of emitting a photon from an excited nucleus.

The neutron-nucleus cross-section value is a measure of the probability of the interaction between these two systems. The neutron is quite sensitive to light atoms like hydrogen (see Fig. II.13.40), oxygen, boron (see Fig. II.13.41) etc., which have much higher interaction probability with neutrons than with X-rays. In contrast to this, metals comparatively show lower interaction probability with neutrons, thus allowing quite high penetration depth.

As follows are some examples of representative materials neutron cross-section:

- a. Hydrogen,
- b. Boron,
- c. Cadmium.

As an example, the transmission of a 200 meV neutron beam in a 0.1 mm of Cd foil (from Fig. II.13.42) is calculated following the attenuation law

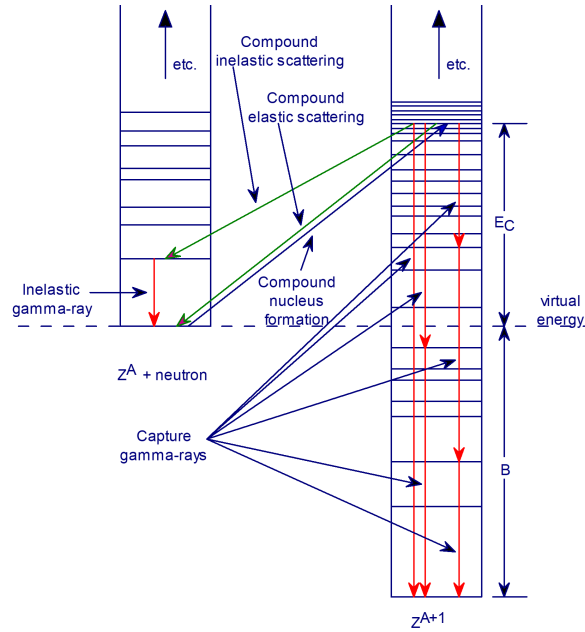


Fig. II.13.39: Diagram of nucleus gamma emission due to a neutron capture.

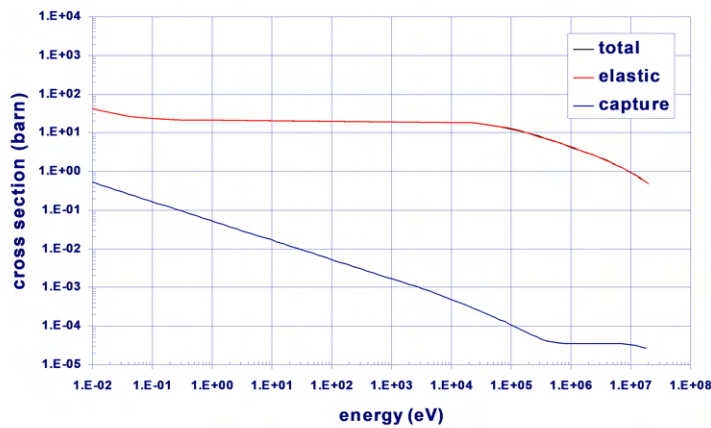


Fig. II.13.40: Hydrogen cross-section as a function of the incident neutron depending on the physical process involved.

$$\frac{N_0 - N}{N_0} = \frac{(N_0 - N_0 \cdot e^{[-10^{-24} \cdot \frac{N_A}{A} \cdot \sigma_{Cd}(200 \text{ meV}) \cdot d]}}{N_0},$$

$$\frac{N_0 - N}{N_0} = 1 - e^{[-10^{-24} \cdot \frac{(6.023 \cdot 10^{23})}{112.42} \cdot (7 \cdot 10^3) \cdot 0.01]},$$

$$\frac{N_0 - N}{N_0} = 1 - 0.69 = 0.31.$$

Therefore the transmission is 31% of the incident neutron beam.

From the graphs above, the most convenient element to stop a neutron beam of 10 eV is a borated material because:

$$\sigma_B(10 \text{ eV}) \approx 300 \text{ barn} \gg \sigma_H(10 \text{ eV}) \approx 30 \text{ barn} > \sigma_{Cd}(10 \text{ eV}) \approx 8 \text{ barn}.$$

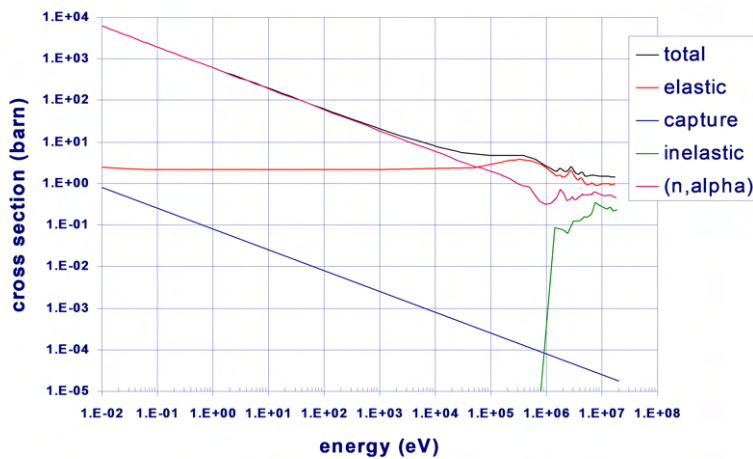


Fig. II.13.41: Boron cross-section as a function of the incident neutron depending on the physical process involved.

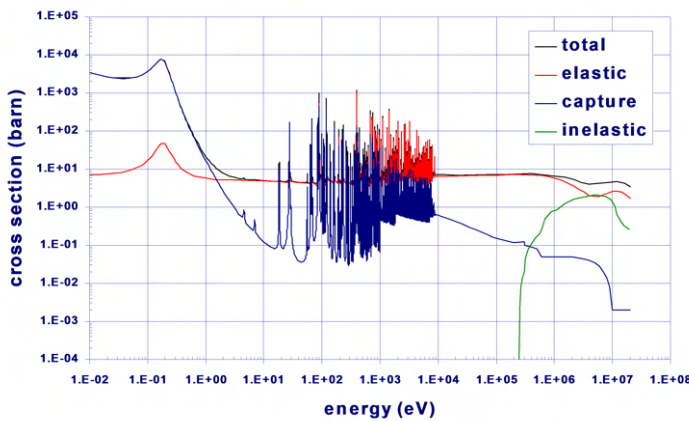


Fig. II.13.42: Cadmium cross-section as a function of the incident neutron depending on the physical process involved.

II.13.4.3.4 Protons

Since a proton is a heavy particle compared with the electrons, and it is charged, in contrast with the neutrons, its interaction with the atom is very strong. Depending on the proton energy, the primary interaction is with the electrons in the shell (low energy) or the atomic nucleus (for high proton energies). The physical processes involved in the proton energy loss are as follows

- i. Ionisation: the proton interacts with an orbital electron, and it is removed,
- ii. Inelastic proton-nucleus scattering: like the Rutherford alpha particle, the proton beam is deflected by the positive charge in the nucleus,
- iii. Spallation: high-energy protons interact with the nucleus producing nucleus fragments (lower atomic mass number) and neutrons.

II.13.4.3.4.1 Proton stopping power

As shown in Fig. II.13.43, even a 10 MeV proton beam can be stopped easily with any metal (see the definition of stopping power in Eq. (II.13.14), $S = \frac{dE}{dt}$). This graph shows the effect of a given energy where the stopping power is minimum, i.e. maximum penetration of the proton beam in the material. Also, it is clear that for light elements (like Al) the stopping power is higher than in the case of Fe or Pb.

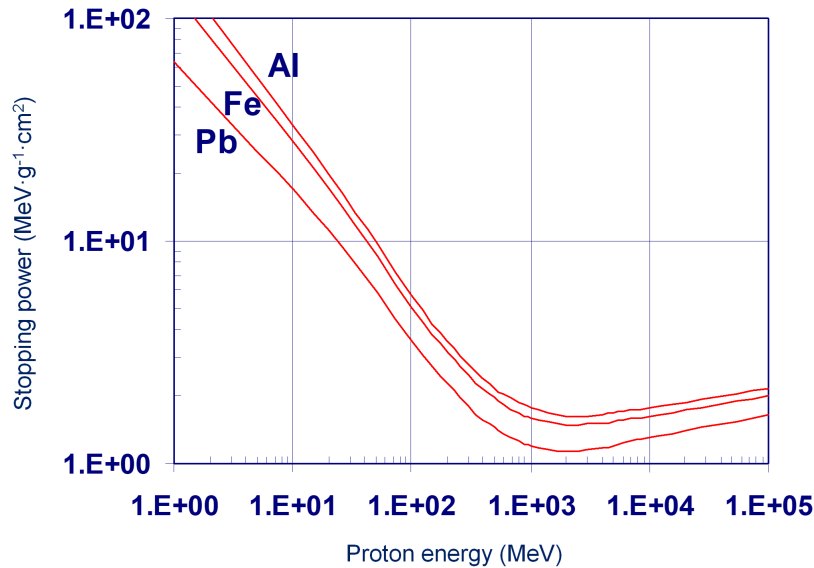


Fig. II.13.43: Proton stopping power for three common elements found in any accelerator.

II.13.4.3.4.2 Protons and electrons CSDA

The continuous slowing down approximation (CSDA) is the average path length travelled by a charged particle as it slows down to rest. It is given by

$$r_{\text{CSDA}} = \int_{E_0}^0 \frac{1}{S_{\text{Total}}} dE \quad . \quad (\text{II.13.27})$$

For a given charged particle energy, it is the length needed to release all the charged particle energy in the material.

As it can be seen from Fig. II.13.44, CSDA increases with the particle energy, and it is bigger for an electron beam with energies between ~ 100 keV and ~ 100 MeV.

II.13.4.3.4.3 Proton-nucleus inelastic interaction

The spallation reaction is a process where a high-energy proton (~ 1 GeV) loses all its energy interacting with a nucleus (see Fig. II.13.45). The products from this reaction are as follows

- Neutrons,
- Protons,

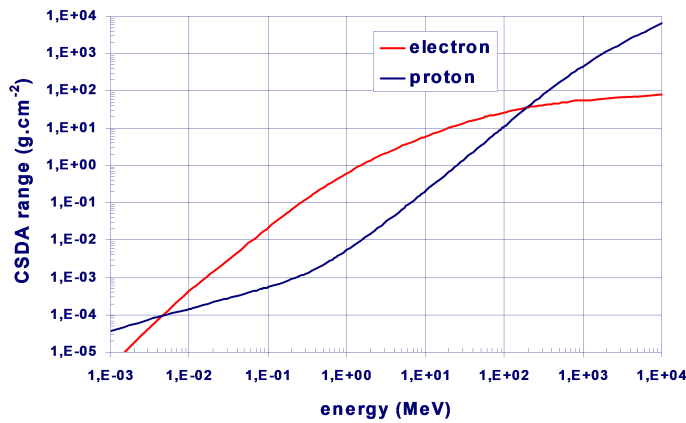


Fig. II.13.44: Comparison of the Continuous Slowing Down Approximation-CSDA for electrons and protons beam in iron.

- A lower A nucleus, which emits γ , α particles, n , D (deuteron).

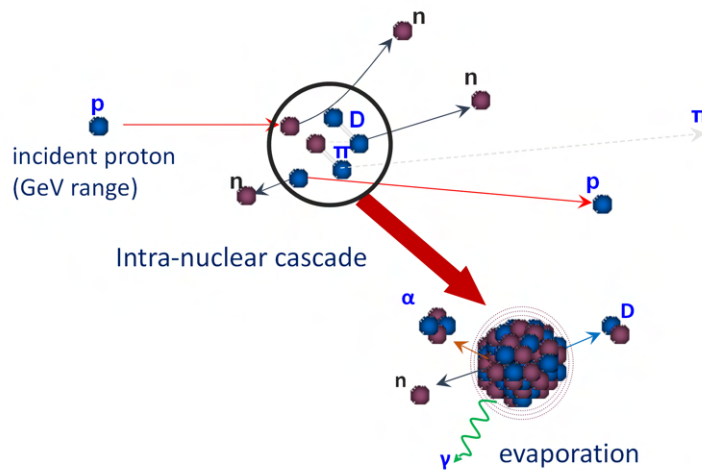


Fig. II.13.45: Schematic diagram of the products resulted from the interaction of a high-energy proton (~ 1 GeV) with a nucleus.

Figure II.13.46 shows the inelastic cross-section for common accelerator components elements (C, Al, Fe, Cu, W and Pb) for proton beams with energy higher than 1 MeV. The maximum cross-section for all these elements is found in the energy range of 10–100 MeV.

As an approximation, the inelastic cross-section as a function of the mass number A is given by Eq. (II.13.28)

$$\sigma_{\text{inelastic}} = 0.042 \cdot A^{0.7} \text{ [barn]} . \quad (\text{II.13.28})$$

In a spallation process, there is an important production yield of neutrons. Depending on the proton energy and the target nucleus material, one proton can generate tens of neutrons (see Fig. II.13.47). In

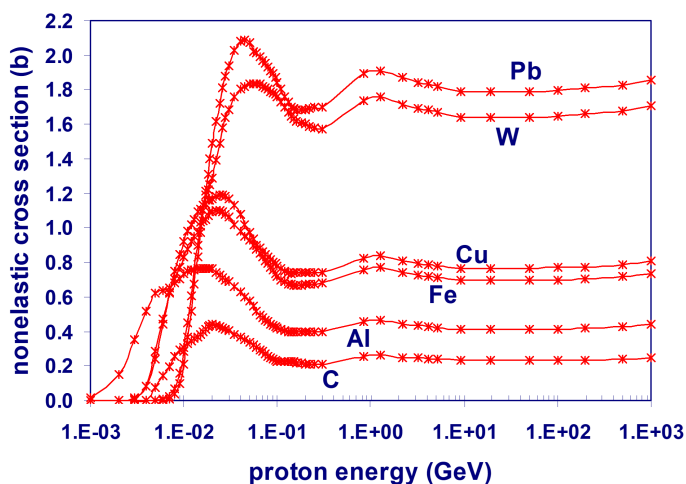


Fig. II.13.46: Inelastic cross-section for proton with energies higher than 1 MeV.

ISIS neutron and muon source at RAL, one proton produces an average of 20 neutrons. This yield is obtained from the incident protons and secondary high-energy neutrons (see Fig. II.13.48).

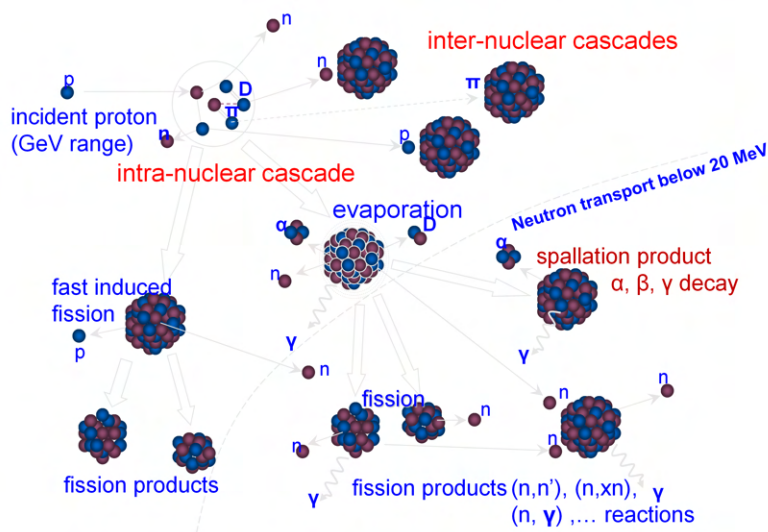


Fig. II.13.47: Spallation cascade process which shows the effects of the interaction of the secondary particles with other nuclei or fragments of the target nuclei.

In summary, from ionisation radiation particles shielding point of view, as shown in Fig. II.13.49, a sheet of paper could be enough to stop a heavy charged particle such as an alpha particle; in the case of beta particles, a metal foil is enough. To stop X-ray and γ -ray, a thick lead plate is sufficient, and to stop neutrons, the most convenient materials are water or concrete because they contain a lot of hydrogen. All these assumptions are for particle energies produced in nuclei disintegration; in the case of particle acceleration, this approach might not be enough.

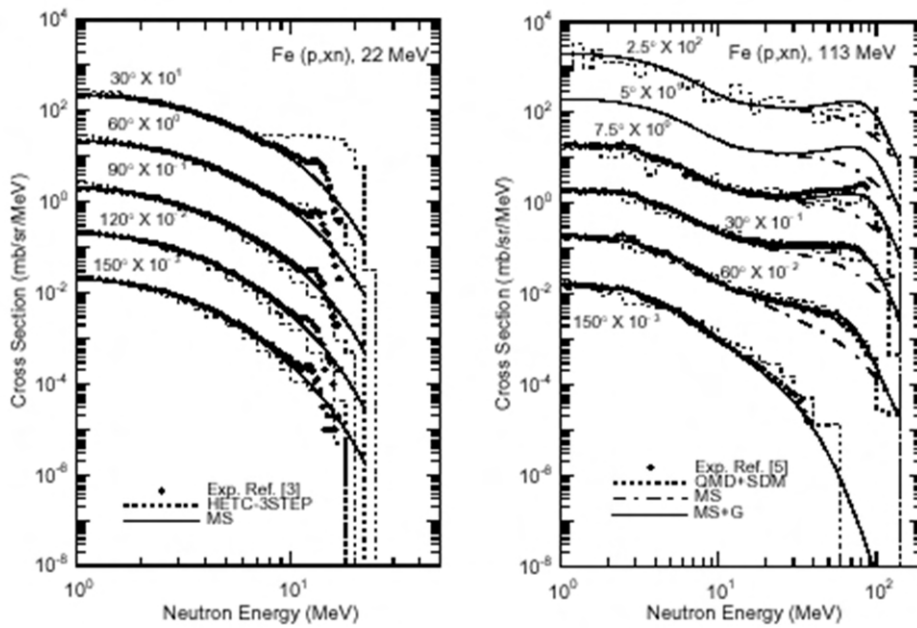


Fig. II.13.48: Comparison of the iron proton reaction for two neutron beam energies, 22 MeV and 113 MeV.

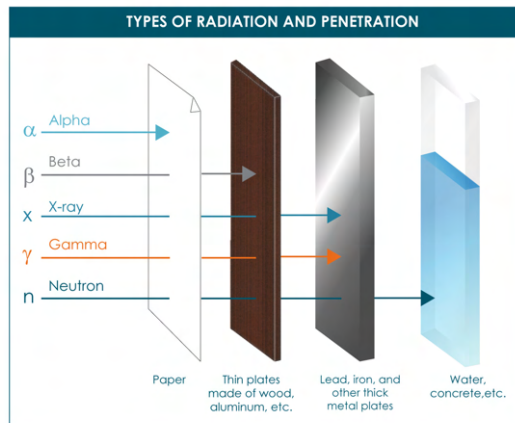


Fig. II.13.49: Schematic representation of the type of material needed to stop the radiation [32].

II.13.5 Radiation shielding

II.13.5.1 Neutron fluence in electrons and proton accelerators facilities

Both in electron and proton accelerators, the main particles to be shielded are photons and neutrons. Although other types of IR particles might be generated, the shielding material characteristics to stop photons and neutrons will shield any other particle.

The photon and neutron fluence produced by an accelerator will depend on the accelerated particle, its energy and current, and the material that contains the accelerator component where the accelerated beam collides.

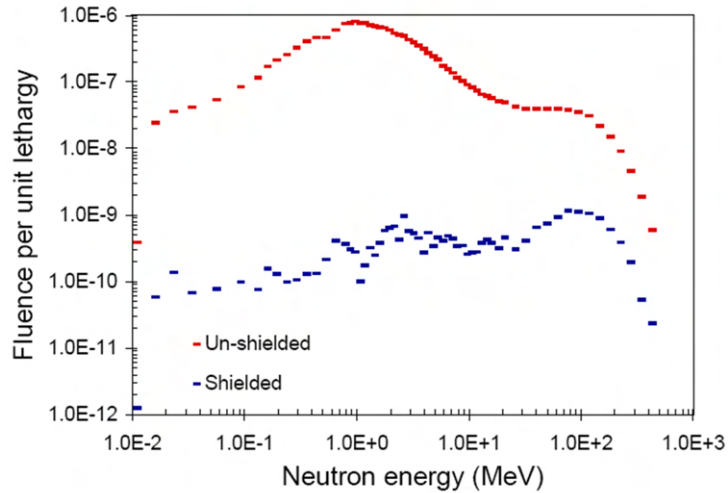


Fig. II.13.50: Calculated neutron spectra for the 1.7 GeV BESSY storage ring (Courtesy of Klaus Ott).

The main difference between electron and proton accelerators is the neutron fluence produced and the resulting neutron flux producing activated material (in solid, liquid or gas state). In the case of synchrotron electron accelerators, the neutron fluence is several orders of magnitude lower compared with the proton one (see Fig. II.13.50 and Fig. II.13.51).

As shown in Fig. II.13.50, the fluence can be reduced by three orders of magnitude in shielded areas, comparable to the neutron fluence natural background.

However, in the case of high-energy proton accelerators (12 GeV, as shown in the Fig. II.13.51), the fluence values and the neutron spectrum are even higher than in a nuclear reactor, making the radiation shielding in high-energy proton accelerators a very different problem compared with the nuclear reactor environment.

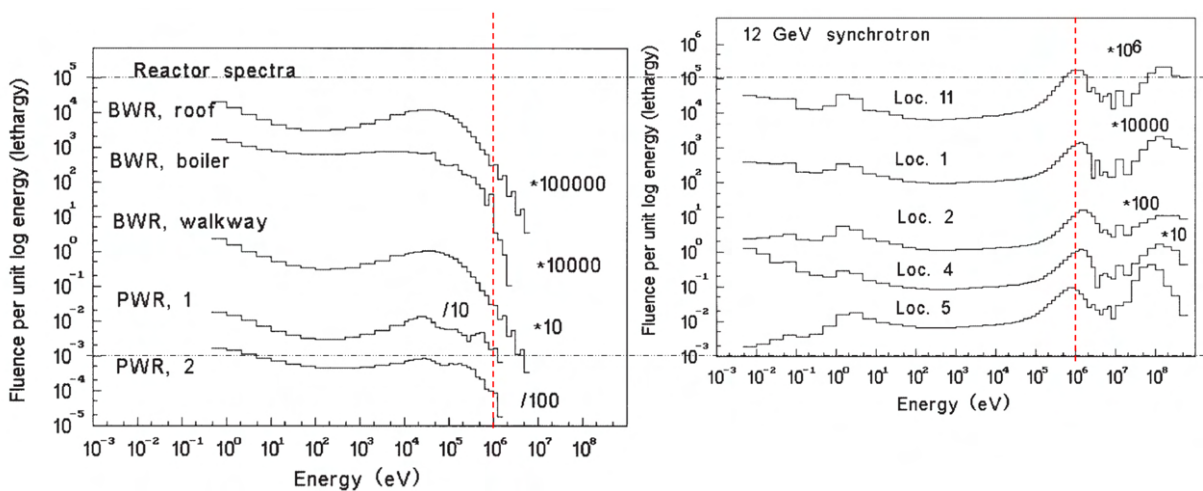


Fig. II.13.51: Comparison of the lethargy (i.e. energy times flux) neutron spectrum between nuclear reactors (left) and 12 GeV proton synchrotron accelerator (right).

II.13.5.2 Estimation of the beam particle losses

It is essential to understand the radiation source term to calculate the characteristics of the needed shielding (geometry, dimensions and material). In any accelerator, the source term is given by estimating how much of the accelerated beam can be lost while in the accelerator [34]. For this reason, the location where the accelerated beam may be substantially lost must be assigned. In general, the beam losses can be produced by

- A change in the accelerator aperture (different vacuum pipe, the presence of a collimator beam or beam scraper),
- Mis-steering of the beam in any place where the beam trajectory changes, bent trajectories and beam transfer lines,
- A systematic failure of an accelerator component (vacuum, magnet, or RF power supplies).

For each of the beam loss points considered, the radiation produced by this loss must be calculated in the main directions

- Forward and backward,
- Sided forward,
- Towards inside and outside,
- Towards the roof and the floor,
- The skyshine component (due to scattered radiation in the air),
- Across any labyrinth and penetrations (for personnel access and ancillary plants, such as electrical power and cooling circuits).

Figure II.13.52 shows the electron beam loss points for the ALBA LINAC and the radiation directions considered, in the horizontal and vertical points.

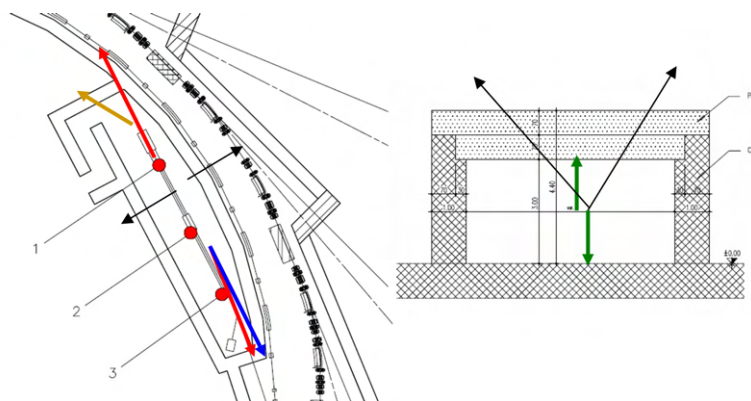


Fig. II.13.52: Electron beam point losses and radiation direction in the case of the ALBA LINAC.

Table II.13.11 and Fig. II.13.53 show the location of all the electron beam loss points in the case of the ALBA accelerators. The number of points chosen has to be large enough to ensure that all the areas outside the shielding (outwards and inwards) have at least one source point assigned.

Table II.13.11: List of electron beam point loss locations in the case of the ALBA accelerators, from the LINAC to the Storage Ring.

#	Accelerator Component	Accelerator Area
0	LINAC pre-buncher	LINAC bunker
1	LINAC RF Cavity-1	LINAC bunker
2	LINAC RF Cavity-2	LINAC bunker
3	Beam Scrapper	LINAC bunker
4	Bending Magnet - Transfer line LINAC to Booster	Tunnel (inner side)
5	Injection Septum - Booster	Tunnel (inner side)
6	Extraction Septum - Booster	Tunnel (inner side)
7	Bending Magnets (25 point losses) - Booster	Tunnel (inner side)
8	Extraction Septum - Booster	Tunnel (inner side)
9	Bending Magnet-1 - Transferline Booster to Storage Ring	Tunnel (center side)
10	Bending Magnet-2 - Transferline Booster to Storage Ring	Tunnel (center side)
11	Injection Septum – Storage Ring	Tunnel (outer side)
12	Bending Magnets (27 point losses) - Storage Ring	Tunnel (outer side)

Once the beam point loss location is assigned, the next step is to estimate the amount of accelerated beam loss in each point. This analysis can be done from a beam dynamic and expected components failure point of view but also must be done taking into account the experience of any similar accelerator. This is an essential step because it determines the dose produced by the accelerated beam in the given location in the main directions considered.

For example, Table II.13.12 shows the estimated values of the beam losses for any point loss considered for the ALBA accelerators. It indicates the current loss and energy. In each location, further considerations must be taken into account, such as the activation of material components and water circuit cooling of air. All these points must be checked once the accelerator commissioning starts.

Table II.13.12: A list of the estimated values of the percentage beam electron loss and their current (in e⁻/s) and energy at the expected locations.

#	Machine Point	% loss	LOSS	Electron per second		Energy [GeV]
				IN	OUT	
0	Linac pre-buncher	-	-	$7.02 \times 10^{+10}$	$9.24 \times 10^{+10}$	0.00009
1	Linac-1	10%	$9.24 \times 10^{+9}$	$9.24 \times 10^{+10}$	$8.32 \times 10^{+10}$	0.05
2	Linac-2	10%	$8.32 \times 10^{+9}$	$8.32 \times 10^{+10}$	$7.49 \times 10^{+10}$	0.1
3	Transf. line Linac→Booster-1	5%	$3.74 \times 10^{+9}$	$7.49 \times 10^{+10}$	$7.11 \times 10^{+10}$	0.1
4	Transf. line Linac→Booster-2	5%	$3.56 \times 10^{+9}$	$7.11 \times 10^{+10}$	$6.76 \times 10^{+10}$	0.1
5	Injection septum	20%	$1.35 \times 10^{+10}$	$6.76 \times 10^{+10}$	$3.38 \times 10^{+10}$	0.1 to 3
6	Extraction septum	15%	$1.01 \times 10^{+10}$	$3.38 \times 10^{+10}$	$3.38 \times 10^{+10}$	0.1 to 3
7	Point sources-Booster	15%	$1.01 \times 10^{+10}$	$3.38 \times 10^{+10}$	$3.38 \times 10^{+10}$	0.1 to 3
8	Extraction septum	15%	$5.07 \times 10^{+9}$	$3.38 \times 10^{+10}$	$2.87 \times 10^{+10}$	3
9	Transf. line Booster→SR-1	5%	$1.44 \times 10^{+9}$	$2.87 \times 10^{+10}$	$2.73 \times 10^{+10}$	3
10	Transf. line Booster→SR-2	5%	$1.36 \times 10^{+9}$	$2.73 \times 10^{+10}$	$2.59 \times 10^{+10}$	3
11	Injection septum	40%	$6.48 \times 10^{+9}$	$2.59 \times 10^{+10}$	$1.30 \times 10^{+10}$	3
12	Point sources-Storage Ring	30%	$6.48 \times 10^{+9}$	$1.30 \times 10^{+10}$	$1.30 \times 10^{+10}$	3

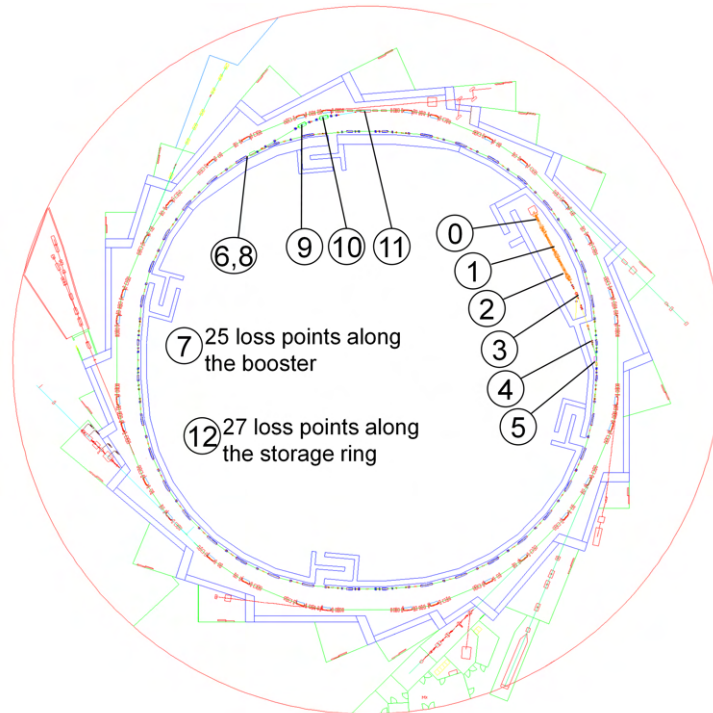


Fig. II.13.53: Electron beam point loss location for all the ALBA accelerators, formed by the LINAC, booster accelerator, transfer lines and Storage Ring.

II.13.5.3 Machine modes

The accelerators are designed to operate in such a way that they produce the expected outcome as an irradiator, a collider, a synchrotron light source, and a neutron spallation source, among others. This way of operation is known as the “user mode”. In the user mode, the accelerator runs in a well-known way, where their set-up parameters and conditions are well established, the beam losses are controlled, and they are ALARA.

However, it is widespread, mainly in the accelerators used for research, to dedicate some time over the year to improve its performance and check any change done in any of the accelerator components. This is called the “machine test mode” or “machine physics mode”, where the accelerated beam losses can be higher than in the “user mode” because some experiments are ongoing to understand or improve the behaviour of any part of the accelerator. In commercial accelerators, this can be labelled as the “maintenance mode”. In general, the machine test mode is a small percentage of the total time of the operation, but it depends from one facility to another. The design shielding must consider both modes to ensure that the total annual dose expected will never be exceeded.

There is a third mode with significant uncertainty about the beam losses because it is the first time the accelerator is “on” or a significant change has been made. This is called the “commissioning mode”. In this mode, the expected doses outside the shielded areas can be exceeded temporarily, and some administrative control measures must be in place to monitor and control the doses in those areas. In principle, the design shielding characteristics do not cover the commissioning mode. If the losses are still high once the commissioning is done, some consideration on the shielding or the accelerator running

parameters must be put in place to achieve the targeted annual dose.

II.13.5.3.1 Accelerator “user mode”

This mode represents the primary usage time for the 8,760 hours of the calendar year. It depends on each accelerator facility but varies from 4,000 to 6,000 hours per year. During this period, the accelerator(s) are running so that the beam losses are minimal. The routine tasks for the ALBA case are as follows

- Injection time,
- Acceleration time,
- Store beam time,
- Operation time.

The dedicated time for the above tasks varies from one accelerator to another. For instance, in the case of the synchrotron light sources, the injection happens a few times daily because the beam is stored in the Storage Ring. However, nowadays, it is very common to run in a “top-up mode” where a minimal current is injected frequently to compensate for the beam losses in the storage ring. In contrast to this, in the case of a neutron spallation source, the beam could be injected fifty times per second in pulsed sources.

In the case of the ALBA facility, the breakdown of the “user mode” time is given in Table II.13.13, where the total expected operating time and the number of injections is specified. In this example, the “user mode” represents around 75% of the calendar year.

Table II.13.13: List of the routine accelerator task and timing on the “user mode”.

Accelerator task	Time	Unit
Operating time /day	24	hours
Operating time/year (250 days/year)	6000	hours
Storage time /filling	5	hours
Injections / day	5	
Injections / year	1200	
Booster operation / injection	12	minutes
Booster operation / year	250	hours
Min. injection time/ injection	169	seconds
Min. injection time/ year	59	hours
Max. injection time/ injection	507	seconds
Max. injection time/ year	176	hours

II.13.5.3.2 Accelerator “machine test mode”

In well-established accelerators, this mode represents a small part of the total year but might produce a significant dose in a calendar year. It can affect the whole accelerator or only a part of it, such as the LINAC, or some part of it, the transfer (or injection) lines and the main accelerator (in general, a

synchrotron). The tasks are very similar to the “user mode”, but the number of injections and the mode of injection can vary from one test to another.

Table II.13.14 shows the time breakdown values for each task in the case of the ALBA accelerators. It is clear that the number of injections considered and their timing, in this case, is several times higher than the user mode.

Table II.13.14: List of routine accelerator task and timing on the “machine test” mode.

Accelerator task	Time	Unit
Machine test weeks / year	12	hours
Injections / day	10	hours
Injections / year	600	hours
Synchrotron operation / injection	48	minutes
Synchrotron operation / year	476	hours
Min. injection time / injection	169	seconds
Min. injection time / year	28	hours
Max. injection time / injection	2535	seconds
Max. injection time / year	422	hours

II.13.5.4 Annual dose target

Once the beam loss point characteristics and the operation times have been established, the last step is calculating the shielding characteristics that will allow us to achieve the calendar year dose target. The value of this dose determines the operational conditions of the areas outside the shielding, following the legal requirements, and it has to be decided by the top-level managers of the accelerator facility.

If the total annual dose in the calendar year is smaller than one mSv/year above the natural background, the administrative control measures will be minimal, and it is highly recommended to take this value as a target. However, depending on the facility characteristics, this is not always possible, and more restricted access control and monitoring areas must be in place for those areas. For example, in the ALBA case, the dose limit is 1 mSv/y across the site.

II.13.5.4.1 Calculation of the total annual dose

The following Eq. (II.13.29) gives the total equivalent dose in an electron or proton accelerator

$$D = \sum_{i=1}^3 D_i = D_{\gamma\text{-ray}} + D_{\text{giant-neutron}} + D_{\text{fast-neutron}}, \quad (\text{II.13.29})$$

where D_i is the total annual dose for each of the IR particle (i), and it is given by Eq. (II.13.30)

$$D_i(\vec{s}) = i_{\text{loss}}(s) \cdot t(s) \cdot \dot{H}_i(\vec{s}), \quad (\text{II.13.30})$$

where s is the accelerator loss beam point and direction, $i_{\text{loss}}(s)$ is the beam particle loss rate at s -point,

$t(s)$ is the time that the e-loss occurs (at s -point), and $\dot{H}_i(\vec{s})$ is the dose rate (at s -point) generated by the i -particle.

II.13.5.4.2 Calculation of the dose rate produced by a loss particle

This is the central problem of the radiation shielding. It consists of calculating the dose rate produced by a beam loss particle after colliding with an accelerator part of a component and transporting the IR dose to a point behind the shielding material (see Fig. II.13.54). The calculation of the dose rate consists of three different phases for the IR point of view

- Production,
- Transportation,
- Attenuation.

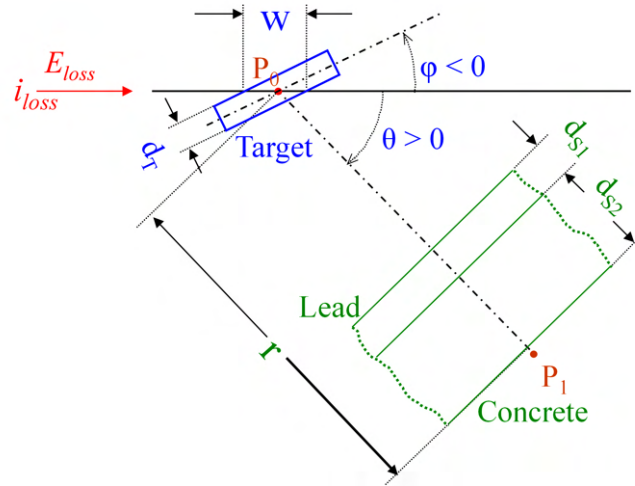


Fig. II.13.54: Layout of the geometry to calculate the dose produced at a doubled shielded (with lead and concrete) P_1 by an incident loss current of the beam at P_0 after colliding with a part of the accelerator.

Generally, the target is a piece of iron, copper, aluminium or stainless steel. However, in some cases, we must consider a liquid or gaseous target.

The equivalent dose at P_1 , per incident loss particle at P_0 , is given by Eq. (II.13.31)

$$\dot{H} = \dot{H}(E_{loss}; w(d_T, \varphi, \rho_T); r, d_{S1}, \rho_{S1}, d_{S2}, \rho_{S2}, \theta). \quad (\text{II.13.31})$$

In the case of ALBA, where the stored beam is of 400 mA with an energy of 3.0 GeV and the target material is stainless steel, the shielding materials and thicknesses are as follows

- Lead (5 cm),
- Concrete: normal and heavy (1.5 m for the front walls and tunnel walls), and normal (1.4 m for the roof tunnel).

In the case of photon, \dot{H} can be calculated by (assuming the source-point distance is important)

$$\dot{H}_p = \sum_i \frac{\dot{H}_0 \cdot e^{[-(\mu/\rho)_i \cdot \rho_i \cdot d]}}{r_p^2}, \quad (\text{II.13.32})$$

where \dot{H}_p is the dose rate equivalent rate (in Sv/h) in a given point- p (out of the shielding area), \dot{H}_0 is the dose rate equivalent rate (in Sv/h) at 1 m from the source (without the shielding), d is the shield thickness (in cm), $(\mu/\rho)_i$ is the mass attenuation coefficient (in cm^{-1}) for the material- i , r_p is the distance from the source point to the dose point- p (in m), and i is summed over different materials.

As an example, a dose of 1 Sv/h of 100 keV photon source, attenuated by 10 m of dry air is given by

$$\dot{H}_p = \frac{1 \cdot e^{[-(0.1541 \cdot 0.00123) \cdot 1000]}}{10^2} = 8.3 \text{ mSv/h}.$$

II.13.5.4.3 Build-up factor

In some cases, the calculated shielded dose is lower than the measured one because the material attenuation and distance square factors are insufficient. The effect of the scattered radiation in the shielding material must be considered because the shielding material acts as a lens of the radiation. This effect is called the shielding material build-up factor (see Fig. II.13.55).

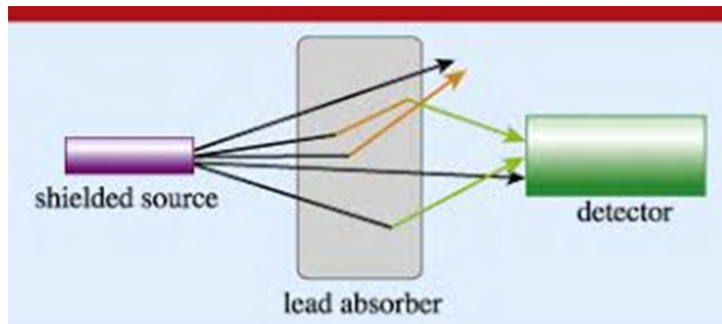


Fig. II.13.55: Scheme representing the shielding build-up factor.

II.13.5.5 Synchrotron radiation facilities

Up to now, the radiation shielding approach can be applied to any particle accelerator. However, the synchrotron facilities contain the areas where the users put their samples to be irradiated by the synchrotron radiation. This paragraph explains the shielding specific to this type of facility, particularly for the ALBA facility case.

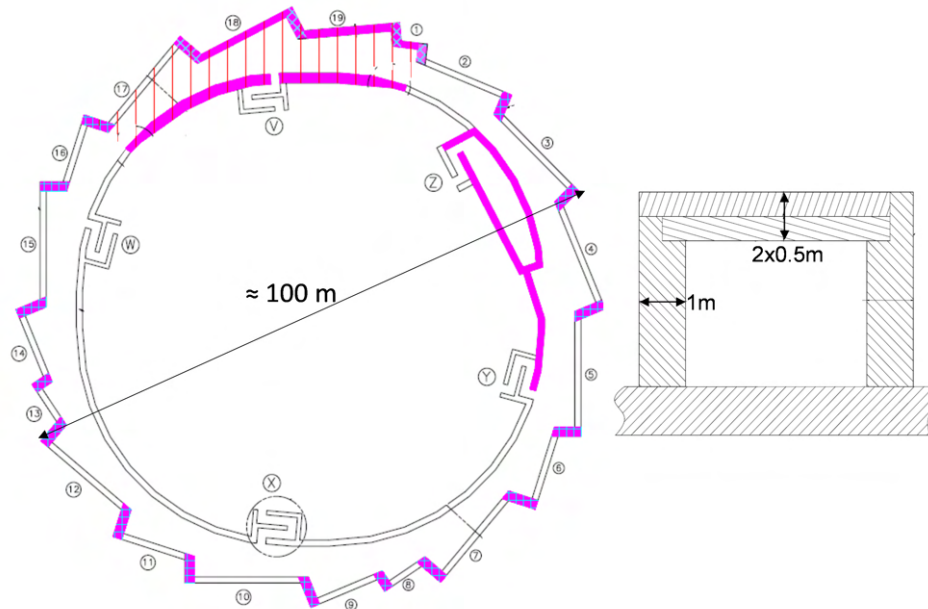
II.13.5.5.1 Accelerator shielding

Considering the electron beam loss points, the current and energies (see tables from Table II.13.11 to Table II.13.14) the accelerator shielding characteristics are summarised in Table II.13.15 and Fig II.13.56.

The resulting total annual dose rates are below 1 mSv/year, and only three areas of the annual dose are slightly higher (see Fig. II.13.57), mainly outside the injected areas.

Table II.13.15: ALBA shielding characteristics.

Tunnel Part Characteristic	Value
Inner and side walls thickness	1 m
Inner wall thickness at injection	1.65 m
Side wall thickness at injection	1.25 m
Roof thickness	1 m
Roof thickness at injection	1.4 m
Linac walls thickness	1 m
Labyrinths walls thickness	0.7 m
Front walls thickness	1.5 m
Number of side/front walls	19
Concrete density	2.4 g/cm ³
Heavy concrete density	3.2 g/cm ³

**Fig. II.13.56:** ALBA synchrotron shielding. Top view of accelerator shielding structures and tunnel cross-section.

II.13.5.5.2 Synchrotron light sources: beamlines shielding

II.13.5.5.2.1 Overview

In synchrotron light sources, the synchrotron radiation is generated in the Storage Ring bending magnets (dipoles) and in the straight sections where periodic magnetic structures (undulators and multipole wigglers) are inserted. Synchrotron radiation spectrum covers soft to hard X-ray (10–100 keV). Superimposed with this radiation, a high-energy gamma radiation is produced from the collision of the electron beam with the residual gas (called “gas bremsstrahlung”). The energy of this radiation covers some hundreds of MeV up to the electron beam energy, in the ALBA case, up to 3 GeV. In both cases, the intensity

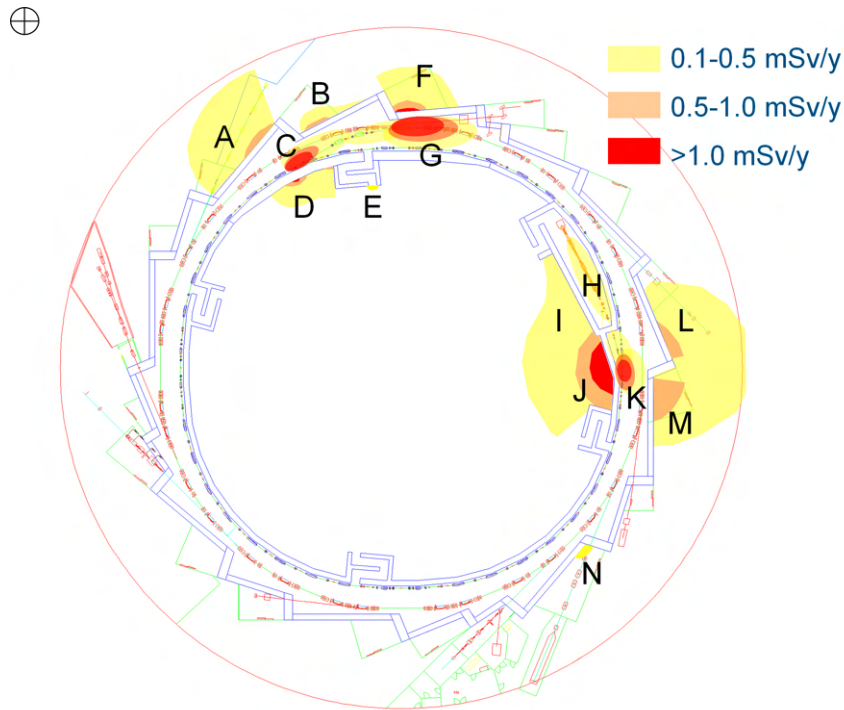


Fig. II.13.57: ALBA annual equivalent dose mapping.

of the radiation is proportional to the beam current.

A hole in the tunnel must be made to extract the synchrotron radiation. This hole must be aligned with the Storage Ring straight section or tangential with a bending magnet. This radiation is guided outside the concrete wall tunnel through a straight line of components called “front-end”. The radiation reaches the other side of the front-wall tunnel in the lead-shielded area called the “optical hutch” and is subsequently guided to where the sample is placed (see Fig. II.13.58).

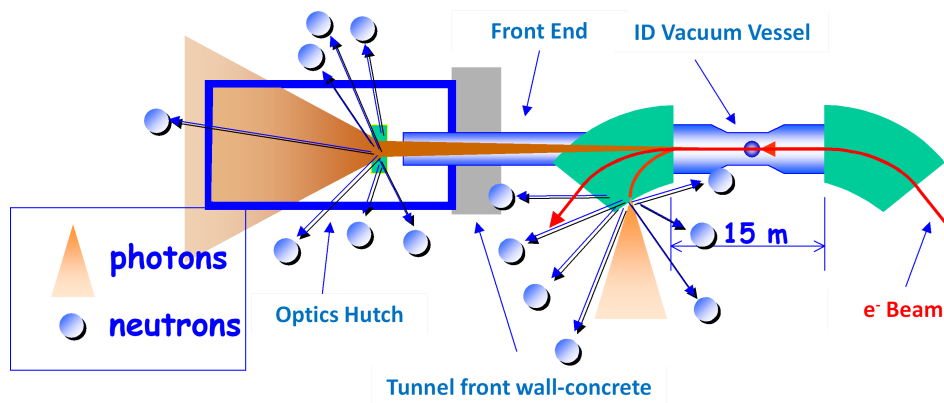


Fig. II.13.58: Top-view scheme of the radiation types in a synchrotron radiation beamline.

The synchrotron radiation (very intense) and the high-energy gas bremsstrahlung arrive in the optical hutch. Because of the interaction between the high-energy photons (from the gas bremsstrahlung) and the nuclei of the optical hutch components, neutron radiation can be produced.

II.13.5.5.2.2 Synchrotron radiation spectrum

Figure II.13.59 shows the photon beam brightness for different synchrotron radiation sources, covering the energy range from the infrared to the hard X-ray.

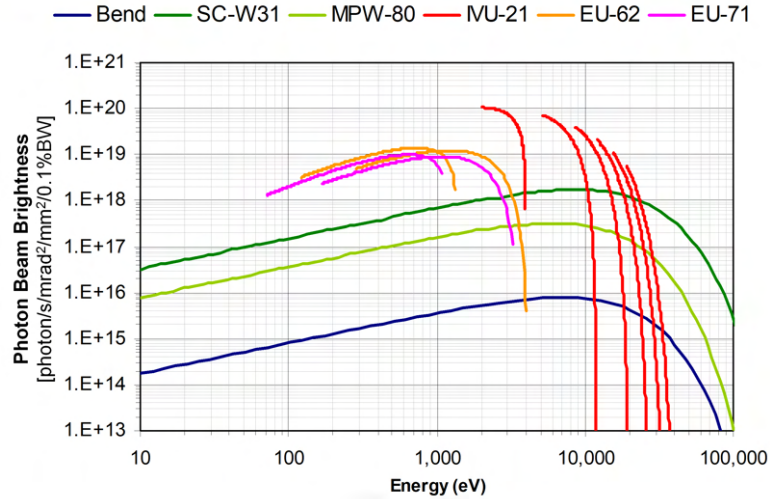


Fig. II.13.59: Photon beam brightness produced by different synchrotron radiation sources (Bend: bending magnets, SC: superconducting wiggler, MPW: multipole wiggler, IVU: in-vacuum undulator and EU: elliptical undulator).

II.13.5.5.2.3 Gas bremsstrahlung

Synchrotron light sources contain long straight sections where insertion devices longer than four meters are placed. If the vacuum level inside the vacuum pipes of these long devices are not low enough, the electron beam collides with the residual gas (mainly N₂ and O₂ molecules), see Fig. II.13.60. As a result of this interaction, high-energy photons can reach the other side of the front-wall tunnel. To avoid this, a tungsten shutter is placed in the front-end side.

The equivalent dose rate at a point “O” at a distance “*d*” from the end of the vacuum pipe is proportional to the beam current and the vacuum pressure inside the pipe, see Eq. (II.13.33)

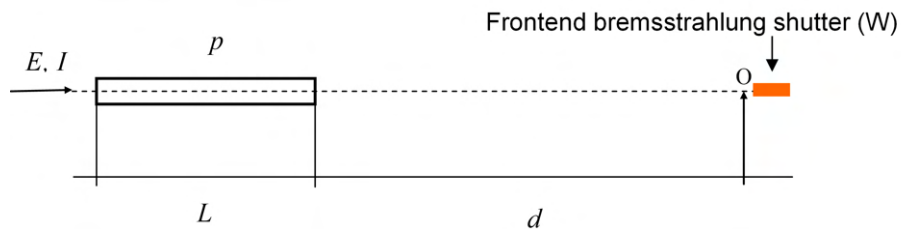


Fig. II.13.60: Schematic drawing of the gas bremsstrahlung radiation generated in a long straight section.

$$\dot{D}_0 = 2.5 \cdot 10^{-27} \cdot \left(\frac{E}{m_e \cdot c^2} \right)^{2.67} \cdot \frac{L}{d \cdot (L + d)} \cdot I \cdot \frac{p}{p_0}, \quad (\text{II.13.33})$$

where \dot{D}_0 is the dose rate at O-point, if $L = 4$ m, $d = 18$ m, $I = 400$ mA, $p = 1.4 \cdot 10^{-9}$ mbar, then $\dot{D}_0 = 0.6$ Gy/h.

Gas bremsstrahlung heavily depends on the electron beam energy, comparing two situations at 2.0 GeV against 3.0 GeV. The dose rate in the second one is three times higher than in the first case (assuming the other parameters are the same)

$$\frac{\dot{D}]_{3 \text{ GeV}}}{\dot{D}]_{2 \text{ GeV}}} = \frac{3^{2.67}}{2^{2.67}} \approx 3 .$$

The electron beam current depends on the vacuum quality, so higher currents imply higher pressure (lower vacuum). Figure II.13.61 shows this dependence for two different straight section lengths in ALBA.

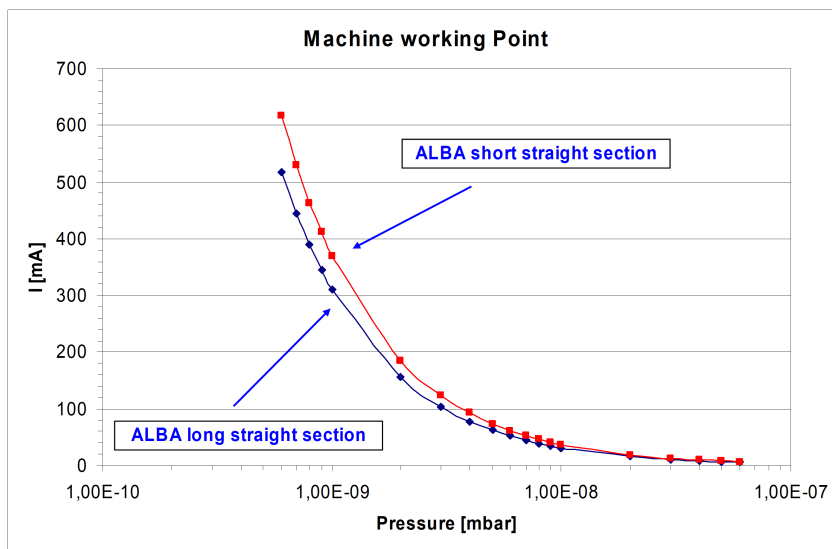


Fig. II.13.61: Electron beam current vs vacuum vessel dependence for a short and long ALBA straight sections.

II.13.5.5.2.4 Beamlines shielding

The maximum annual dose in ALBA is 1 mSv/year, which means that on average, assuming a worker is working 2000 hours/year and is exposed during all the working hours, the average dose rate must be smaller than 0.5 μSv/h. The dose rate produced by the synchrotron and gas bremsstrahlung sources is close to 1 Sv/h, therefore, the optical hutch shielding must be reduced by 10⁶ times.

For all the ALBA optical hutches (cabinets), and in general for a 3.0 GeV synchrotron accelerator, the optical shielding requirements are as follows (see Fig. II.13.62)

- Lead side walls, back walls, and roof to shield all the scattered radiation,
- Photon beam stopper: to shield the high-energy forwarded photon beam,
- Photon beam shutter: in case of an experimental lead hutch in place, it allows access to the experimental hutch while the front-end shutter is kept open,
- Lead screen: place close to the first scattering component to minimise the back wall thickness,

- Backwall lead reinforcement: in some cases, to improve the shielding in the direct photon beam area.

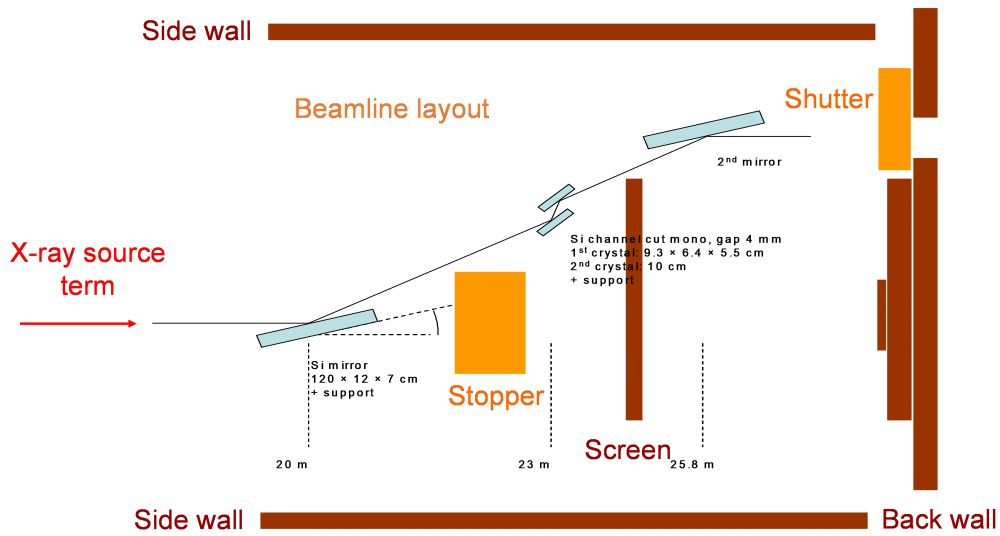


Fig. II.13.62: ALBA beamline optical hutch shielding components, side and back walls, photon beam stopper and shutter and lead screens.

II.13.5.6 Specific shielding situation in electron and proton accelerators

II.13.5.6.1 Beam dump

In any accelerator (linear or circular) it is very convenient to allocate a refrigerated block of metal to dump the beam (“beam dump”). It is a passive component and it must ensure that all the accelerated beam (and secondary generated particles) are contained in it. To guarantee that, the longitudinal and transversal dimensions must be long enough to allow that all the beam energy is deposited on it.

In the case of ALBA, the beam dump is inside the LINAC bunker (see Fig. II.13.63). The bunker is formed by a baritated concrete wall ($3.2 \text{ g}\cdot\text{cm}^{-3}$), 1 m thick.

The ALBA beam dump is a Cu cylinder of 20 cm in diameter and 30 cm in length, which represents several attenuation lengths. In the transversal direction, the dimension that defines that all the incident and secondary particles are not escaping the beam dump is the Molière radius. It is defined as the radius of a cylinder containing, on average, 90% of the shower’s energy deposition (see Fig. II.13.64).

The Molière radius value is given by Eq. (II.13.34)

$$\rho_M[\text{cm}] = 0.0265 [\text{cm}^3/\text{g}] \cdot X_0 \cdot (Z + 1.2), \quad (\text{II.13.34})$$

where $X_0[\text{g}/\text{cm}^2]$ is the radiation length (for Cu = $12.86 \text{ g}\cdot\text{cm}^{-2}$), Z is the atomic number (for Cu = 29), therefore $\rho_M = 10.29 \text{ cm}$.

Figure II.13.65 shows two photos of the ALBA diagnostic beamline placed in the LINAC and a detail (right) of the partially shielded beam dump.

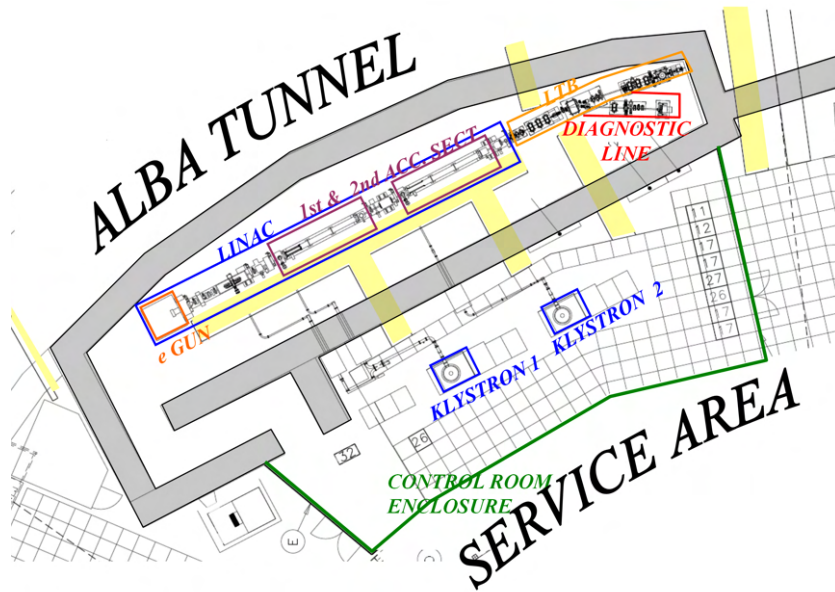


Fig. II.13.63: Location of the electron beam dump in the ALBA LINAC, at the end of the diagnostic line.

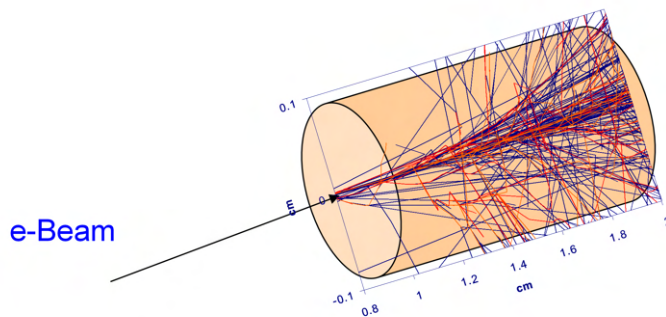


Fig. II.13.64: Electron beam dump characteristics.

II.13.5.6.2 Radiation produced by the induced activity

As shown in the interaction of photons, neutrons, electrons and protons, several particle nucleus reactions end in an unstable (excited) nucleus. This is the process where activation material is produced. In the case of electron accelerators, there are two main physical processes:

- Photonuclear reactions,
- Thermal and slow neutron reactions.

These reactions can also happen in proton accelerators, however, there are two other ways to produce activated (unstable nucleus) material:

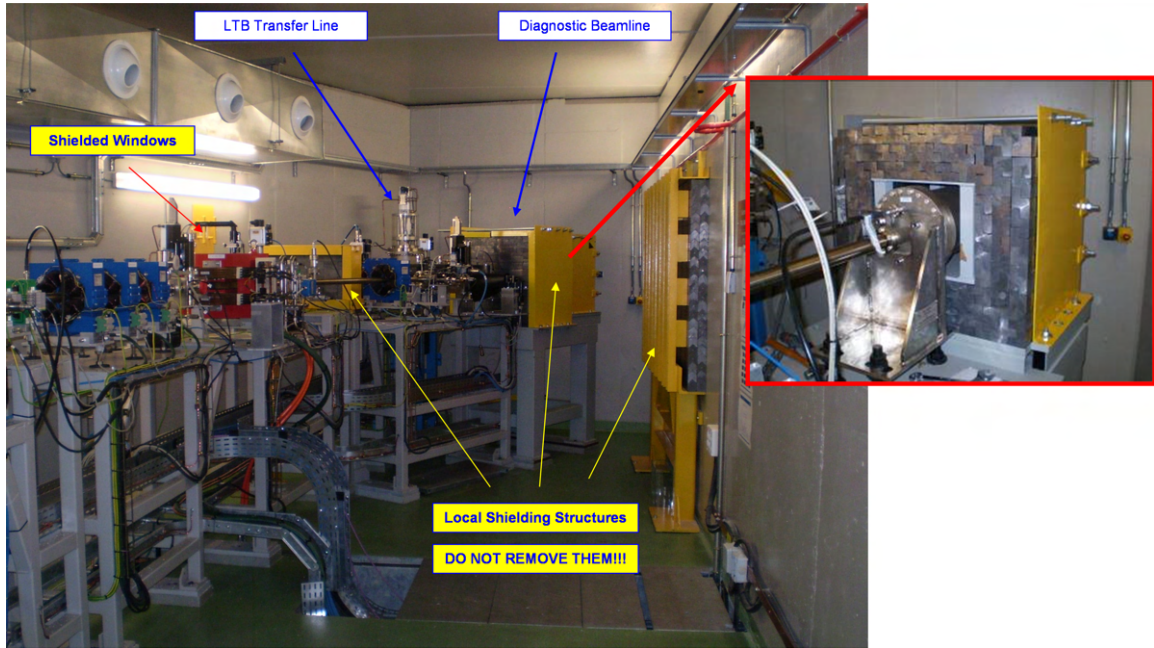


Fig. II.13.65: A photo of the LINAC diagnostic beamline at ALBA. Top right: a detail of electron beam dump [2].

- Medium energy neutron reactions,
- Nuclear reactions at high energy (spallation).

Once the accelerator is switched off, if the radiation levels due to the activated material are very high (see Table II.13.16), a work permit for people entering tunnels must be in place, and management for the activated accelerator components must ensure that the personnel and environment are protected. This is specifically important during the decommissioning of facilities where the activation is very high, like in the neutron spallation sources, such as in ISIS.

Table II.13.16: Activation level depending on the material type.

Relatively insensitive to activation	Moderately susceptible to activation	Highly susceptible to activation	Fissionable
Ordinary concrete, Pb, Al, wood, plastics	Fe (steel, ferrites), Cu	Stainless steel, W, Ta, Zn, Au, Mn, Co, Ni	U, Pu, Th

Figure II.13.66 shows the radionuclides that are present after the irradiation of stainless steel in electron accelerators. After a year of cooling time, only Co-60 is the relevant activated material.

In proton accelerators, as shown in Fig. II.13.47, the material activation is mainly driven by the spallation process, where a large number of energetic neutrons and nucleus fragments are produced. Table II.13.17 shows the most common radionuclides in this type of accelerators.

Cobalt 60 (can be written $^{60}_{27}\text{Co}_{33}$, or ^{60}Co , or Co-60, or Co60) is a very common radionuclide present either in electron or proton accelerators with stainless steel components (see Fig. II.13.66 and Table II.13.17). $^{60}_{27}\text{Co}_{33}$ ($A = 60, Z = 27, N = 33$) decays to $^{60}_{28}\text{Ni}_{32}$ ($A = 60, Z = 28, N = 32$) emitting

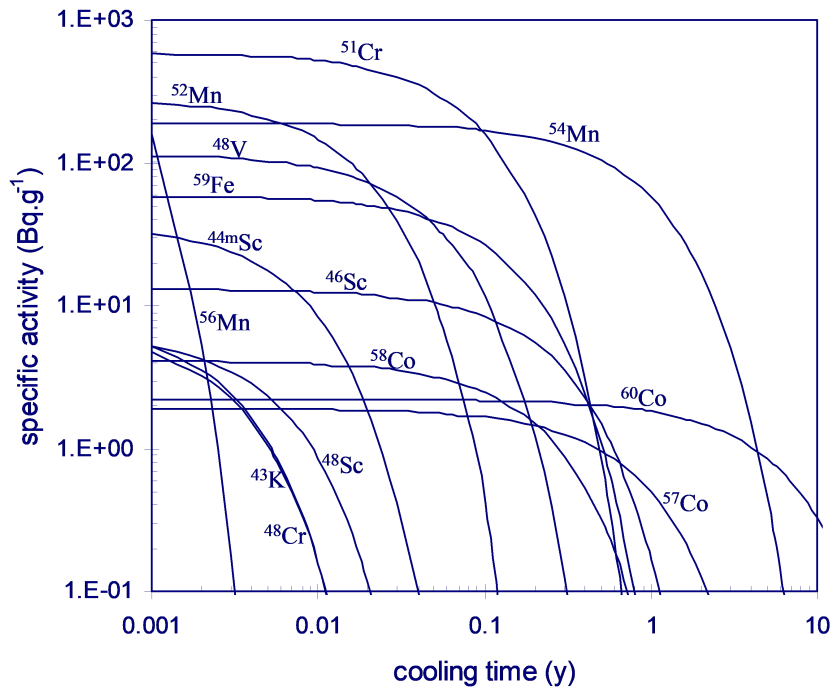


Fig. II.13.66: Cooling down (decay graph) of the activated nuclei for irradiated steel in electron accelerators.

a β^- particle and 2γ (see Table II.13.18), and following the decay diagram given in Fig. II.13.67.

The time needed to reduce to half its activity is 5.27 years, and the dose rate for a Co60 source of 1 GBq is $357 \mu\text{Sv/h}$ (see Table II.13.18). Therefore the dose rate of a Co60 source of 1 Bq at 1 m in air is $3.57 \cdot 10^{-7} \mu\text{Sv/h}$.

As an example of the effect of being exposed to a radionuclide, we calculate the dose $D(t)$ received by a person irradiated by a radioactive source of 1 kBq of Co60, (the dose rate in air is $357 \cdot 10^{-6} \mu\text{Sv/h}$), where the decay of the activity must be taken into account, as given in Eq. (II.13.35)

$$\dot{D}(t) = k \cdot A(t). \quad (\text{II.13.35})$$

Then

$$D(t) = \int_0^t k \cdot A(t) \cdot dt = \int_0^t k \cdot A_0 \cdot e^{-\lambda \cdot t} \cdot dt.$$

After solving the integral, results the following expression

$$D(t) = \frac{k \cdot A_0}{\lambda} \cdot (1 - e^{-\lambda \cdot t}). \quad (\text{II.13.36})$$

Replacing the life-time by the half-life $t_{1/2} = \frac{\ln 2}{\lambda} = \tau \cdot \ln 2$, then $\tau = \frac{t_{1/2}}{\ln 2} = 2.398 \cdot 10^8 \text{ s}$, and $t_{1\text{year}} = 0.315 \cdot 10^8 \text{ s}$. Therefore, the accumulated dose over a year is

Table II.13.17: List of the main radioactive isotopes produced in proton accelerator by spallation reactions, their decay mode and the dose rate per Bq at 1 meter.

Isotope	Half-life	Decay mode	fSv·h ⁻¹ · Bq ⁻¹ (at 1 m)
⁷ Be	53 d	EC	7.8
¹¹ C	20 min	β ⁻	140
¹⁸ F	1.8 h	β ⁻	132
²² Na	2.6 y	β ⁻	298
²⁴ Na	15 h	β ⁻	560
⁴⁶ Sc	84 d	β ⁻	283
⁴⁸ Sc	1.8 d	β ⁻	455
⁴⁸ V	16 d	β ⁻	397
⁵¹ Cr	28 d	EC	4.3
⁵² Mn	5.7 d	β ⁻	326
⁵⁴ Mn	303 d	EC	114
⁵⁶ Co	77 d	β ⁻	350
⁶⁰ Co	5.3 y	β ⁻	340
⁶⁵ Zn	245 d	EC	76

Table II.13.18: ⁶⁰Co dose rate emission.

Nuclide	Half-life	Radiation Particle	Principal Energies	Gamma dose rate at 1 metre (μSv/h/GBq)
⁶⁰ Co	5.27 y	β ⁻	0.32 MeV (100%)	357
		γ	1.17 MeV (100%)	
			1.33 MeV (100%)	

$$D(t_{1year}) = 10.5 \text{ mSv} \quad .$$

There are two interesting limit cases depending on the time considered (from Eq. (II.13.36), replacing λ by $\frac{1}{\tau}$),

$$D(t) = k \cdot A_0 \cdot \tau \cdot (1 - e^{-t/\tau}) \quad .$$

a. If $t \ll \tau$,

$$e^{-t/\tau} \cong 1 - \frac{t}{\tau} \quad ,$$

$$D(t) = k \cdot A_0 \cdot t \quad .$$

In this case, the accumulated dose is linear with the exposed time.

b. If $t \gg \tau$,

$$e^{-t/\tau} \cong 0 \quad ,$$

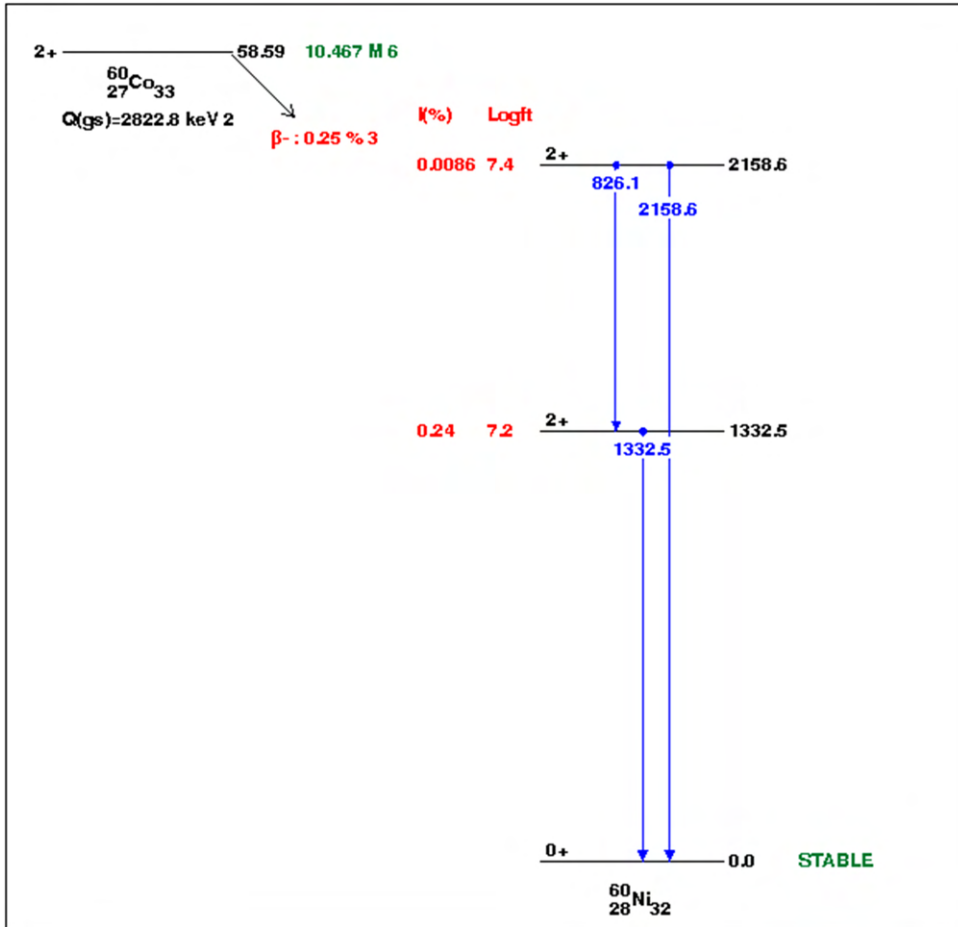


Fig. II.13.67: $^{60}\text{Co}_{33}$ decay diagram to $^{60}\text{Ni}_{32}$.

$$D = k \cdot A_0 \cdot \tau .$$

At this limit, the accumulated dose is a constant value depending on the type of the radioactive source (k and τ) and the initial activity A_0 .

II.13.5.6.3 Radiation produced by the RF generator plants and cavities

II.13.5.6.3.1 RF generators

To generate RF power, an electron beam is accelerated by a voltage of around 32 kV (IOT case) or over 250 kV (klystron case), see Fig. II.13.68. In both cases, the beam is stopped by a metal block, producing high-intensity bremsstrahlung X-rays because the current involved is of the order of 1 A. For this reason, these devices are shielded by lead to ensure that the dose rate on contact is not higher than 0.5 $\mu\text{Sv/h}$.

II.13.5.6.3.2 RF cavities

The conventional (non-superconducting) RF cavities are made of Cu, the internal shape of the cavity ensures that the stationary electromagnetic field accelerates the beam each time it passes through the cavity volume. The shape and structure of the cavity depends on the electromagnetic field characteristic

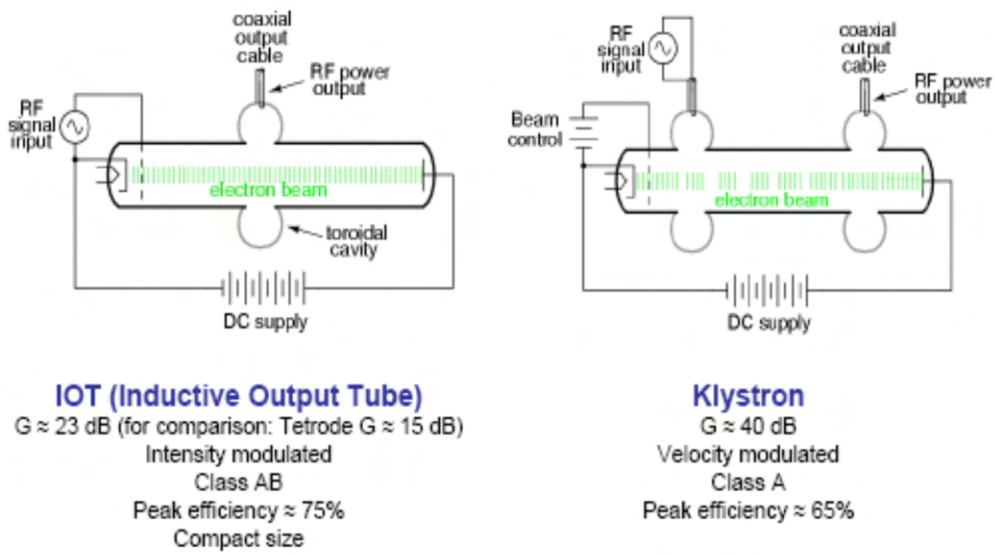


Fig. II.13.68: Two ways of generating RF.

inside (see Fig. II.13.69). Inside the cavity, there is a high voltage and high electric field gradient (see Table II.13.19).

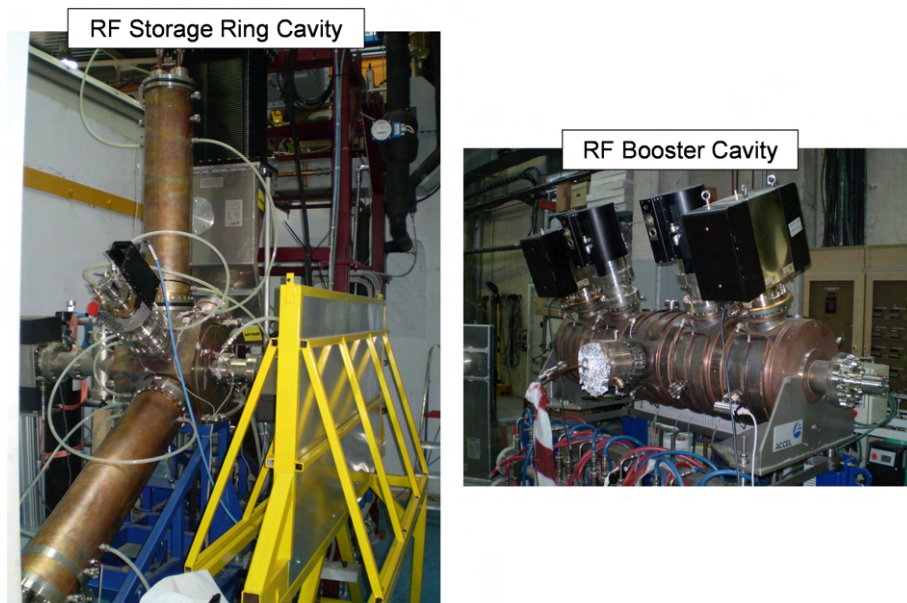


Fig. II.13.69: Two types of RF cavities used in ALBA, for the Storage Ring (left) and for the Booster (right).

Before the cavity is installed in the accelerator, a power test must be done to check that the stability of the applied power is achieved. This cavity conditioning is done without any beam inside. Although there is no beam, a very high gradient electric field can be produced due to the high electrical voltage and the impurities in the metal surfaces (electric field tip effect). Under these conditions, the electromagnetic field structure inside the RF cavity can extract and accelerate electrons from the metal surface. This

current is called dark current on the RF cavity surface, and the value of the current density as a function of the electric field (E) is given by

$$j(E) = \frac{A_{FN} \cdot A_e \cdot (\beta_{FN} \cdot E)^2}{\varphi} \cdot \exp\left[-\frac{B_{FN} \cdot \varphi^{3/2}}{\beta_{FN} \cdot E}\right],$$

where A_{FN} and B_{FN} are constants, A_e is the area emitter, φ is the metal work function, and β_{FN} is the field enhancement factor.

Table II.13.19: ALBA RF cavities electrical characteristics.

	Booster	Storage Ring
Voltage on axis (kV)	1350	750
Maximum E field on surface (MV/m)	2.0	6.2

The dose rate produced by the ALBA Storage Ring cavities (generated X-rays, see Fig. II.13.70) can be as high as 14.05 mSv/h at 20% of the maximum power (80 kW). Figure II.13.70 shows that very energetic X-rays are produced, higher than the expected by the nominal voltage, due to the local tip effect located in the metal surface.

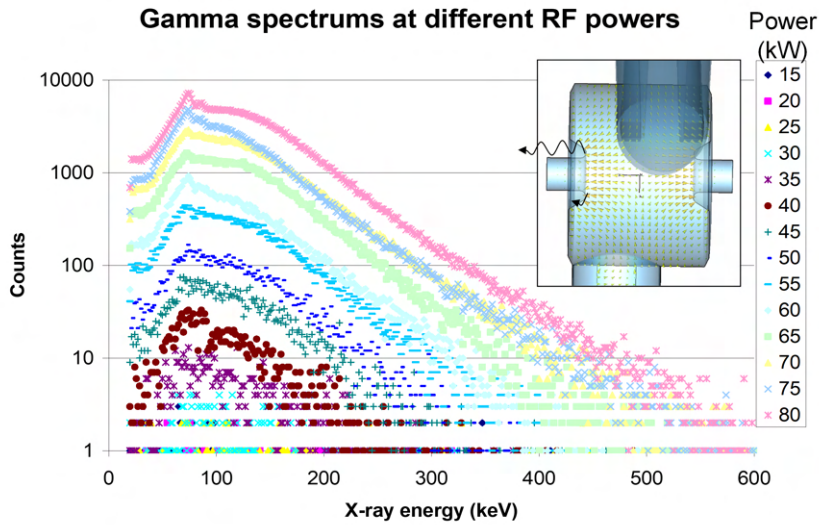


Fig. II.13.70: X-ray spectrum produced during the conditioning phase of the ALBA Storage Ring Cavities, for different power applied.

II.13.6 Radiation safety systems

II.13.6.1 Engineering solution

As it was explained in Sec. II.13.2.1.1, once it has been decided that the source of the hazard cannot be eliminated nor substituted, the third level in the hierarchy of risk control is implementing engineering measures. The engineering measures must be established so that it is very unlikely that someone can modify them unless it is a severe offence or a high degree of negligence. In radiation safety, two main categories of engineering solutions are shielding and interlocks.

II.13.6.1.1 Radiation shielding

Radiation shielding was explained previously in Sec. II.13.5. In the case of synchrotron light sources, the primary shielding is installed around the accelerators using concrete walls and in the beamlines, using lead panels, see Fig. II.13.71 for the accelerators case and Fig. II.13.72 for the beamlines.

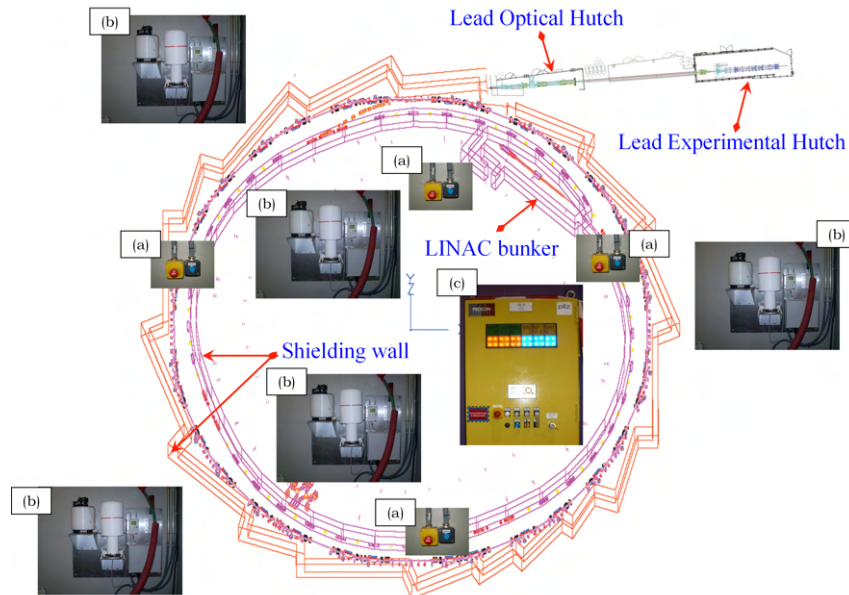


Fig. II.13.71: Top view of the ALBA shielding elements for the LINAC (bunker), Booster and Storage Ring (Tunnel) and beamlines (Optical and Experimental hutches), and the interlocked components (a) Search and Emergency stop buttons, (b) Gamma and neutron radiation monitors, and (c) Interlock access cabinet.

It is essential to ensure that any shielding component cannot be moved nor modified. For this reason, regular inspections after major modifications of any of the components inside the shielding must be done and registered. Special attention must be given to all the shielding penetrations, which must be registered and checked that no modification has occurred.

II.13.6.1.2 Interlocks

The set of interlocks, electrical circuits, and programming used to lock up any accelerator area and stop any accelerator component immediately is called the Personnel Safety System (PSS) or the Personnel Protection System (PPS). This system can be based on hardware interlocks and switches or on a Programmable Logic Controller (PLC).

On the one hand, the PSS' objective is to ensure that nobody is left inside the shielded areas, in the case of the ALBA synchrotron, inside the LINAC bunker, the ALBA tunnel and the shielded beamlines. Also, it is very unlikely that a full-time worker receives more than 1 mSv/year outside the shielded areas.

To avoid somebody being left inside the shielded area, a trained patrol formed by two people has to ensure that nobody is left behind them pressing the search buttons in the correct sequence and at the right time. At the end of the search procedure, the patrol leaves the shielded area and interlocks all the access doors.

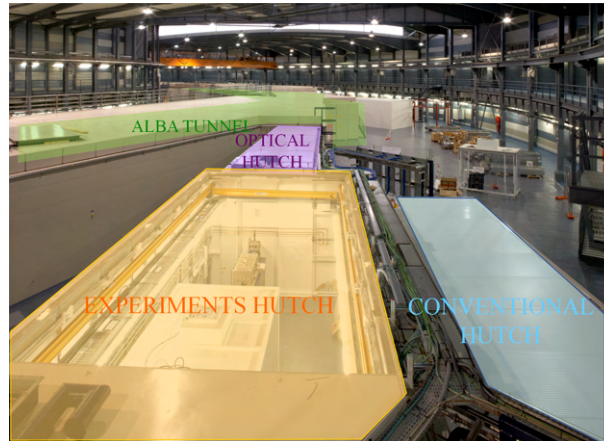


Fig. II.13.72: Top perspective view from the back of an ALBA beamline, showing the Experimental hutch lead shielding (roof removed), Optical Hutch lead shielding and the ALBA tunnel (concrete).

Before the accelerators are energised, a Public Address (PA) system informs that the accelerators are close to starting. In the improbable situation where somebody is left behind, and the shielded areas are locked up, this person must press any emergency stop button to abort any acceleration operation and to unlock the shielded area.



Fig. II.13.73: PSS Main Control Cabinet and the monitor display (detailed) where the interlock elements for the LINAC bunker are displayed.

It is recommended that the PSS be implemented following the IEC-615081 standard, covering the life cycle of the system. In the case of the ALBA facility, the main technical specifications cover the LINAC, booster, Storage Ring and all the beamlines. The Safety Integrity Level-SIL for ALBA is SIL-3, based on redundant and diverse solutions to stop radiation sources.

The technology used in the ALBA facility is based on SIL-3 PLCs, and in ISIS, it is hardwired for

the accelerators and PLCs for the beamlines. In both cases, it is a modular structure solution that allows it to act independently in the LINAC, accelerators and beamlines.

To ensure that the different phases of the PSS are designed, installed and commissioned by different teams, each of them must be checked by external teams from the ones involved in any of those phases, and all the PSS systems must be certified by an external company not involved in any of the life cycle steps.

All the components interconnected in the PSS systems are controlled by a dedicated cabinet control (see Fig. II.13.73). The PSS elements that support the search and lock-up of the shielded areas are, search buttons, emergency stops buttons, loud speakers, captive keys, as shown in Fig. II.13.74 for the accelerators areas, and in Fig. II.13.75 for the beamlines (ALBA case).

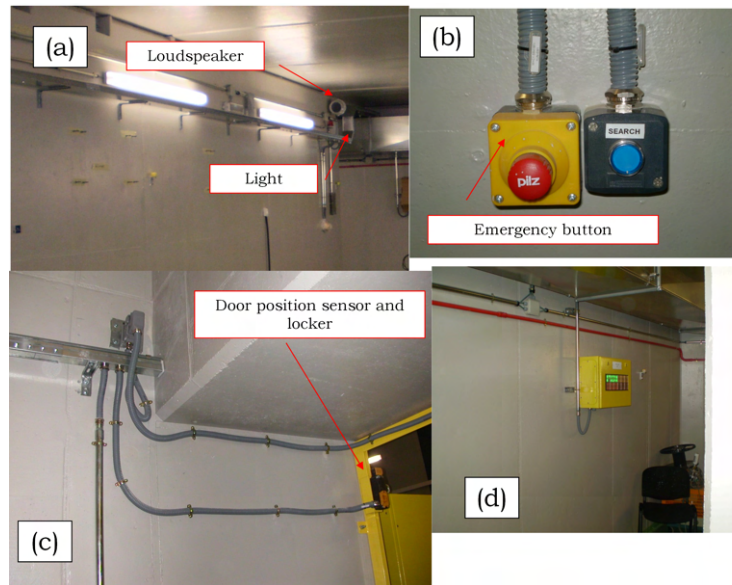


Fig. II.13.74: Search and lock-up PSS components for the ALBA tunnel: (a) PA loudspeakers and light, (b) search and emergency stop buttons, (c) door shut sensor and locker, and (d) status panel.

In any emergency situation, when somebody is left inside the shielding, or a radiation monitor detects a dose higher than expected, the PSS must be capable of stopping the cause of the radiation, i.e. the accelerators, or to blocking the radiation to avoid any unwanted exposure, which could happen in the beamlines. For example, to stop the ALBA accelerators, the PSS must switch off the following components:

1. The LINAC 's elements are as follows:

- (a) Electron gun,
- (b) RF klystron,
- (c) Bending magnet,
- (d) Bremsstrahlung shutter.

2. The booster 's elements are as follows:

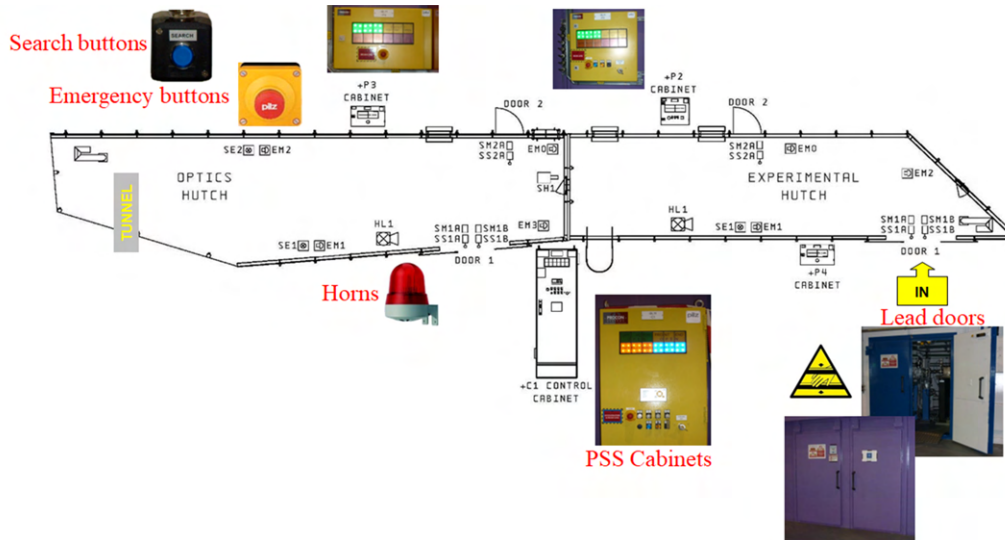


Fig. II.13.75: An example of an ALBA beamline PSS components and their locations inside and outside the lead panel shielding.

- (a) RF IOT,
 - (b) Dipoles power supplies.
3. The storage ring's elements are as follows:
- (a) All the RF IOTs,
 - (b) Dipoles power supplies.

In the case of the ALBA beamlines, the PSS acts independently in each of the beamlines, in such a way that the accelerators can run if beamline access doors are opened once the search and lock-up have finished. Only in some very specific circumstances, can the beamline elements stop all the accelerators.

The beamline elements which the PSS are connected to are the photon shutter (they are refrigerated copper blocks to absorb the infrared radiation), the bremsstrahlung shutters (tungsten blocks placed next to the photon shutters) located in the ALBA Storage Ring front ends, and the safety shutters (consisting of a tungsten block), situated between the optical and the experimental hutches.

The network of the radiation monitors is connected to the PSS by dedicated SIL-3 relays, to ensure that if any of the radiation monitors around the ALBA accelerators and beamlines detects an accumulated dose higher than 4 μSv in 4 hours, all the accelerators are stopped in some milliseconds. Figure II.13.76 shows how the radiation monitors are connected to the PSS and Fig. II.13.77 indicates the radiation monitors deployment across the ALBA accelerators and beamlines.

II.13.6.2 Administrative approach

Once all the engineering control measures are in place, they are insufficient to control the ionising radiation risk. This is the purpose of the administrative approach, where a set of programmes, manuals, plans,

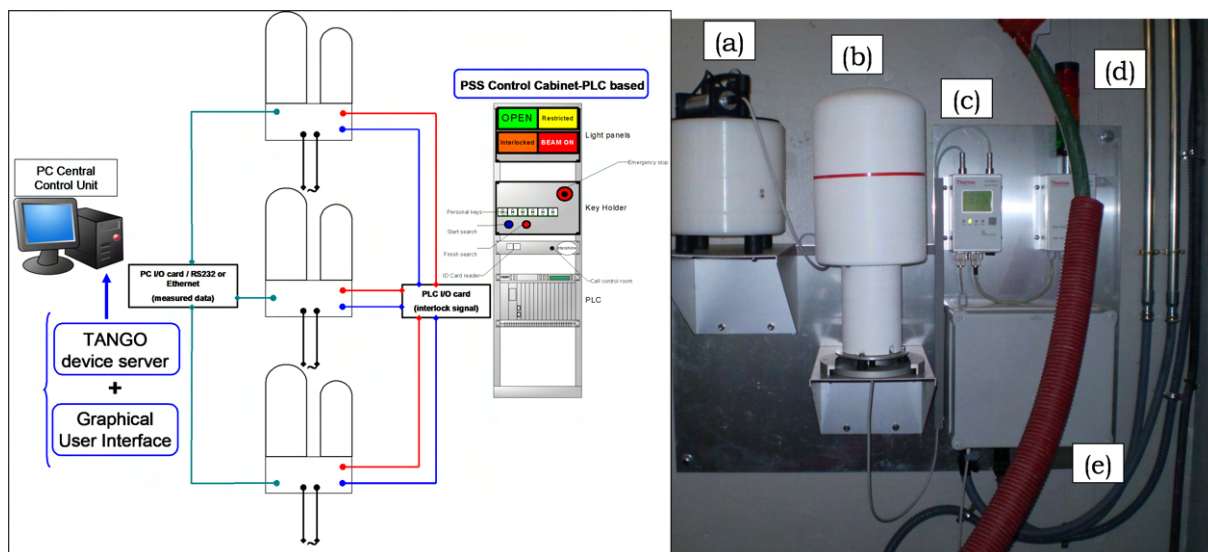


Fig. II.13.76: (Left) diagram showing the connections between the network of the radiation monitors and the PSS cabinet. (Right) one of the radiation monitors attached to the ALBA tunnel wall, indicating (a) neutron probe (Wendi model), (b) gamma probe (FH-190 model), (c) control unit, (d) light and horn unit, and (e) relay and communication box.

procedures, action lists, and check lists must be established to reach the ALARA stage. Two examples of these administrative control measures are how to manage the access and egress of relevant areas close to the radiation sources and how to control the use of these radiation sources, i.e. how to guide the correct use of all the accelerators and the components that have a direct impact in producing the ionising radiation.

II.13.6.2.1 Access and egress control

A common practice to inform and monitor the people that are next to a radiation source area is providing training and placing the right signage in all the access doors. If there is no risk at all to be exposed above the 1 mSv/year limit, the signage access door may be used to indicate the access to the area name, see as an example Fig. II.13.78.

However, if there is a possibility that a person is exposed to an annual dose value higher than 1 mSv/year (supervised or controlled areas), it is very important to ask them to wear a personal (passive or electronic) dosimetry and control and record the values of these readings (see Fig. II.13.79).

There are two basic rules when a personal dosimetry is issued. The first one is that everybody in the designated areas (supervised or controlled) must wear a personal dosimeter, and the second is that they must wear the personal dosimeter (a TLD for the ALBA and ISIS facilities) during the whole workday and wear it in a visible place (chest) and do not knock it nor warm it up (i.e. do not put it next to a heater). Depending on the task use an EPD to get an instant reading (like in the signage shown in Fig. II.13.80).

In some areas, and sometimes on a temporary basis, a prohibited access “do not enter” signage is needed to ensure that nobody is in a presence of high dose rate levels (see Fig. II.13.81).

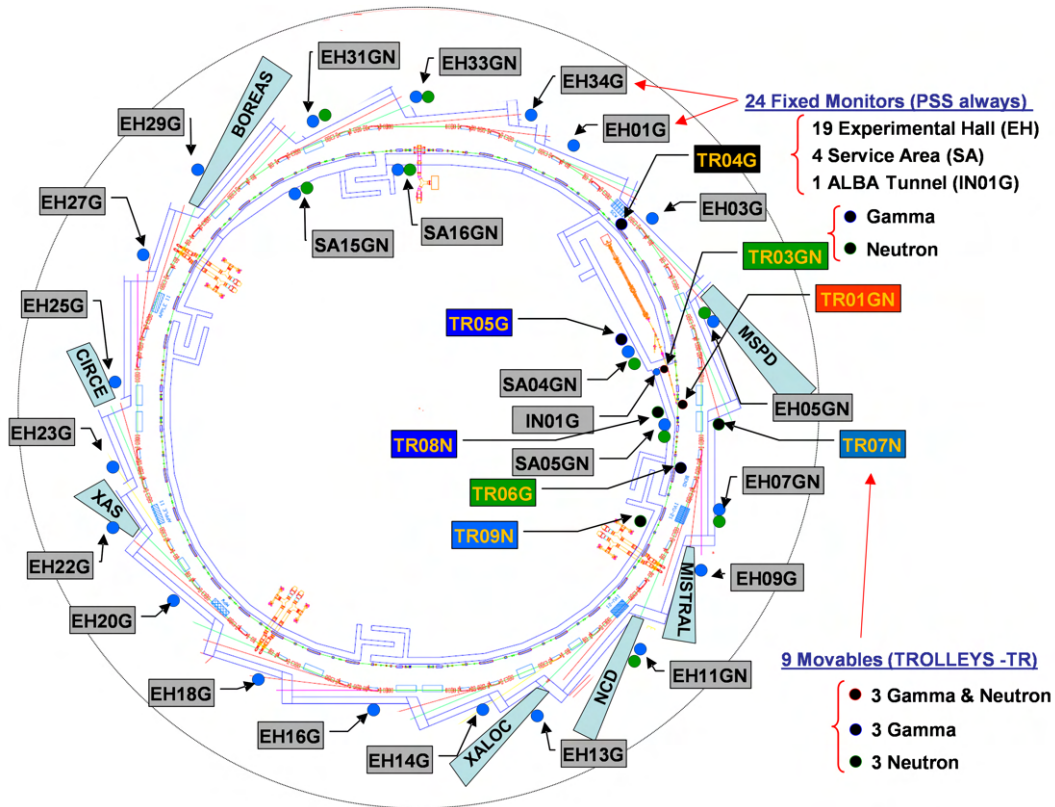


Fig. II.13.77: Top view scheme of the location of the radiation monitors attached to the ALBA tunnel walls and beamline lead panel hatches.



Fig. II.13.78: An example of door signage indicating the free access to the ALBA Experimental Hall.

II.13.6.2.2 Operational control

The signage of all the access doors must be coordinated and supervised by the staff who are operating the accelerators, i.e. the Control Room Crew. They must always know what the machine conditions are and adapt all the information to the operating conditions.

The most critical situation in any accelerator is during commissioning, where it is the first time a beam is accelerated or after a significant accelerator improvement. Following the flowchart given in Fig. II.13.82 is very important in establishing the minimum current values needed for the diagnostic system. Once a current is established, measure the radiation levels, and if the values are higher than expected, stop and take action. Perform a radiation risk assessment of the known condition and decide what to do next. This kind of approach must be agreed upon by all the teams involved in the commissioning



Fig. II.13.79: Example of the two types of personal dosimeters used to monitor the individual dose in controlled areas in ALBA (left) TLD gamma personal badge and (right) Electronic Personal Dosimeter-EPD and log file.



Fig. II.13.80: An example of door signage indicating the restricted access to the ALBA Experimental Hall and the requirement for using an EPD.

and supported by the facility's senior management.

II.13.7 Radiation monitors

II.13.7.1 Gamma detectors

II.13.7.1.1 *Passive type for personal dosimetry*

The standard way of controlling the annual dose limits is providing a dosimeter to all the workers exposed to ionising radiation sources in order to measure the possible radiation fields X-rays (γ -rays), beta and neutron radiation. The personal dosimeters must be worn whenever the worker is exposed to radiation during the calendar year.

There are two types of personal dosimeters, depending on the readout process. If the dosimeters have to be read by an external process, they are called passive dosimeters. In the case of an electronic-based reading, they are called electronic dosimeters. Both methods provide an estimation of the dose received by the worker. The personal electronic dosimeters provide an instant reading compared with the passive one, allowing one to assess the dose level after any task where dose control is critical.

However, the passive dosimeters are read depending on the type of work and the characteristics of the exposure to the radiation, and the personal dosimeters might be read monthly or quarterly, and in some situations after a high dose task is finished.

In case of the passive dosimeters, it is widespread to use thermoluminescence crystal detectors (TLD, see Fig. II.13.83) to measure X-ray, γ -ray or beta. These detectors are based on LiF doped with



Fig. II.13.81: An example of door signage indicating the prohibited access to the ALBA Experimental Hall.

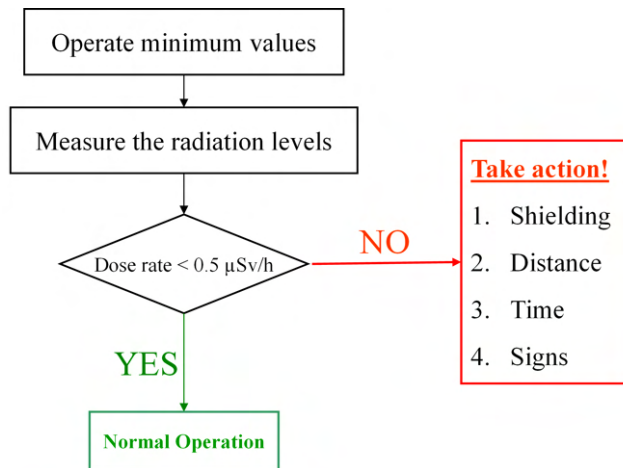


Fig. II.13.82: Flow diagram indicating the steps to follow during the commissioning of any of the accelerators or beamlines.

Mg, Cu and P and can measure from 20 μSv to 10 Sv. The crystal is mounted in a support with a filter system to distinguish the energy radiation and type of particle (photons or beta). The location of the personal (body) dosimeters is close to the chest and uncovered. The body personal dosimeters (passive or electronic) can be supported by extra specific dosimeters (passive or electronic) to measure the doses received at the hands, fingers (see Fig. II.13.84), wrist, belly (for the fetus) or eyes, depending on the workers' activities.

II.13.7.1.2 Gas-filled detectors

When a pressurised gas inside a chamber is exposed to ionising radiation and a controlled electric field is applied, the electrons generated produce a tiny current proportional to the intensity of the ionising radiation (see Fig. II.13.85).



Fig. II.13.83: An example of TLD badge and crystal distribution with the filters and windows locations.



Fig. II.13.84: (Left) is another example of a TLD dosimeter badge (body) and the right wearing location. (Right) is an example of a finger TLD dosimeter.

The amount of charge produced (see Eq. II.13.37) is proportional to the energy absorbed by the gas (E)

$$N_{pairs} = \frac{E}{w}, \quad (\text{II.13.37})$$

where w is the energy needed to ionise one atom (see Table II.13.20 for some common gases used). Therefore the dose rate is proportional to the rate of the charge created, as given by Eq. (II.13.38)

$$\frac{dD}{dt} \propto \frac{w}{\rho_{gas} \cdot V_{gas}} \cdot \frac{dN_{pairs}}{dt}, \quad (\text{II.13.38})$$

where ρ_{gas} and V_{gas} are the gas density and volume.

Thus it is proportional to the current circulating in the circuit, then Eq. (II.13.38) can be expressed as

$$\frac{dD}{dt} \propto \frac{w}{e \cdot \rho_{gas} \cdot V_{gas}} \cdot I. \quad (\text{II.13.39})$$

It means that for a given gas condition, the dose rate is proportional to the current. This is the basics of a gas detector. Depending on the voltage applied on the pressurised gas, there are three different regions on the curve current vs voltage (see Fig. II.13.86).

The three zones define the operation regimes as follows:

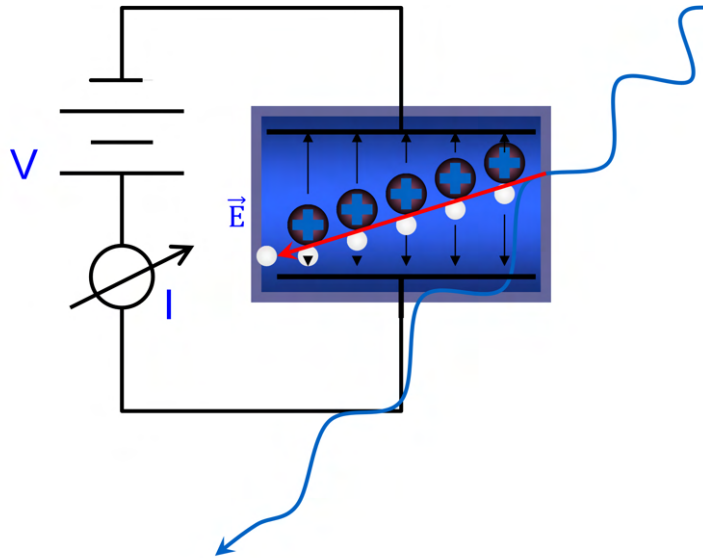


Fig. II.13.85: Diagram of the electric circuit where the ionising radiation produces a pair electron-hole in a gas under a high voltage (V) electric field, and the current (I) is measured.

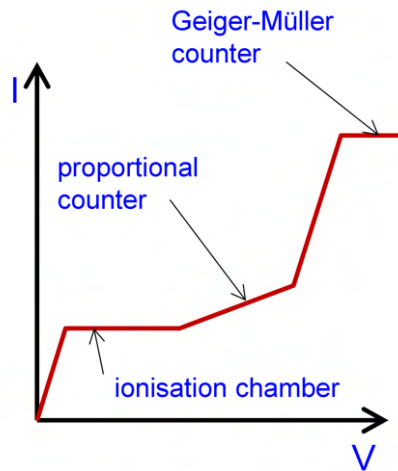


Fig. II.13.86: Characteristics graph, applied voltage- V vs measured current (I) in a filled gas chamber, indicating the different regimes: ionisation chamber, proportional counter and Geiger-Müller counter.

- Ionisation chamber: at low voltage variations the current is kept constant (see Fig. II.13.87),
- Proportional counter: at higher voltage, the current is proportional to the voltage applied (see Fig. II.13.88).
- Geiger-Müller counter: the current is saturated at very high voltage (see Fig. II.13.89).

Table II.13.20: Ionisation energy (w) for different types of particles as a function of the filled gas.

w	H2	He	O2	Ar	Air
e^-	36.3 eV	41 eV	31 eV	26.4 eV	34 eV
α	36.5 eV	44 eV	32.4 eV	26.4 eV	35.3 eV



Fig. II.13.87: Three examples of handheld monitors based on ionisation chamber detectors.



Fig. II.13.88: One example of handheld monitors is based on a proportional counter detector (right) and the possibility to use multiple probes with different detector types, such as ionisation chambers.

II.13.7.2 Neutron detectors

II.13.7.2.1 Passive type for personal dosimetry

To measure neutron doses, one possible material is the one based on poly-allyl diglycol carbonate (PADC, also called CR-39, see Fig. II.13.90), and they can measure doses from 200 μ Sv to 200 mSv.

In both cases, the operational personal dose provided is given in personal dose equivalent $H_p(10)$ (10 mm depth) or $H_p(0.07)$ (0.07 mm depth).

The values provided by the passive detectors, for gamma or for neutrons, are calculated using algorithms that convert the measure magnitude, in the case of the PADC film “number of dots”, to personal dose equivalent in mSv. Figure II.13.91 shows a set-up of a measurement carried out with two different suppliers of neutron badges, being irradiated by an AmBe neutron source in the same way in a controlled environment. The badges are placed in between by 5 cm thickness block in two different locations.

The results of this test is shown in Table II.13.21, where it can be seen that the values from the same badges supplier (Sup1 or Sup2) in the same layer are very similar, but there is a significant variation



Fig. II.13.89: Three examples of handheld gamma monitors based on Geiger-Müller counter.



Fig. II.13.90: An example of a neutron dosimeter badge (bottom) and the PADC film (clear-top left and exposed-top right).

if we take the same layer but from different suppliers.

Table II.13.21: Comparison of the neutron dose values from two different suppliers (Sup1 and Sup2).

#	POSITION	Poly thickness [cm]	Sup1 Dose [mSv]	Sup2 Dose [mSv]	(Sup1-Sup2) [%]
1	1a	0	25.63	22.80	11.04%
2	1b	0	28.28	22.50	20.44%
3	2a	5	9.33	12.20	-30.76%
4	2b	5	10.22	11.90	-16.44%
5	3a	10	3.96	4.70	-18.69%
6	3b	10	4.65	5.10	-9.68%
7	4a	15	1.63	2.40	-47.24%
8	4b	15	1.68	1.90	-13.10%

II.13.7.2.2 Moderated neutron detectors

The electronic neutron detectors are based on the reaction between the neutron and an atom. As a result of this reaction a charged or a energetic photon is produced, and the effect of these secondary particles with the detector sensor produce a current or a voltage and this output is converted in equivalent ambient dose in Sv or Sv/h, or in more general case in counts per unit time.

Reactions (II.13.40) and (II.13.41) show two different neutron reactions with ^3He and ^{10}B atoms

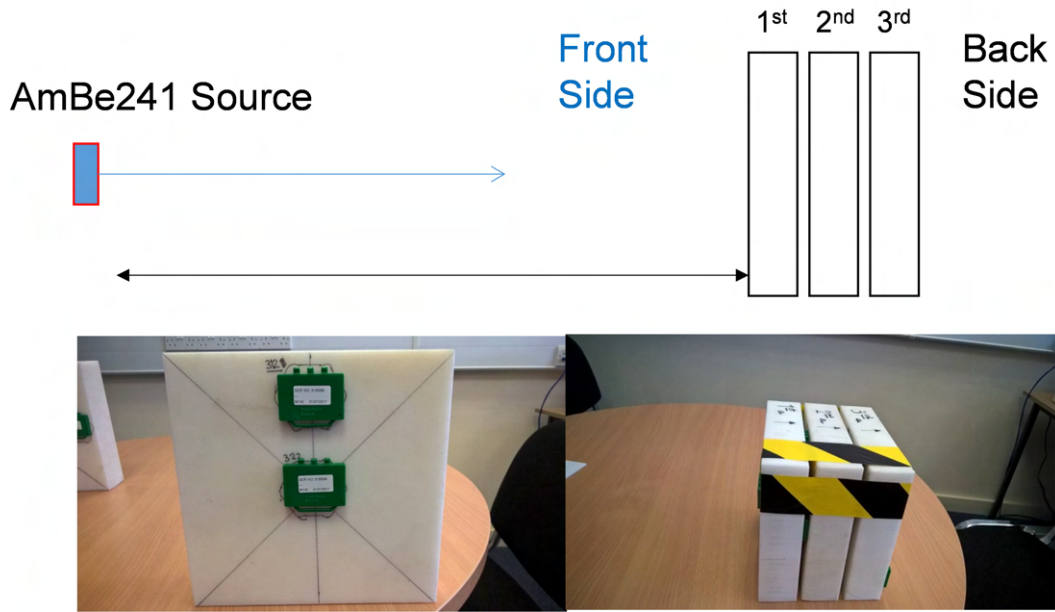


Fig. II.13.91: (Top) side view of the test carried out to check the spread of data reading depending on the passive neutron supplier. (Bottom) detailed of the location of the neutron badges in the polyethylene layers, and the set exposed to the AmBe241 source.

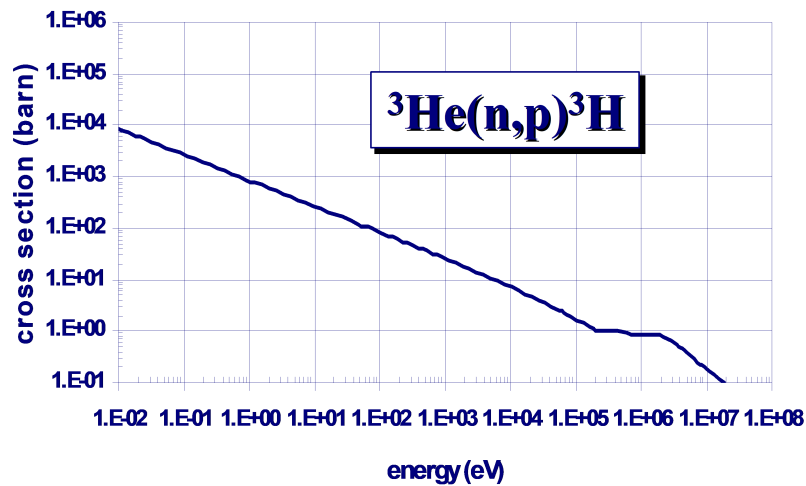
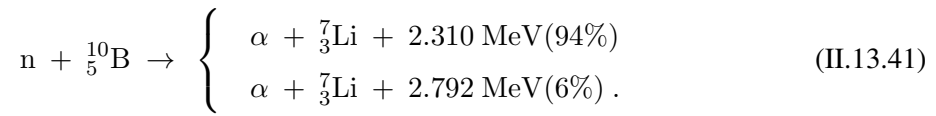


Fig. II.13.92: ${}^3\text{He}(n,p){}^3\text{H}$ cross-section reaction for neutron energies in the range of 10 meV to 100 MeV.

respectively, producing in both cases high-energy photons that interacting with the atoms of the detector sensor will produce electronic charge, and then an electric current





The value of this current will depend on the neutron flux and its energy. The probability of interaction with these atoms (cross-section) is almost decreasing linearly with the neutron energy as it is shown in Fig. II.13.92 and Fig. II.13.93 for the two in question materials. Above 10 keV, the value of the cross-section is reduced by three orders of magnitude.

To enhance the detection in the region above 10 keV, the high energy neutrons must be moderated and therefore they can be detected more easily. To achieve this behaviour, it is very common to put a neutron moderator (polyethylene) to increase the response in this energy range.

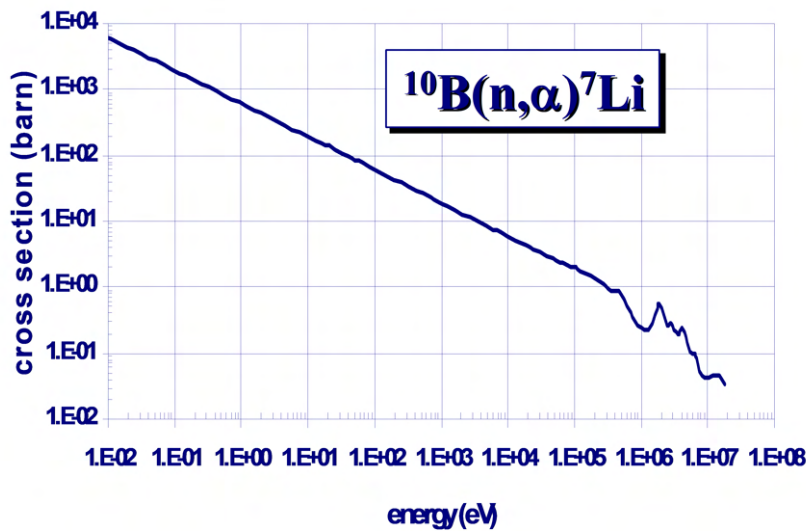


Fig. II.13.93: ${}^{10}\text{B}(n, \alpha) {}^7\text{Li}$ cross-section reaction for neutron energies in the range of 10 meV to 100 MeV.

Figure II.13.94 shows the energy response for the Cramal-31 detector. It is a portable monitor for the measurement of neutron ambient dose equivalent and ambient dose equivalent rate. The monitor comprises a 200 mm diameter polyethylene sphere for neutron moderation with a cadmium liner, which encloses a ${}^3\text{He}$ filled proportional counter. This monitor was originally designed for measurement of neutrons with energies from 2 keV to 15 MeV. Some examples of commercial handheld neutron detectors are shown in Fig. II.13.95.

To reduce the photon flux reaching the sensor part of the detector, it is very common to put a layer of lead or tungsten to suppress the spurious current. Figure II.13.96 shows two different neutron detectors design using a moderator and lead layers. In this way, the energy response for both can reach above 1 MeV neutrons.

The neutron energy response depends heavily on the detector material, moderator and shield-

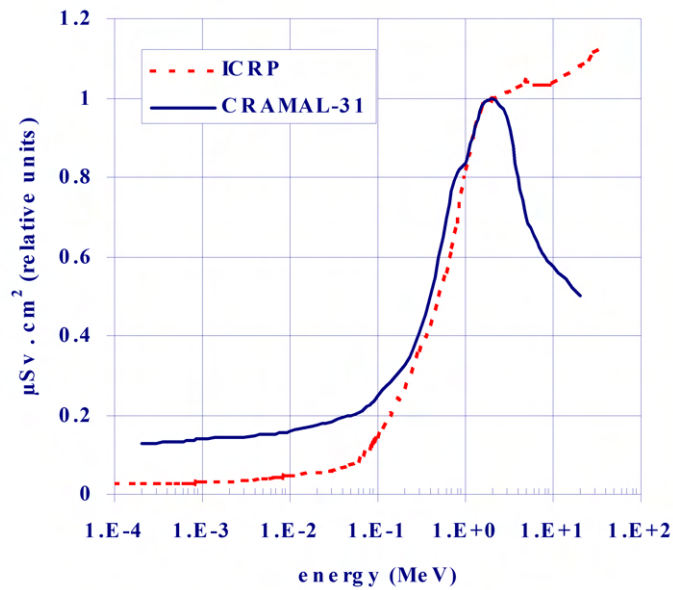


Fig. II.13.94: Cramal-31 handheld detector energy response compared with the ICRP data.



Fig. II.13.95: Three examples of handheld neutron monitors based on polyethylene moderator.

ing material and the geometry. The difference can be more than 40% depending on the range of energy considered. Due to the fact that the neutron equivalent dose depends on the neutron energy (see Sec. II.13.3.1), the equivalent dose measure by one detector can be substantially different to another. Figure II.13.97 shows the response function (counts/cm²) for four different commercial detectors, where there is more than one order of magnitude difference between them and also within the same detector.

To check this behaviour, a test with seven neutron detectors, in five different positions (see Fig. II.13.98 Right), was carried out in ISIS on the top of the intermediate target, where a fraction of the 800 MeV proton beam collides with a small block of carbon producing muons. Figure II.13.98 (Left) shows the measured dose rate values for each location. The biggest difference (six times higher) is in the central position, while on the sides the values are only two times higher. Even with the same type of detectors (Priscila case), the readings are higher for all the positions (the same accredited laboratory calibrated both detectors).

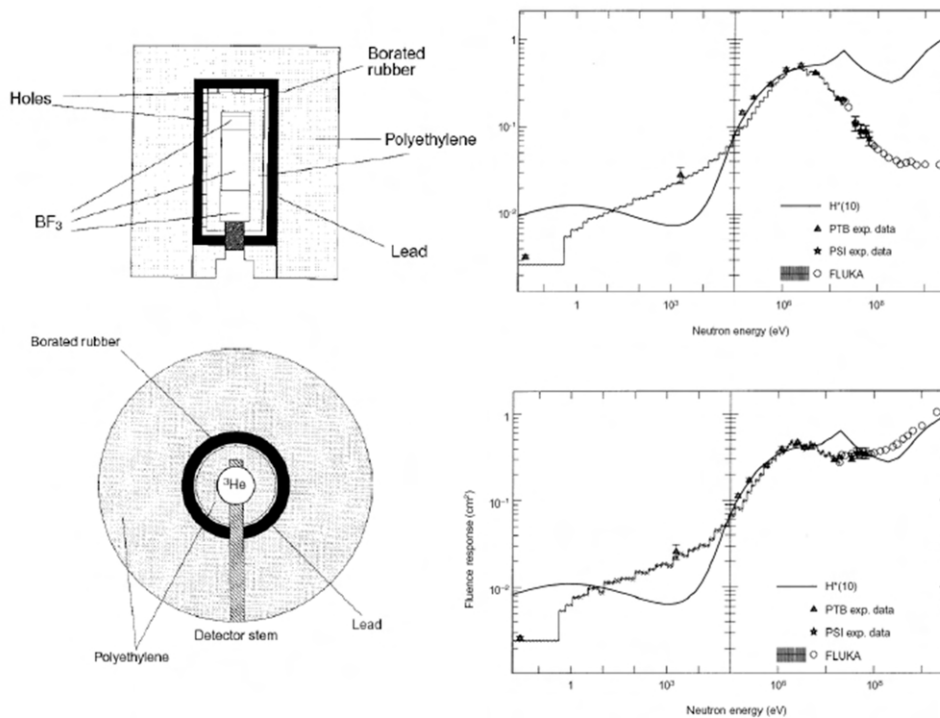


Fig. II.13.96: Neutron response using lead-shell in moderator type for two different counters (BF3 and He3 based).

In summary, Table II.13.22 presents the main characteristics (particle detected, energy range, measuring range, energy response, quantity displayed, type of detector, the sensitive material and the dead time) for three handheld instruments.

II.13.7.3 Network of area radiation monitors

The accelerator beam current stability is one of the main challengers in operational beam dynamics. There are several factors that may affect the stability of the beam, such as:

- Magnet power supplies stability,
- RF power supplies stability,
- RF cavities temperature,
- Cooling water circuit temperature for magnets and RF cavities,
- Air temperature in the accelerator enclosure,
- Mechanical vibrations.

All these instabilities can produce changes on the beam position or on the beam size, or on both. As a consequence of that, the beam losses can increase in some accelerator areas, and therefore the dose rates outside the shielded area can change (increase). To monitor and record all these changes a network of radiation monitors (see Fig. II.13.77) is used. For instance, in the “top-up mode” in a synchrotron light facility, every ten minutes a small beam is injected in the Storage Ring, the changes in the Storage Ring can produce more beam current losses and could be monitored remotely by this network as shown in

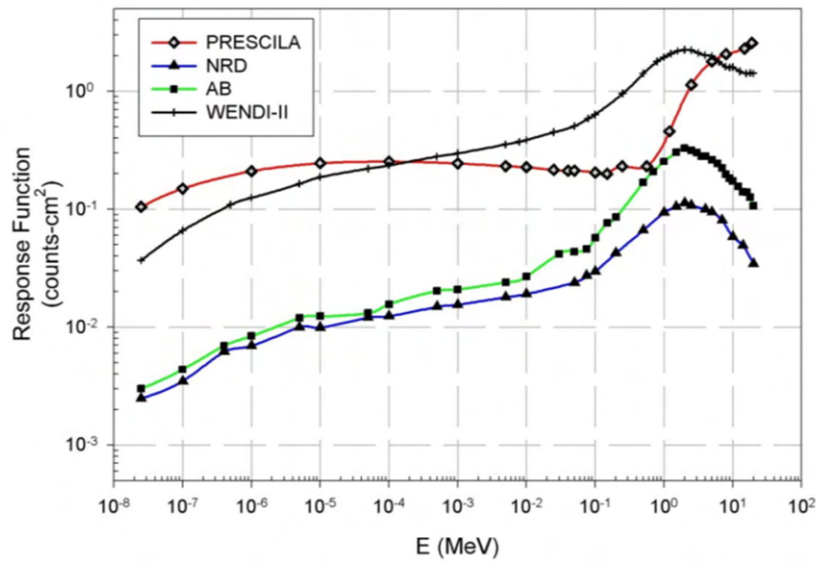


Fig. II.13.97: Neutron energy response for different handheld neutron detector manufacturers.

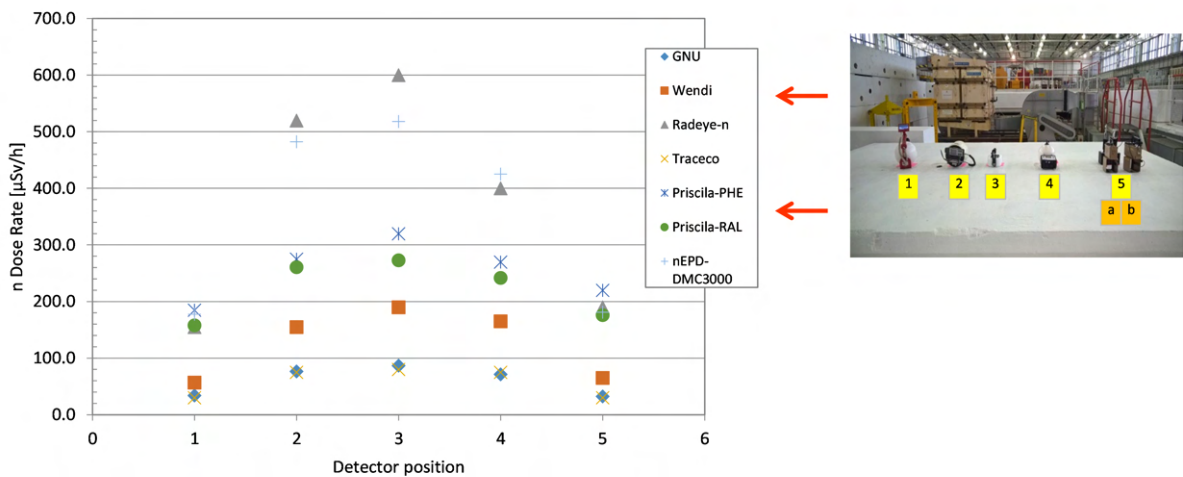


Fig. II.13.98: Left: intercomparison for a given location in ISIS facility for different handheld neutron detector manufacturers. Right: neutron dose rate for the five different locations.

Fig. II.13.99). The changes in the stored current at every injection are shown at the bottom of the figure, and the peak in the dose rate is at the top.

During accelerator commissioning it is very frequent to experience beam current instabilities. At ALBA facility, a set of movable radiation monitor units were deployed in areas such as the Booster to Storage Ring transfer line, where the beam losses were expected. Figure II.13.100 shows the position of all these monitors.

Using the accumulated total dose data (integrated over four hours), see Fig. II.13.101, it was very clear when it was necessary to change the area designation from controlled to supervised.

Table II.13.22: List of the main characteristics of typical handheld monitors used in accelerator-based facilities.

#	Characteristics, model and manufacturer	FHT192 (Thermo)	FHT 762 (Wendi-2) (Thermo)	EPD (Thermo)
1	Particle	Photons	Neutrons	Photons
2	Energy range	30 keV–7 MeV	25 meV–5 GeV	15 keV–10 MeV
3	Measuring range	100 nSv/h–1 Sv/h	1 nSv/h–100 mSv/h	Resol. 1 mSv/h: < 0.5 Sv/h–4 Sv/h Resol. 1 Sv/h: 4–50 Sv/h
4	Energy response	Calibration factor resp. Cs-137: For low dose rate: 0.01–0.02 (μSv/h)/cps For high dose rate: 1.9–2.2 (μSv/h)/cps	Calibration factor: ± 30% from 17 keV–6 MeV ± 50% from 6 MeV–15 MeV	Ref. Cs-137
5	Quantity	Hp(10)	Hp(10)	Hp(10)
8	Type	Active ionisation chamber	Active proportional counter	Active semiconductor dosimeter
9	Sensitive material	Inert gas (7 bar)	He-3 (2 bar) + polyethylene moderator	Silicon diode detectors
10	Dead time	Dead time for high dose rate: 6–7 μs	Dead time: 1.8 μs	–

Also it allows to understand the contribution of the gamma and neutron dose rates (measured every two seconds) to the accumulated total dose, and the presence of spurious losses that produce high dose rate peaks (see Fig. II.13.102).

Another application of measuring and recording the dose rate using a computer is to monitor the effect of a machine physics test during the commissioning phase. In particular, to measure the beam size delivered by the LINAC to the Booster synchrotron in ALBA, a movable collimator (“scraper”) was used. Figure II.13.103 shows the effect of the beam losses depending on the scraper position on the gamma dose rate outside the shielding. This result confirmed that the extra shielding put on the wall (see Fig. II.13.63) effectively reduced the dose rate to a public level even when doing this kind of test.

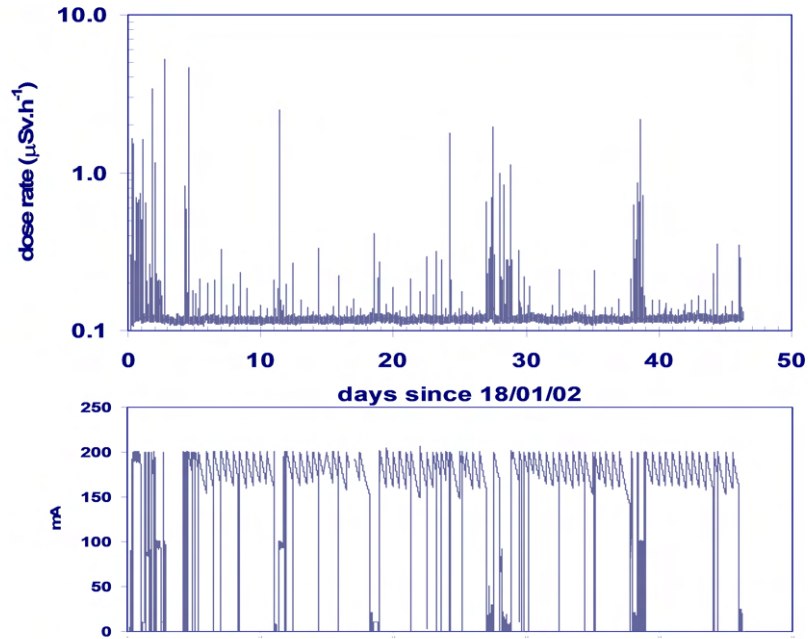


Fig. II.13.99: (Top) photon dose rate measurement in a location outside the ESRF storage ring shielding. (Bottom) beam current in the storage ring.

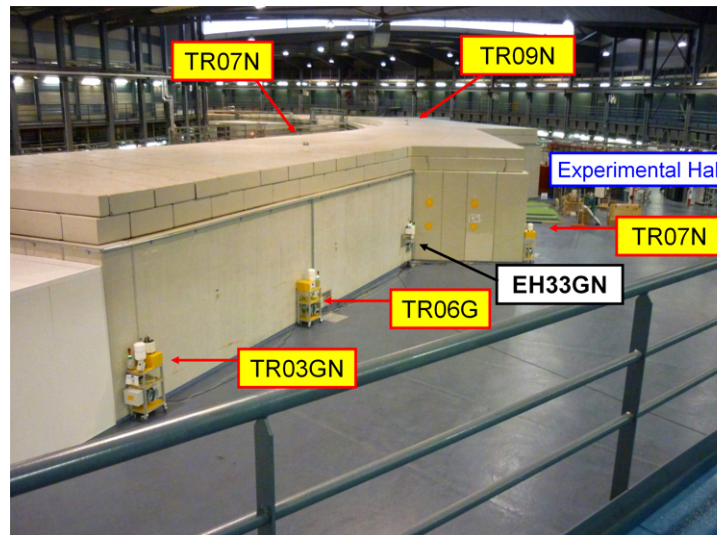


Fig. II.13.100: Photo showing the deployment of the movable radiation monitor units outside the ALBA tunnel during the Storage Ring commissioning phase next to the injection Booster to the Storage Ring.

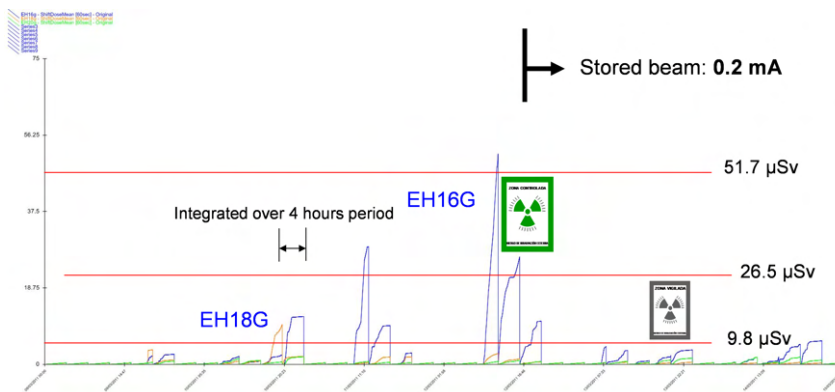


Fig. II.13.101: Time vs accumulated dose (over 4 hours) outside the ALBA tunnel shielding during the Storage Ring commissioning, before and after the stored beam was achieved.

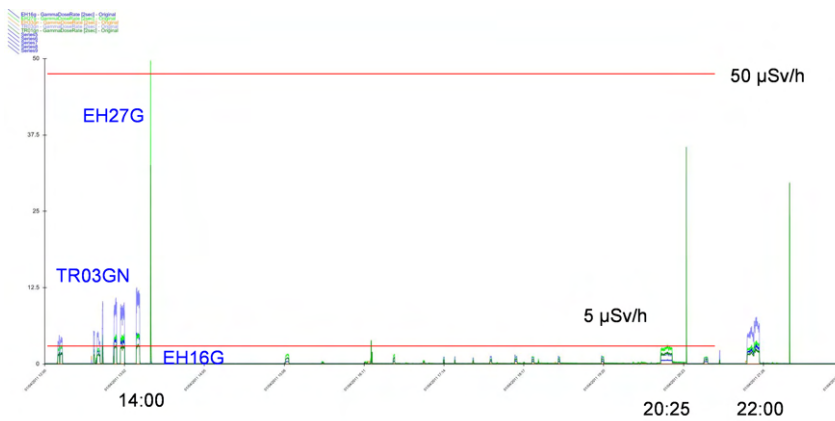


Fig. II.13.102: Time vs gamma dose rate (two-second data) outside the ALBA tunnel during the beam current increase attempts in the commissioning phase.

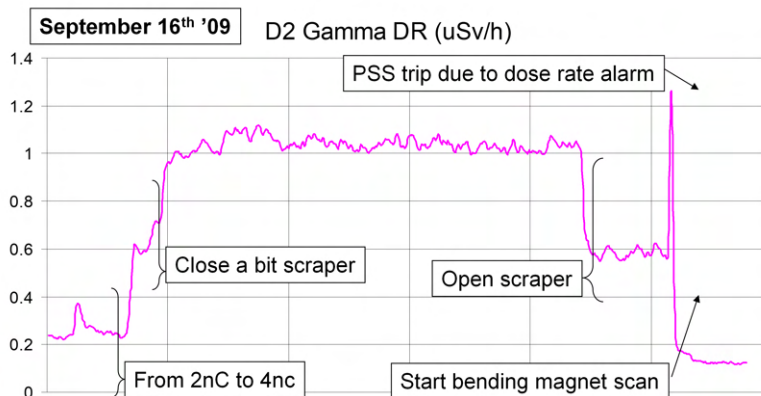


Fig. II.13.103: Time vs gamma dose rate (two-second data) outside the ALBA LINAC bunker during a beam size measurement.

II.13.8 Exercises

II.13.8.1 Multiple answer questions

- 1) In the high-energy accelerators scenario, the dose rate out of the shielding area is mainly due to:
 - a. Synchrotron radiation
 - b. Gas bremsstrahlung radiation
 - c. Activation of the solid accelerator components
 - d. Solid bremsstrahlung radiation
 - e. Electromagnetic cascade

- 2) If we have to designate a zone as a public zone, the dose-rate level that we have to use as a reference is (in the International System unit and the background removed):
 - a. 1 $\mu\text{Sv/day}$
 - b. 0.1 $\mu\text{Sv/h}$
 - c. 0.5 mSv/h
 - d. 0.5 mSv/month
 - e. 0.5 $\mu\text{Sv/h}$

- 3) The radiological magnitude that allows the comparison of the influence of the radiation nature is (according to the type of the particle involved):
 - a. Activation
 - b. Effective dose
 - c. Exposure
 - d. Absorbed dose
 - e. Equivalent dose

- 4) The gas-filled detectors are based on the following physical phenomena:
 - a. Gas bremsstrahlung by a charged particle
 - b. Photo-electric effect by a neutral particle
 - c. Coherent scattering by a radiation particle
 - d. Gas ionisation by a radiation particle
 - e. Compton scattering by a radiation particle

- 5) The ICRP (International Commission on Radiological Protection) in its publication no. 103 recognises three types of exposure situations:
 - a. Scheduled / Medical / Natural
 - b. Natural / Emergency / Scheduled
 - c. Scheduled / Planned / Natural

- d. Planned / Emergency / Existing
 - e. Isotropic / Planned / Natural
- 6) Generally speaking, any particle with a given energy can produce some dose contribution, but in the radiation protection field, the main contribution comes from:
- a. Alphas, electrons, neutrons and protons
 - b. Quarks, muons, electrons and protons
 - c. Muons, neutrons, electrons and protons
 - d. Betas, electrons, positrons and protons
 - e. Alphas, electrons, neutrons and photons
- 7) For exposed workers, the maximum effective dose per year (on average over a 5-year period, and above the background level) is:
- a. 6 mSv
 - b. 1 mSv
 - c. 50 mSv
 - d. 20 mSv
 - e. 100 mSv
- 8) There are three types of gas detectors: ionisation chambers, proportional counters and Geiger-Müller counters; this classification is based on:
- a. The pressure of the gas
 - b. The volume and pressure of the gas
 - c. The voltage vs. current characteristic
 - d. The voltage of the gas
 - e. The type of the gas
- 9) In all the radiation protection situations, the implementation of the ALARA principle obliges one to deal with three aspects of the radiation source environment:
- a. Distance between the radiation source and the worker involved / Shielding characteristics / Exposure time
 - b. Distance between the radiation source and the detector involved / Shielding characteristics / Average annual hours worked per worker
 - c. Distance between the shielding and the worker / Source characteristics / Exposure time
 - d. Distance between the source and the shielding / Shielding characteristics / Exposure time
 - e. Distance between the radiation source and the worker involved / Shielding characteristics / Average annual hours worked per worker
- 10) According to the ICRP, the ALARA principle is one of the three key principles of radiological protection, and it stands for:

- a. As Light As Reasonably Achievable
- b. As Low As Reasonably Approved
- c. As Low As Reasonably Achievable
- d. As Light As Reasonably Approved
- e. As Late As Reasonably Achievable

11) The unit (International System) and the symbol for the effective absorbed dose is:

- a. Sievert / sb
- b. Gray / Gy
- c. milliSievert / mSv
- d. Sievert / Sv
- e. Siemens / S

12) The electromagnetic cascade explains the interaction of:

- a. Protons with matter
- b. Photons with neutrons
- c. Electrons with matter
- d. Electrons with photons
- e. Photons with matter

13) When the Personnel Safety System (PSS) has to stop the accelerator, this feature is based on the following principle:

- a. It must be redundant and diverse
- b. It must be tested regularly
- c. It must be quick and safe
- d. It must be efficient and fast
- e. It must be redundant and quick

14) The specific characteristic that defines a beam dump for an electron beam is:

- a. The radius of the beam dump
- b. The location of the beam dump
- c. The length of the beam dump
- d. Only the material of the beam dump is relevant
- e. The Molière radius of the beam dump, for a given material

15) The Personnel Safety System (PSS) is an engineering solution used in order to guarantee that:

- a. The accelerator is working fine
- b. The RF cavities and the bending magnets are off

- c. The ionisation radiation hazard is completely removed
- d. The injection components are disabled
- e. Nobody is inside the accelerator bunkers and nobody receives more than 1 mSv in a year (above the background level)

16) For unexposed workers and the public, the maximum allowed effective dose per year is (above the background level):

- a. 1 Sv
- b. 1 μ Sv
- c. It will depend on the ALARA principle
- d. 1 mSv
- e. 0 Sv

17) The natural background level depends on the local area conditions. However, it is possible to say that the effective dose that we are exposed to coming from the background is in the order of (in a year):

- a. 0.5 μ Sv
- b. 5 mSv
- c. 0.1 mSv
- d. 0 mSv
- e. 240 mSv

18) The particle-matter interaction is usually defined by a physical magnitude called cross-section and, if for a given particle energy and material this value is very high, it means that:

- a. The probability for this interaction is higher than 0.5
- b. The probability for this interaction is very low
- c. It has no relation at all with the probability for this interaction
- d. There is no relation between the probability for this interaction and the cross-section
- e. The probability for this interaction is very high

19) The interaction of the photons with the matter follows the law given by:

- a. An exponential function
- b. The proportionality of the material density
- c. It depends on the photon energy
- d. The inverse of the thickness square of the material
- e. The proportionality of the material cross-section

20) “Once the high-energy particle accelerator is switched off, the radiation risk disappears”, this sentence is correct:

- a. For all cases

- b. Only for high-energy protons
- c. Never
- d. Only for high-energy electrons
- e. If we do not take into account the induced-activity phenomena

II.13.8.2 Problems

1) If we write the decay exponential law for a given radioactive nuclide A as

$$N_A(t) = N_A(0) \cdot e^{-\lambda t}$$

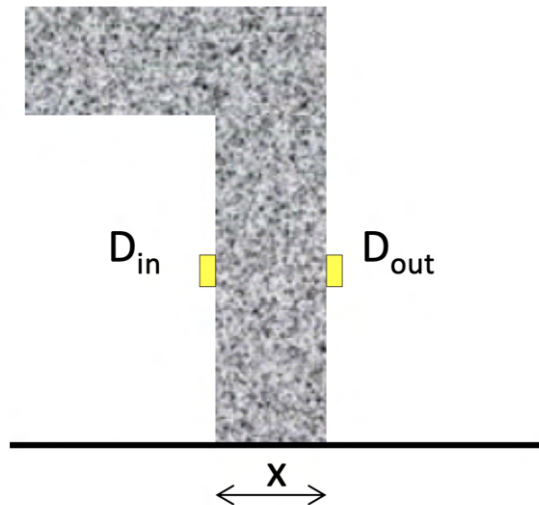
Q1: Define the nuclide lifetime τ .

Q2: What is the relation between τ and λ ?

Q3: Define the half-life of a nuclide $T_{1/2}$ and its relation with τ .

Q4: If we have a Na22 source of 10^6 Bq, what will be its activity after 100 days ($T_{1/2}[\text{Na22}] = 2.6018$ years)?

2) In a high-energy electron accelerator, there is a barite concrete shielding wall (see figure below).



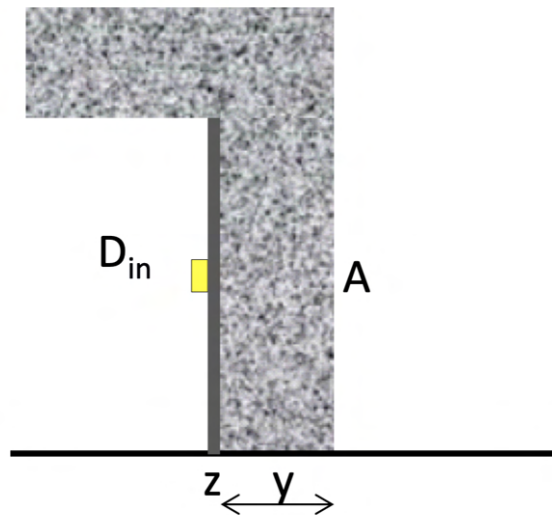
Inside the wall and attached to it (at 1.4 m height), there is a photon passive detector, and on the opposite position (out of the wall) there is another one (labelled as D_{in} and D_{out} respectively). After one year, the data measured from these detectors (effective dose, once the background contribution is removed) is $D_{in} = 228.3$ Sv and $D_{out} = 2.5$ mSv. Assuming that:

- a. The dose is mainly coming from 2 MeV photons
- b. The build-up factor is negligible
- c. The mass attenuation factor for the barite concrete $\left(\frac{\mu}{\rho}\right)_{\text{barite}} = 4.296 \times 10^{-2} \text{ cm}^2/\text{g}$
- d. The density for the barite concrete $\rho_{\text{barite}} = 3.35 \text{ g/cm}^3$

Q: What is the value of the wall thickness x (in meters)?

3) Following with the same accelerator as in the previous exercise, we have put a 1 cm iron layer (z) inside the shielding (see figure below). Taking into account the same considerations as in the previous exercise and assuming that:

- a. The barite concrete thickness $y = 1.5$ m
- b. The value of $D_{in} = 228.3$ Sv
- c. The mass attenuation factor for iron $\left(\frac{\mu}{\rho}\right)_{iron} = 4.265 \times 10^{-2} \text{ cm}^2/\text{g}$
- d. The density for iron $\rho_{iron} = 7.874 \text{ g/cm}^3$



Q: Can the zone next to the outside shielding wall be designated (point A, see figure above) as a public zone? And why?

4) A given nuclide has a half-life of 30.08 years with an initial activity of 2.53×10^{10} Bq.

Q1: How long do we have to wait to get an activity value of 3% of the initial one (give the result in years)?

Q2: If 1 GBq of this nuclide generates a dose rate (at 1 m) $75 \mu\text{Sv/h}$, how long do we have to wait to designate the area farther than 1 m of the nuclide source as public?

II.13.9 Solutions to the exercises

II.13.9.1 Solutions to the multiple answer questions

- 1) d
- 2) e
- 3) e
- 4) d

- 5) d
- 6) e
- 7) d
- 8) c
- 9) a
- 10) c
- 11) d
- 12) c
- 13) a
- 14) e
- 15) e
- 16) d
- 17) b
- 18) e
- 19) a
- 20) e

II.13.9.2 Solutions to the problems

- 1)
- Q1

$$N_A(t) = N_A(0) \cdot \exp\left(-\frac{t}{\tau}\right)$$

$$\lambda = \frac{1}{\tau}, \quad \tau \text{ is the nuclide lifetime}$$

$$N_A(t) = N_A(0) \cdot \exp\left(-\frac{t}{\tau}\right) \Rightarrow \frac{N_A(t)}{N_A(0)} = \exp\left(-\frac{t}{\tau}\right) \Rightarrow \ln\left[\frac{N_A(0)}{N_A(t)}\right] = \frac{t}{\tau}$$

If $t = \tau$, then

$$\ln\left[\frac{N_A(0)}{N_A(\tau)}\right] = 1 \Rightarrow N_A(\tau) = \frac{N_A(0)}{e}$$

The lifetime τ is the time needed for a reduction of the initial radionuclide quantity $N_A(0)$ by a factor of $1/e \approx 0.368 = 36.8\%$.

- Q2

$$\lambda = \frac{1}{\tau}$$

Q3

$T_{1/2}$ is defined as the time such that the initial quantity of radioactive nuclide is reduced to half of its initial value:

$$N_A(T_{1/2}) = N_A(0) \cdot \exp\left(-\frac{T_{1/2}}{\tau}\right) = \frac{N_A(0)}{2} \Rightarrow \exp\left(-\frac{T_{1/2}}{\tau}\right) = \frac{1}{2}$$

Taking the logarithm yields

$$\ln(1) - \ln(2) = -\frac{T_{1/2}}{\tau} \Rightarrow T_{1/2} = \tau \cdot \ln(2) \approx 0.7 \cdot \tau$$

Q4

$$100 \text{ days} = \frac{1 \text{ year}}{365 \text{ days}} \times 100 \text{ days} = 0.274 \text{ years}$$

$$N_A(t) = N_A(0) \cdot \exp(-\lambda t) = N_A(0) \cdot \exp\left(-\frac{\ln(2)}{T_{1/2}} \cdot t\right)$$

$$N_A(t) = 10^6 \cdot \exp\left(-\frac{\ln(2)}{2.6018} \cdot 0.274\right) = 10^6 \cdot \exp(-0.073) = 10^6 \cdot 0.93 \approx 9.3 \times 10^5 \text{ Bq}$$

2) Assuming an exponential law for the attenuated dose on the other side of the shielding:

$$D_{\text{out}}(x) = D_{\text{in}}(0) \cdot \exp\left[-\left(\frac{\mu}{\rho}\right)_{\text{barite}} \cdot \rho_{\text{barite}} \cdot x\right]$$

$$\ln\left(\frac{D_{\text{out}}}{D_{\text{in}}}\right) = \ln\left(\frac{2.5 \times 10^{-3} \text{ Sv}}{228.3 \text{ Sv}}\right) = \left(-\frac{\mu}{\rho}\right)_{\text{barite}} \cdot \rho_{\text{barite}} \cdot x$$

$$\left(\frac{\mu}{\rho}\right)_{\text{barite}} = 4.296 \times 10^{-2} \text{ cm}^2/\text{g} \quad , \quad \rho_{\text{barite}} = 3.35 \text{ g/cm}^3$$

$$x = \frac{-\ln\left(\frac{2.5 \times 10^{-3}}{228.3}\right)}{4.296 \times 10^{-2} \times 3.35} = -\frac{\ln(1.095 \times 10^{-5})}{0.144} = \frac{11.13}{0.144} = 0.8 \text{ m}$$

The factor $1/r^2$ does not apply because of the short distance between the passive detectors.

3)

$$D_{\text{out}}(z) = D_{\text{in}}(0) \cdot \exp\left[-\left(\frac{\mu}{\rho}\right)_{\text{iron}} \cdot \rho_{\text{iron}} \cdot z\right]$$

$$D_{\text{out}}(y) = D_{\text{out}}(z) \cdot \exp \left[- \left(\frac{\mu}{\rho} \right)_{\text{barite}} \cdot \rho_{\text{barite}} \cdot y \right]$$

$$D_{\text{out}}(y) = 228.3 \times \exp(-0.335) \times \exp(-21.5874) = 6.9 \times 10^{-8} \text{ Sv} < 1 \text{ mSv}$$

The zone can be designated as a public area because the annual dose is less than 1 mSv.

4)

Q1

$$A(t = 0) = A(0) = A_0 = 2.53 \times 10^{10} \text{ Bq}$$

$$A(t) = A(0) \cdot \exp \left(-\frac{t}{\tau} \right) = 0.03 \times A_0$$

Replacing:

$$T_{1/2} = \tau \cdot \ln(2)$$

Then:

$$t = 2384 \text{ years.}$$

Q2

$$A(t) = A(0) \cdot \exp \left(-\frac{t}{\tau} \right) \Rightarrow D(t) = 75 \mu\text{Sv/h} \cdot \exp \left(-\frac{t}{\tau} \right) = 0.5 \mu\text{Sv/h}$$

$$-\frac{t}{\tau} = \ln \left(\frac{0.5}{75} \right)$$

Therefore, we will have to wait for 217.4 years.

Acknowledgement

My sincere thanks to P. Berkvens [33] for offering me the opportunity to give this lecture, providing all his experience on the structure of the content and supplying a large part of the material used. Also, I wish to thank K. Ott [34] for helping me a while ago in my first steps toward this exciting subject of radiation safety. Without their help, support and contribution, the presented chapter would not have been achieved. Lastly, to all the JUAS lecturers and staff who, in early 1994, guided and transmitted their passion to me in this breathtaking world of accelerator physics and technology.

References

- [1] For more information: <https://www.cells.es/en/>.
- [2] Copyright Consortium for the Construction, Equipping and Exploitation of the Synchrotron Light Source (CELLS).

- [3] For more information: <https://www.isis.stfc.ac.uk/Pages/home.aspx>. Photo copyright STFC.
- [4] Copyright UK Research and Innovation (UKRI-STFC).
- [5] Safety Glossary, Terminology Used in Nuclear Safety and Radiation Protection. Wien: IAEA, 2018, [IAEA Safety Glossary: 2018 Edition](#).
- [6] For more information <https://www.nobelprize.org/prizes/themes/marie-and-pierre-curie-and-the-discovery-of-polonium-and-radium/>.
- [7] For more information: <https://americanhistory.si.edu/girlhood/work/radium-girls>.
- [8] Copyright <https://americanhistory.si.edu/girlhood/work/radium-girls>.
- [9] For more information: <https://pubmed.ncbi.nlm.nih.gov/8696882/>.
- [10] For more information: <https://www.ncbi.nlm.nih.gov/pmc/articles/PMC7446021/>.
- [11] Copyright: <https://www.ncbi.nlm.nih.gov/pmc/articles/PMC7446021/>.
- [12] For more information: <https://www.iaea.org/topics/chornobyl>.
- [13] V. Saenko *et al.*, The Chernobyl accident and its consequences *Clin. Oncol.* **23** (2011) 234–43, [doi:10.1016/j.clon.2011.01.502](https://doi.org/10.1016/j.clon.2011.01.502).
- [14] K. Coeytaux *et al.*, Reported radiation overexposure accidents worldwide, 1980–2013: A systematic review, *PLOS ONE* **10**(3) (2015) e0118709, [doi:10.1371/journal.pone.0118709](https://doi.org/10.1371/journal.pone.0118709).
- [15] For more information: <https://www.unscear.org/unscear/en/index.html>.
- [16] For more information: <https://www.iaea.org/>.
- [17] Document link
https://www.unscear.org/docs/publications/2017/UNSCEAR_2017_Annex-B.pdf.
- [18] Document link:
https://www.unscear.org/docs/publications/2001/UNSCEAR_2001_Report.pdf.
- [19] ICRP Organisation link: <https://www.icrp.org/>.
- [20] ICRU Organisation link: <https://www.icru.org/>.
- [21] IRPA Organisation link: <https://www.irpa.net/>.
- [22] ICRP Publication 103: The 2007 Recommendations of the International Commission on Radiological Protection. *Ann. ICRP* **37**(2–4) (2007), <https://journals.sagepub.com/toc/anib/37/2-4>.
- [23] RASSC Committee link: <https://www-ns.iaea.org/committees/rassc/default.asp>.
- [24] ICRP Publication 1: Recommendations of the International Commission on Radiological Protection: Adopted September 9, 1958, *Ann. ICRP OS* **1**(1) (1959), [doi:10.1016/S0074-27402880016-X](https://doi.org/10.1016/S0074-27402880016-X).
- [25] ICRP Publication 26: Recommendations of the International Commission on Radiological Protection, *Ann. ICRP* **1**(3) (1977), [ICRP Publication 26](#).
- [26] ICRP Publication 60: 1990 Recommendations of the International Commission on Radiological Protection, *Ann. ICRP* **21**(1–3) (1991), [ICRP Publication 60](#).
- [27] NCRP Report No 51: Radiation Protection Design Guidelines for 0.1–100 MeV Particle Accelerator Facilities. s.l.: NCRP, 1979.

- [28] NCRP Report No 144: Radiation Protection for Particle Accelerator Facilities. s.l.: NCRP, 2003.
- [29] Topics in Accelerator Health Physics, Professional Development School, Health Physics Society, 2008.
- [30] Accelerator Radiation Physics for Personnel and Environment Protection, J. Donald Cossairt, Matthew Quinn, CRC Press, 2019.
- [31] National Institute of Standards and Technology (NIST) “Stopping Powers and Ranges for Electrons” database <https://physics.nist.gov/PhysRefData/Star/Text/method.html>.
- [32] Mirion Technologies, *Types of ionising radiation*, 2015, <https://www.mirion.com/discover/knowledge-hub/articles/education/types-of-ionizing-radiation>.
- [33] P. Berkvens, Radiation Safety. s.l.: JUAS, 2007.
- [34] K.Ott, The shielding design of BESSY II. New York: IEEE, 1999, Vol. Proceedings of the 1999 Particle Accelerator Conference.
- Recommended references for radiation safety in accelerators:**
- [35] IAEA Report No. 188: Radiological Safety Aspects of the Operation of Electron Accelerators. Vienna: IAEA, 1979.
- [36] IAEA Report No. 283: Radiological Safety Aspects of the Operation of Proton Accelerators. Vienna: IAEA, 1988.
- [37] IAEA. Compendium of Neutron Spectra and Detector Responses for Radiation Protection Purposes – Technical Reports Series no. 403, IAEA, Vienna: IAEA, 2001.